Technische Universität München, TUM School of Natural Sciences

# From Black Pulp to Liquid Gold – Single-Cell Oil Production with *Cutaneotrichosporon oleaginosus*

**Zora Selina Rerop**

Vollständiger Abdruck der von der TUM School of Natural Sciences der Technischen Universität München zur Erlangung des akademischen Grades einer

**Doktorin der Naturwissenschaften (Dr. rer. nat.)**

genehmigten Dissertation.

| | | |
|---|---|---|
| Vorsitz: | | Prof. Dr. Tom Nilges |
| Prüfer der Dissertation: | 1. | Prof. Dr. Thomas Brück |
| | 2. | Prof. Dr. Michael Zavrel |
| | 3. | Prof. Dr. Johannes Kabisch |

Die Dissertation wurde am 25.09.2023 bei der Technischen Universität München eingereicht und durch die TUM School of Natural Sciences am 10.11.2023 angenommen.

*Selber Denken ist das oberste Gebot!*

- Klaus R. Rerop

# Acknowledgements

Die Fertigstellung meiner Doktorarbeit markiert nicht nur das Ende eines langen und intensiven Forschungsprozesses, sondern auch den Beginn eines neuen Kapitels in meinem Leben. Es gibt einige Menschen, denen ich in diesem Zusammenhang gerne danken möchte.

Zunächst möchte ich Prof. Dr. Thomas Brück, meinem Doktorvater, meinen Dank aussprechen. Vielen Dank für das Stellen des Forschungsprojektes und der Thesis und das Vertrauen in mich beides erfolgreich abzuschließen. Herzlichen Dank für die Unterstützung, das Wissen und die Expertise von der ich profitieren durfte.

Ein großer Dank gilt auch dem Projektträger, dem BMBF, das unser Forschungsprojekt "Xylophon" finanziell unterstützt hat. Das Projekt "Xylophon" wurde am WSSB von einem tollen Team bearbeitet und ich hatte Glück ein Teil davon zu sein. Vielen Dank an Mahmoud für deine Betreuung, das Vertrauen, die Unterstützung und das Wissen welches du an mich weitergegeben hast. Vielen Dank an Petra für deine unschätzbare Zuverlässigkeit, die Unterstützung und Energie die du in unser Projekt gesteckt hast und von der ich so viel profitieren konnte. Ein außerordentlicher Dank geht - natürlich - an Niko, dafür, dass du mein Projektpartner warst, ein toller Wissenschaftler bist, immer die Ruhe bewahrt hast, alles mit einem zwinckernden Auge betrachten kannst und genauso viel Leidenschaft und Energie für unsere Forschung aufgebracht hast wie ich. Ohne dich wäre das Projekt nicht dasselbe gewesen.

Ein weiterer Dank geht an meine hoch geschätzten Kollegen, sowohl innerhalb als auch außerhalb des WSSB Forschungsteams. Ihre Beiträge, Diskussionen und Zusammenarbeit haben mein Verständnis vertieft und meine Arbeit bereichert. Insbesondere möchte ich zudem Marion Ringel hervorheben, die mich seit meiner Masterarbeit nicht nur inhaltlich, sondern auch emotional immer unterstützt und beraten hat. Zudem danke ich allen Studenten die ich in Praktika und Abschlussarbeiten betreuen durfte und die alle einen wertvollen Anteil zu meiner Forschung beigetragen haben. Ich danke allen meinen tollen Kollegen und ehemaligen Kollegen: Michi, Nate, Nadim, Sophia, Linda, Manfred, Kevin, Melli, Selina, Felix, Martina, Gülnaz, Petra, Elias, Mahmoud, Norbert, Daniel, Dania, Gabi, Sam, Babak, Philipp, Pariya, Tobi, Jan und Monika.

Schließlich möchte ich meinen Freunden und meiner Familie danken. Euer Vertrauen in mich und Eure bedingungslose Unterstützung haben mir die Kraft gegeben, Hindernisse zu überwinden und weiterzumachen, auch in schwierigen Zeiten. Danke Mama, Sindram und Dirk für Euren unglaublichen Rückhalt.

Danke Mo, dass du immer für mich da bist.

# Zusammenfassung

Die Produktion von Öl und oleochemischen Plattformchemikalien basiert heute auf der Verwertung von fossilen und pflanzlichen Ölen und Fetten. Die Anwendungsgebereiche der Öle reichen von der Kraftstoffherstellung über die pharmazeutische, die kosmetische Industrie bis hin zur Lebens- und Futtermittelindustrie. Nicht jedes Öl ist für jede Anwendung geeignet, da dies von den Produktionskosten, der Reinheit, der Zusammensetzung und der Menge abhängt. Seit geraumer Zeit streben wir eine Abkehr von fossilen Rohstoffen an und setzen aus vielerlei Gründen auf die Produktion nachwachsender Rohstoffe. Die Produktion von Pflanzenölen kann aber auch erhebliche Probleme mit sich bringen, wie z.B. einen hohe Flächenverbrauch, die Zerstörung von natürlichen Lebensräumen und einen erhöhten Eintrag von Pestiziden.

Die mikrobielle Produktion von Ölen und oleochemischen Plattformchemikalien kann eine nachhaltigere Alternative darstellen. Das Ausgangsmaterial für den Prozess kann aus Neben- oder Reststoffströmen der Forst-, Agrar- und/oder Lebensmittelindustrie gewonnen werden. Dieser Reststoff wird ggf. zunächst vorbehandelt und zu einem Nährmedium formuliert. Anschließend kann er als Nährstoffquelle für die ölbildenden Hefe *Cutaneotrichosporon oleaginosus* (ATCC 20509) in einem Bioreaktor zu mikrobiellem Öl umgesetzt werden. Die verwendete Hefe ist eine natürlich vorkommende, nicht genetisch veränderte Spezies. Um die Produkteigenschaften zu verbessern oder die Ausbeute zu erhöhen, wären Methoden zur genetischen Adaption der Hefe notwendig, die jedoch noch nicht ausreichend erforscht sind.

Im ersten Teil dieser Arbeit wurde ein Reststoff aus der Papierindustrie, ein lignocellulosehaltiges Hydrolysat (LCH), aufbereitet und erfolgreich in ein Fermentationsmedium überführt. In einer Fed-Batch Fermentation mit der ölbildenden Hefe *C. oleaginosus* als Produktionsplattform wurde das LCH in Hefeöl umgewandelt. Der Fermentationsprozess basierte auf LCH als Ausgangskohlenstoffquelle und einer verbrauchsabhängigen Essigsäurezufuhr während des Fermentationsprozesses. Durch den Austausch der Kohlenstoffquelle Glucose durch pentosehaltiges LCH wurden deutliche Verbesserungen, sowohl in der Biomassenbildung, als auch im Lipidgehalt erzielt. Die erzielte Lipidproduktion war mit einem Titer von 42,1 g/L und 75,5% Öl in der Trockenmasse eine der höchsten in der Literatur beschrieben Ausbeuten. Um den Prozess weiter zu optimieren, wurde ein hybrider Ansatz gewählt, der verbrauchsbasierte und kontinuierliche Feeding-Methoden kombinierte, um die Bioverfügbarkeit des aus LCH gewonnenen Kohlenstoffs zu maximieren. Darüber hinaus zeigte eine techno-ökonomische Analyse, dass die Verwendung von LCH anstelle von Glukose im industriellen Maßstab eine deutliche Kostenreduktion ermöglicht.

Im zweiten Teil der Arbeit wurden die Werkzeuge zur genetischen Modifikation von *C. oleaginosus* gezielt erweitert, um deren Potential hinsichtlich Substrataufnahme, Produktspezifität und Effizienz in Zukunft zu erhöhen. Dazu wurde die Struktur potentieller endogener Promotorse-

quenzen untersucht und Motive für regulatorische Elemente und translationsinitiierende Stellen identifiziert. Diese wurden verwendet, um vier potentielle Promotorsequenzen zu annotieren, die wiederum erfolgreich zur Expression eines bekanntes Resistenzgen verwendet wurden. PPIp, einer der verwendeten endogenen Promotoren wurde für die anschließende Markerentwicklung eingesetzt. Zwei neuartige dominante Resistenzmarker, Aminoglykosid-3'-phosphotransferase (APH) und N-Acetyltransferase (NAT), wurden zur Selektion in *C. oleaginosus* verwendet. Die beiden Markergene erwiesen sich als kompatibel für den Einsatz sequentieller oder simultaner Integration. Die Implementierung dieser vier endogenen Promotoren und zwei neuartiger Resistenzmarker in *C. oleaginosus* eröffnet neue Möglichkeiten für das Genetic Engineering und die Stammentwicklung dieser Hefe. In Kombination mit gezielten genomischen Integrationsmethoden erschließt diese erweiterte Auswahl an neuen Werkzeugen ein breites Spektrum an genetischen und Metabolic Engineering-Möglichkeiten, für die industrielle Anwendung der ölbildenden Hefe.

Die Ergebnisse dieser Arbeit sind somit ein Schritt auf dem Weg zu einer nachhaltigeren Produktion von Öl und oleochemischen Plattformchemikalien. Diese können mit Hilfe des optimierten Fermentationsprozesses aus Reststoffen der Papierindustrie in einem industriell relevanen Kostenrahmen hergestellt werden. Durch die Erweiterung der genetischen Werkzeuge um vier endogene, konstitutive Promotoren und zwei dominante Selektionsmarker kann *C. oleaginosus* zukünftig auch durch Metabolic Engineering weiter optimiert werden. Dies ermöglicht potenziell eine breite Substratnutzung, eine Spezifizierung der Produktzusammensetzung sowie eine Steigerung der Produktionseffizienz. Diese Dissertation trägt dazu bei, das mikrobielle Öl aus der Grundlagenforschung in die industrielle Entwicklung zu überführen.

# Abstract

The production of oil and oleochemical platform chemicals currently relies on the utilization of fossil oils and vegetable oils. These oils find applications in various fields such as energy storage, pharmaceuticals, cosmetics, foods, and animal feeds. However, not all oils are suitable for every application due to factors such as production cost, composition, purity, and quantity. There is a growing desire to shift away from fossil resources and to focus on renewable materials. However, the production of vegetable oils also comes with serious problems, including intense land usage, destruction of natural habitats, and pesticides utilization.

Microbial production of oils and oleochemical platform chemicals offers a sustainable alternative. Feedstocks for this process can be obtained from by-products or waste streams from forestry, agriculture, and the food industry. This material is then pretreated and formulated into a growth medium enabling its conversion to microbial oil, for example, using the oil-producing yeast *Cutaneotrichosporon oleaginosus* (ATCC 20509) in a high cell density process. Initially, the yeast used is a naturally occurring, non-genetically modified variant. However, methods for genetic adaptation of this unconventional yeast, which have not been extensively studied, would be desirable for optimization of the product properties.

In the first part of this work, lignocellulosic hydrolysate (LCH), a residue from the paper industry, was processed and successfully converted into a fermentation medium. Through a fed-batch fermentation using the oil-producing yeast *C. oleaginosus* as the production platform, LCH was converted to yeast oil. The fermentation process relied on LCH as the carbon source and a consumption-based supply of acetic acid during the fermentation process. Using the pentose-rich LCH significantly improved biomass formation and lipid content compared to glucose as carbon source. The obtained lipid production, with a titer of 42.1 g/L and 75.5% oil in dry biomass, is among the highest yields reported in the literature. To further optimize the process, a hybrid approach combining consumption-based and continuous feeding methods was chosen. This strategy was used to maximize the bioavailability of the carbon derived from LCH. Furthermore, a techno-economic analysis showed that using LCH instead of glucose allows for a significant cost reduction on an industrial scale.

In the second part of the work, the tools for genetic modification of *C. oleaginosus* were specifically extended to increase the potential of the yeast for substrate uptake, product specification, and efficiency in the future. The structure of potential endogenous promoter sequences was investigated, and motifs of regulatory elements and translation initiation sites were identified. These findings were used to annotate four potential endogenous promoter sequences, which were successfully used to express a known resistance gene. One endogenous promoter, PPIp, was used for subsequent marker development. Two novel dominant resistance markers, Aminoglycoside-3'-

phosphotransferase (APH) and N-Acetyltransferase (NAT), were used for selection in *C. oleaginosus*. In addition, these two marker genes were compatible for both sequential and simultaneous integration. The implementation of these four endogenous promoters and two novel resistance markers in *C. oleaginosus* provides new possibilities for genetic engineering and strain development of this yeast. Combined with targeted genomic integration methods, this expanded toolkit offers a wide range of genetic and metabolic engineering strategies for the industrial application of oil-producing yeast.

The results of this work are therefore a significant step towards a more sustainable production of oil and oleochemical platform chemicals. The results provide a new strategy to generate these valuable products from waste materials, such as those from the paper industry, using the optimized fermentation process within an industrially relevant cost framework. The addition of four endogenous constitutive promoters and two dominant selection markers to the genetic tools will allow future optimization of *C. oleaginosus* by metabolic engineering. This will potentially enable broader substrate utilization, tailored product composition and increased production efficiency. Thus, this work contributes to bridging the gap between basic research on microbial oil and its cost-efficient industrial production.

# Contents

# Part I.

# Introduction

# 1 Introduction

## 1.1 Single-cell oil -a modern substitute for fossil and vegetable oil

Oils, fats, and other oleochemicals are used in a variety of different industries, such as energy storage, mobility, plastics, pharmaceuticals, cosmetics, foods, and feeds. However, their production is often based on fossil resources [1, 2]. The shift towards vegetable oils as renewable sources, has already improved the carbon footprint of certain oleochemicals and their derived products. However, the production of vegetable oils comes with numerous drawbacks, including extensive land use, large monocultures leading to decreased biodiversity, and intensive pesticide use, overall resulting in negative impacts on the global environment. Therefore, relying solely on vegetable oil production cannot be the only solution to meet the increasing demand in the future. A promising approach to address this challenge is the microbial production of single-cell oils, fats, and oleochemicals [3]. Microbial biomass production can be efficiently scaled up by employing large bioreactors with compact cultivation volumes on a small land area [4]. In addition, the production process is significantly faster, requiring only a few days for one batch rather than an entire season. Single-cell oil producers encompass various unicellular organisms such as bacteria, algae, protozoa, or yeasts [5]. While these microorganisms have their respective advantages and disadvantages, non-conventional oleaginous yeasts have demonstrated the highest lipid production yields [4, 6, 7]. These specialized yeasts serve as production platforms offering great potential for land-efficient and commercially viable lipid production, independent of weather and climate conditions, pesticides, and harmful monocultures [4].

## 1.2 Relevance of the industrial side stream valorization

Waste or side streams generated from industrial processes, such as agriculture, forestry, pulping, and municipal waste, are often used for energy recovery in anaerobic digestion or combustion. The result of these processes is energy that is often used for the operation of on-site production facilities [8, 9, 10]. However, not all waste-producing locations have the infrastructure for energy recovery systems. Moreover, the energy conversion rates are limited and vary, depending on the specific side stream and the respective process [8]. A valorization of the side and waste streams towards high-value products, such as oleochemicals, is very attractive for some of the biomaterials [11]. Especially, streams containing pentose sugar-rich lignocellulose derived from wood or various other crops [12, 13]. Fortunately, these compounds are the ideal starting material for the ecologically friendly and economically viable production of valuable products such as single-cell oils [5]. Instead of resorting to combustion or anaerobic fermentation, utilizing the carbon from these by-product streams to create new products allows for the establishment of a circular bio-economy, promoting waste upcycling across multiple applications.

## 1.3 Genetic engineering for innovations inspired by nature

In public perception, genetic engineering is to date mainly associated with risks and drawbacks rather than with the advantages and possibilities it offers [14]. The natural capabilities of microorganisms are remarkable and can already be used under optimized process conditions to produce a wide range of products. However, synthetic biotechnology can be applied to further improve the capabilities, performance, or production of organisms by transferring or modifying their genetic information. This adaptation can result in microbial hosts capable of producing valuable products such as pharmaceuticals, energy storage, cosmetics, food, and beverages [15, 16, 17]. Through continued optimization, adaptation, and customization, microorganisms with tailored properties for industrial applications can be developed, making them economically viable. For many processes, this goal still requires extensive research on the individual production organism. In particular, for microorganisms capable of producing commercially relevant products, genetic optimization can be the decisive factor in bringing the process to an economical industrial scale [18]. In this context, drawing inspiration from nature for innovation holds great potential for benefiting humankind.

## 1.4 Objective of the work

The objective of this work was the optimization of single-cell oil production process using the promising unconventional yeast *C. oleaginosus*. A cheap side stream from the pulp and paper industry was investigated as raw material and made accessible for the yeast. Furthermore, the fermentation procedure was scaled up to a laboratory bioreactor level, and genetic engineering of the production organisms was explored. The developed technology represents a significant advancement towards the efficient production of single-cell oils, fats, and other oleochemicals in terms of land and time utilization, while also contributing to general waste reduction.

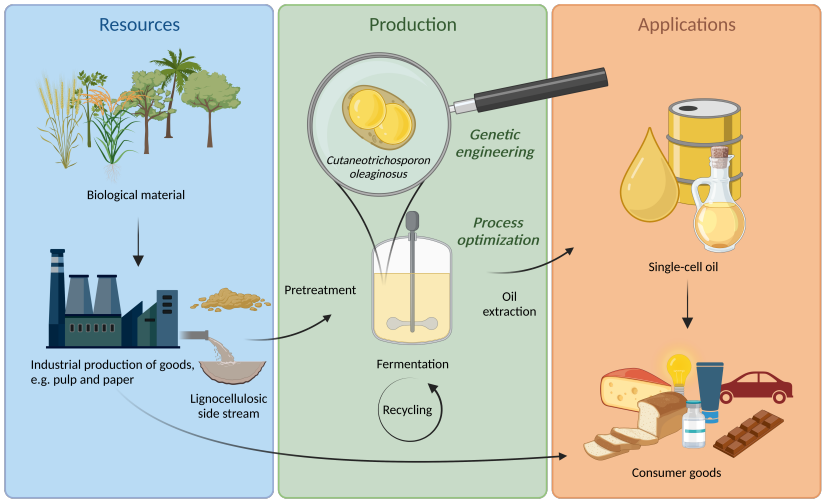


**Figure 1.1.:** Summary of the circular bioeconomy approach for single-cell oil (SCO) production using the oleaginous yeast *C. oleaginosus*. The upcycling of industrial by-products to SCO is shown, including process optimization and genetic engineering, as well as possible applications of the yeast oil. Created in BioRender.com

# 2 Background

## 2.1 Industrial side and waste streams

### 2.1.1 Utilization of waste streams and by-products for bio-conversion

Many industries generate waste streams or by-products that have the potential for value creation but are often not fully exploited. These biomass streams originate from various industrial sectors, including forestry (e.g. sawdust), fiber production (e.g. pulp liquor), agriculture (e.g. wheat bran, manure), food industry (e.g. used cooking oil, municipal waste), and marine residues (e.g. algae) [19, 20, 21, 22]. The utilization of these biomasses is often implemented within a circular bioeconomy framework, with social, economic, and environmental benefits [8]. In these concepts, the biorefinery plays a vital role in creating new value from biomass, particularly from waste materials. This approach aims to minimize waste disposal and environmental pollution through the holistic utilization of waste materials [8]. Commonly practiced methods include incineration and anaerobic digestion of biomass to produce chemicals, heat, and energy [8, 9, 10]. However, this practice generates only low value compared to the production of high-value materials and, in some cases, even contributes to further environmental pollution [8, 22].

### 2.1.2 Lignocellulosic hydrolysates

Lignocellulosic biomass is the most abundant renewable resource globally [23]. It is derived from plants and can be hydrolyzed to access its monomeric constituents [12]. The main components of lignocellulosic biomass are cellulose, hemicellulose, and lignin [12, 13]. Cellulose, a polysaccharide comprised of D-glucose, constitutes up to 50% of the biomass. It is often the most abundant compound in biomass material, and has the most applications and the best bio-accessibility [11]. Lignin is a complex polymeric structure composed of phenolic compounds, including non-phenolic aromatic compounds, such as benzoic acid and cinnamic acid, as well as phenolic compounds, like coniferyl aldehyde, vanillic aldehyde, and 4-hydroxy-benzoic acid [11, 24]. Hemicellulose is a heteropolymer, a polysaccharide matrix, that is complex in its structure and varies from plant to plant; it is commonly composed of xylan, xyloglycan, mannan, or glucomannan or others [11, 25]. Upon chemical hydrolysis with mineral acids, hemicellulose yields hexose and pentose sugars, uronic acids, and acetic acid originating from acetyl groups [11].

Hydrolysis of plant material can be achieved through various methods, including chemical and physicochemical lysis as well as enzymatic and cell-based approaches that can be employed individually or in combination [26, 27, 28]. Hydrolysis can be used for fractionation and to increase the accessibility of the carbon sources from the material for further processing [12, 28]. However, the industrial practices and scientific research vary for each material because of differences in com-

position, fractionation, and product application [28]. A major challenge associated with hydrolysis is the formation of inhibitory by-products that can be toxic to microbial growth [11]. Industrial methods might use acids such as $H_2SO_4$, $SO_2$, HCl, and $H_3PO_4$ to hydrolyze polymeric hemicellulose constituents and saccharides [11]. In other chemical processes such as Kraft pulping, an alkaline treatment with, e.g., NaOH and $Na_2S$ results in the hydrolysis of lignin and, to some extent, hemicellulose. Mild alkaline conditions with $Ca(OH)_2$ or $NH_3$ are also used for lignin removal [11]. Oxidative methods remove lignin and hemicellulose using chemicals such as $H_2O_2$ and $O_2$ or $O_3$ [11]. Hydrothermal processing is used, which results in the solubilization of hemicelluloses without complete hydrolysis [11]. Enzymatic hydrolysis is often used to lyse poly- to monosaccharides, which is essential for anaerobic fermentation and fiber production [27, 28]. In most industrial processes, physical, enzymatic, and chemical hydrolysis methods are used [11, 12, 27].

### 2.1.3 Waste streams from industrial pulp and paper production

The European pulp and paper industry generates more than 11 million tons of waste material annually making it a major producer of biodegradable waste [29, 30]. The term pulping describes the hydrolysis of wood, to separate cellulose fibers from the rest of the material. Various pulping methods are employed industrially, including alkaline, neutral, and acid pulping [24, 31]. These methods typically involve the addition of sulfate salts to increase hydrolysis efficiency. In acid pulping, sulfuric acid is utilized, which is also called sulfite pulping. Industrially, these chemical pulping processes are combined with a physicochemical steam explosion step, which assists to break down the plant cell walls and separate the valuable cellulose fibers from the remaining biomass [27]. The cellulose content in dry wood strongly varies with tree species, ranging from 42% for softwood and 42-48% for hardwood [24]. More than half of the wood content is not further valorized but is converted to energy wherever possible. This part of the wood is composed of hemicellulose (17 - 28%) and lignin (15-29%), as well as pectin, starch, ash, and other components (0.3-4%), visualized in figure 2.1 [11, 24, 25]. Hemicellulose primarily consists of the O-acetyl-4-O-methylglucurono-D-xylans, O-acetyl- galactoglucomannans, arabino-4-O-methylglucurono-D-xylans, and others [11]. These sugar polymers contain hexose and pentose sugars, but also acetyl groups and uronic acids, such as gulcoronic and galactoronic acid [11]. Hardwood generally exhibits higher cellulose content and lower lignin content compared to softwood or other plants [11, 32]. Furthermore, hardwood has a relatively high amount of acetyl groups that are present in the hemicellulose, resulting in hydrolysates with higher acetic acid content [11].

Typically, waste streams from pulping processes are either disposed of in landfills or combusted/incinerated for energy production [27, 33]. However, combustion requires the water content of the waste to be reduced, which in turn requires energy, reducing its overall energy efficiency [27]. The paper sludge, on the other hand, with its 20 to 75% carbohydrate content can be used in biorefinery processes, such as anaerobic methane production, thermal pyrolysis, biohydrogen production, or the production of value-added chemicals, like ethanol [27]. However, most of these biorefineries are based on the cellulose residues in paper sludge and often do not utilize the lignin-derived compounds and the pentose sugars [27]. The waste stream is typically highly concentrated, and the acetic acid is evaporated and separated from the other components [20]. Acetic acid is rarely recovered and used as a bulk chemical, such as by the Lenzing AG in Austria [34]. For

acetic acid, lignin, and xylose, there are only a few established recovery or valorization technologies [35, 36, 37].

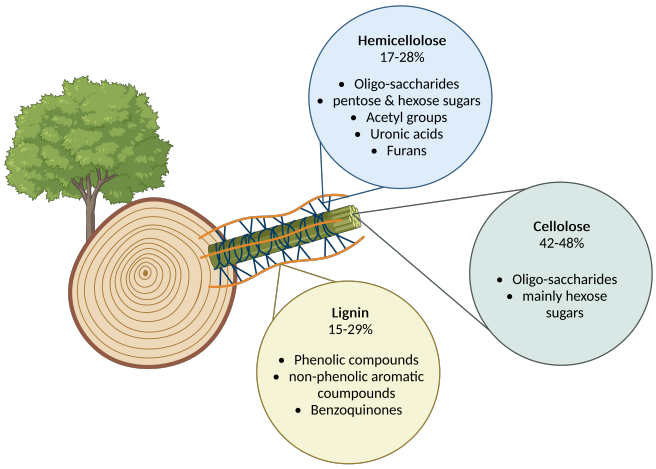


**Figure 2.1.:** Composition of wood and its fiber structure with the components of the main biopolymers hemicellulose, cellulose, and lignin. Created in BioRender.com

### 2.1.4 Pretreatment of pulp hydrolysates for bio-conversion

Pulp sludge and other lignocellulosic hydrolysates often contain inhibitory by-products of hydrolysis, such as furans derived from monomeric sugars, aromatic compounds from lignin, organic acids, metals, and small aliphatic aldehydes [28, 38]. In addition, the sludge is often acidic or alkaline, creating an unfavorable environment for microbial growth. To facilitate fermentative valorization, further pretreatment of the hydrolysate is usually required [11]. Depending on the requirements of the microorganisms used for fermentation, some of the inhibitory components must be reduced or eliminated. Furthermore, the pH of the solution must be changed from extreme values to the optimal one for the respective microorganism [11]. To deal with these inhibitory compounds, strategies such as detoxification by absorption or chemical effects with chemicals, activated carbon, or various polymers can be applied; those on the other hand require more chemicals and consumables [39, 40]. In addition, microbial bioabatement has been applied, although the sugar content of the hydrolysate is reduced with this method [41, 42].

## 2.2 Single-cell oil production

### 2.2.1 Single-cell oil

Single-cell oil (SCO) is sometimes referred to as microbial oil or microbial lipid. Lipid is the molecular description of the sum of molecules naturally present in oil or fat [43]. In general, lipids are hydrophobic or amphipathic small molecules that are formed in whole or in part by carbanion-based condensations of ketoacyl thioesters and/or by carbocation-based condensations of isoprene units [43, 44]. According to the LIPID MAPS classification system, lipids can be divided into eight classes: fatty acids (FA), glycerolipids, glycerophospholipids, sterols and sterol derivatives, sphingolipids, prenol lipids, glycolipids, and polyketides [3, 44]. SCOs are lipids synthesized by microorganisms that can be accumulated intracellularly [7]. Therefore, SCO can be distinguished

from animal fats or plant/vegetable oils by the production organisms. At the molecular level, the composition of SCO shows many similarities, but also some differences compared to animal or vegetable oil [5, 45]. The composition of the oil is always highly dependent on the organism used for production [5]. Lipids serve a variety of functions within cells, including structural components such as cell and organelle membranes, and energy storage [7]. Organisms that produce lipids for energy storage are of particular interest for SCO production as specific conditions can induce lipid accumulation and higher yields [3].

### 2.2.2 Oleaginous microorganisms

While all living organisms can produce lipids, most are channeled into membrane homeostasis, but can also function as structural elements, signaling molecules, mediators of membrane fusion and apoptosis, as well as energy storage [3]. Apart from certain plants and animals that can store large amounts of lipids, unicellular organisms can also produce significant amounts of intracellular lipids or oils [5]. These oleaginous microorganisms can convert various carbon sources, such as sugars or organic waste materials, into lipids through lipid biosynthesis. Among these oleaginous microorganisms, there are microalgae, such as *Chlorella* sp. and *Dunaliella* sp., which can produce microalgal oil on the basis of a carbon source, $CO_2$, and sunlight [6]. The typical lipid content achieved with microalgae ranges from 3 to 30% [46, 47]. More recently, higher contents of 60 to 70% lipid have been demonstrated, e.g. using red instead of white light [48]. Other protists, thraustochytrid marine organisms such as *Schizochytrium* sp. are also capable of producing microbial oil [49, 50, 51]. In addition, some bacteria reach contents of over 50%, such as *Rhodococcus rhodochrous* or *Rhodococcus opacus* [52]. However, in terms of high lipid content and short production times, oleaginous yeasts generally outperform other oleaginous microorganisms, with over 80% lipid in dry cell weight (DCW) and fast batch fermentation times of two to five days [4, 7, 53]. Overall, oleaginous microorganisms can produce significant amounts of single-cell oils for more sustainable oleochemical production [5].

### 2.2.3 Oleaginous yeasts

There are over a hundred, probably several hundred, oleaginous yeast species, defined by a minimum lipid content of 20% lipid per DCW [53, 54, 55, 56]. However, only a few of these have been characterized and new species continue to be discovered every year [54, 57]. The best studied organism of these yeasts is *Yarrowia lipolytica*, a fungus belonging to the phylum Ascomycota of the class Saccharomycetes [58]. *Y. lipolytica* has been used to produce lipids for food-related applications, flavors, polyalcohols, organic acids, emulsifiers, surfactants, and proteins [59]. Other prominent and well-studied yeasts are *Rhodosporidium toruloides* and other *Rhodosporidium* sp., *Lipomyces starkeyi* and other *Lipomyces* sp, *Cutaneotrichosporon oleaginosus* and several *Candida*, *Trichosporon* and *Pseudozyma* species [60, 61]. Among the known oleaginous yeasts, only *Yarrowia lipolytica* has been extensively used for genetic engineering studies [62]. In regards to lipid synthesis *Y. lipolytica* performs both the *de novo* and *ex novo* pathways, where especially the *de novo* synthesis requires genetic engineering to produce substantial lipid yields. Table 2.1 summarizes the performance studies of wild-type oleaginous yeasts fermented on relevant hydrolysates.

**Table 2.1.:** Wild-type oleaginous yeast cultures on industrial hydrolysates for lipid production. Some examples with potentially high yields have been selected. n.d. - not defined, FB - fed-batch

| Oleaginous yeast | Carbon source | Cultivation scale | Lipid per biomass (%) | Lipid titer (g/L) | Lipid product. (g/L/h) | Fatty acid profile (%) | | | | | | | | | Reference |
|---|---|---|---|---|---|---|---|---|---|---|---|---|---|---|---|
| | | | | | | C14:0 | C16:0 | C16:1 | C18:0 | C18:1 | C18:2 | C18:3 | C22:0 | C24:0 | |
| *Cutaneotrichosporon oleaginosus* ATCC 20509 | lignocel. hydrol. from pulping | fed-batch fermentation | 75.5 | 42.1 | 0.58 | 0.4 | 24.5 | 0.28 | 16 | 54.5 | 4.9 | 0.5 | 0.3 | 0.5 | [63], 2023 |
| *Cutaneotrichosporon oleaginosus* ATCC 20509 | brown algae hydrol. | fed-batch fermentation | 64 | 72.9 | 0.59 | | 28.8 | | 8.8 | 47.4 | 13.8 | 1.2 | | | [4, 60], 2019,2021 |
| *Cutaneotrichosporon curvatus* CA-3802 | detoxified lignocel. hydrol. of *A. donax* | FB fermentation | 63.6 | 28.4 | | | 26.9 | | 8.2 | 33.3 | 31.6 | 0 | | | [64], 2019 |
| *Yarrowia lipolytica* | Industrial oleic rapeseed oil/stearin (25/75) | flasks | 41 | 3.4 | 0.009 | | | | | | | | | | [65], 2001 |
| *Rhodosporidium toruloides* | lignocel. hydrol. derived from corn stover | online-FB fermentation | 59 | 31.86 | 0.4 | 1.4 | 26.8 | | 11.2 | 45.8 | 9.8 | 4.1 | | | [66], 2016 |
| *Lipomyces starkeyi* | hemicel. hydrol. from sugarcane bagasse | bioreactor fermentation | 26.1 | 2.51 | 0.06 | 0.3 | 31.3 | 5.5 | 6.3 | 52.6 | 2.6 | | | | [67], 2017 |
| *Rhodoturula glutinis* TISTR 5159 | unconc. sugarcane bagasse hydrol. + glycerol addition | flasks | 33.03 | 8.31 | | 1.2 | 24.5 | 2.2 | 8.4 | 48.5 | 11.4 | 2.8 | | | [68], 2022 |
| *Cryptococcus albidus* | onion and apple hydrol. | cell retention system fermentation | 20 | 2.71 | 0.08 | <1 | 18-27 | | 0.2-3.0 | 1.0-10.0 | 67-74 | | | | [69], 2019 |
| *Candida albicans* SY3 | sugarcane bagasse | flasks | 22.13 | 1.84 | n.d. | | | | | | | | | | [38], 2019 |
| *Meyerozyma guilliermondii* G5 | sugarcane bagasse | flasks | 37.99 | 2.33 | n.d. | | | | | | | | | | [38], 2019 |

### 2.2.4 *De novo* lipid biosynthesis in oleaginous yeast

The formation of lipids in oleaginous yeasts is typically triggered by specific cultivation conditions. The trigger may be nutrient depletion such as nitrogen, phosphate, iron, sulfur, zinc, oxygen limitation, or supplementation with an organic acid, fatty acids, or glycerol [55, 65]. Media containing hydrolysates from agriculture, the food or pulp industry, or marine residues often result in higher lipid formation and content than media containing monomeric sugars [60, 70]. Lipid biosynthesis starts with the uptake of digestible carbon sources, usually sugars, which are channeled into the cellular metabolism to form malonyl-CoA [71]. First, the fatty acids are synthesized via the *de novo* pathway, or external fatty acids are taken up and hydrolyzed [72, 73]. Fatty acid synthesis usually occurs in the cytoplasm of the cell by the FAS complex, and fatty acids with a chain length of up to C16 are formed [72]. The acyl-CoA chains are then channeled into the endoplasmic reticulum (ER), where the fatty acids are elongated and desaturated. Subsequently, di- and triacylglycerols (TAGs) are synthesized within the ER [72, 73]. Phospholipids are also synthesized in the ER, including phosphatidylethanolamine (PE) and phosphatidylcholine (PC) [72, 74]. Lipids are typically accumulated in lipid bodies, which bud from the ER [71, 75]. These lipid bodies consist of a hydrophobic core of neutral lipids, mainly TAGs, surrounded by a phospholipid monolayer membrane. Proteins, such as lipid droplet-associated proteins (LDAPs), coat the surface of lipid bodies, helping to stabilize and regulate their formation [72, 76]. They can enlarge over time, and small lipid bodies can merge to form larger ones [75, 76].

### 2.2.5 Genetic engineering of oleaginous yeasts

#### Evolutionary engineering - chemical and physical mutagenesis methods

Evolutionary engineering can be used to optimize strains without creating an organism classified as a genetically modified organism (GMO). Available methods include chemical mutagens, such as ethyl methanesulfonate (EMS) and N-methyl-N-nitro-N-nitrosoguanidine (NTG), and physical mutagens, such as UV irradiation and ionizing radiation [77, 78]. Chemical mutagenesis with EMS alkylates DNA bases, resulting in point mutations, while NTG induces both point mutations and frame-shift mutations [79, 80]. These mutagens have been successfully used to generate diverse mutant populations in oleaginous yeasts, resulting in improved lipid accumulation phenotypes [81]. In physical mutagenesis methods, the yeasts are exposed to physical agents that induce genetic changes, such as UV irradiation and ionizing radiation. UV irradiation mainly induces point mutations, while ionizing radiation can induce a wider range of genetic changes, including point mutations, chromosomal rearrangements, and deletions. These methods have generated genetic diversity in oleaginous yeasts, resulting in strains with enhanced lipid production capabilities [82]. Mutagenesis is followed by often time-consuming selection and screening to find the mutants with the desired phenotype [78]. Evolutionary engineering offers several advantages, including its simplicity, cost-effectiveness, and ability to induce random mutations throughout the genome. These methods can generate diverse mutants, allowing the identification of novel genetic variations with improved lipid accumulation. However, a limitation is the potential introduction of deleterious mutations and unrelated once to the desired phenotype that affects other parameters. The screening method is critical to find mutants with the desired phenotype and few unwanted mutations.

**Targeted and untargeted genetic engineering**

Sophisticated biotechnological approaches can be used to engineer the yeast genome in a more targeted manner than chemical and physical mutagenesis. However, some methods also involve a random factor, such as untargeted genomic integration, in which a specific genetic sequence is integrated into the genome at a random position. Targeted genetic engineering, on the other hand, can specify the side of genomic integration [83]. To this end, potential genetic targets can be identified and used for genetic engineering for genomics, transcriptomics, proteomics, and metabolomics [84, 85]. Un- or non-targeted methods include electroporation of the yeasts with DNA strands that may randomly integrate into the genome. Still, also methods with assisted random integration, such as with *Agrobacterium tumefaciens* mediated transformation (ATMT), are being applied [58, 86]. Promoters are essential for gene regulation, but only a few promoters have been characterized for many oleaginous yeasts to date. In the genetically best studied oleaginous yeast *Y. lipolytica*, two high-expression promoter systems were described as early as 1982 and 1998: The promoter of the XPR2 gene encoding an alkaline extracellular protease, and the constitutive promoter of TEF encoding translation elongation factor-1 [87, 88]. For this yeast, a wide range of promoters has been described since then, but only little research exists on the comparison of the known promoter strengths [58, 89].

Targeted manipulation of the host can be achieved by inserting DNA into the genome of an organism, but also by maintaining plasmids inside the cells, which is often difficult for eukaryotic cells [90]. For *Y. lipolytica*, a CRISPR Cas system for genomic manipulation was already established in 2016 [91]. Since then, a lot of targeted engineering has been explored over the years to improve lipid productivity and value-added products or substrate adaptation [58, 92]. For genetic engineering, many targets have been addressed in *Y. lipolytica* and some other yeasts, such as the overexpression of key enzymes, the manipulation of transcription factors, or the optimization of the carbon flux [92]. Increasing the expression levels of enzymes involved in lipid biosynthesis, such as ACC, FAS, and DGAT, increases lipid production. Modification of transcription factors such as Mhyp, SREBP, PPAR, and many others can alter the expression of lipid-related genes, thereby affecting lipid production [58, 92, 93]. Rerouting metabolic pathways such as glycolysis, the TCA cycle, and the PPP can optimize carbon allocation for lipid synthesis or value-added products [92]. These genetic engineering strategies promise to enhance lipid biosynthesis in oleaginous yeasts, providing opportunities for increased lipid yields, adaptation to specific substrates, and optimized lipid composition.

## 2.3 *Cutaneotrichosporon oleaginosus*

### 2.3.1 History

The unconventional yeast *Cutaneotrichosporon oleaginosus* ATCC 20509 was primarily isolated in 1978 by Moon et al. and was originally named *Candida curvata* D [94, 95]. Moon et al. used cheese whey to produce single-cell oil and protein with four different isolates from dairy flours and drains in Iowa, USA [94]. They identified some general requirements for cultivating the yeast, such as the need for the vitamin thiamine for growth and the optimal growth temperature of 28°C. The optimal pH was found to be different in the exponential growth phase (5.4) and in the oil-

producing phase (5.8) [94]. Fermentation of the yeast on whey permeate resulted in lipid titers of 15.6 g/L. In addition, Moon et al. hypothesized that the yeast could consume lactic acid and observed slime production in the growth phase, which disappeared in the lipid production phase. The yeast biomass further contained essential amino acids such as threonine, valine, methionine, isoleucine, and leucine [94]. In the 1980s, the name *Apiotrichum curvatum* was used to describe the yeast [96, 97]. In 1986, nitrogen-limited media were tested, and a mathematical model was developed to describe and predict lipid production according to the C/N ratio [96].

Some years after the first descriptions of ATCC 20509 for oil production from cheese whey, a similar setup was chosen to study the cell harvesting and cross-flow oil separation [97]. Chemical mutants of Ykema were generated in 1988 [98]. The yeast was reclassified in 1990 as *Cryptococcus curvatus* [99]. In 1993 however, the organism was also reclassified under the new name *Trichosporon cutanem*. Although this specific name had been given to other organisms, including an organism described as *Trichosporon beigelii*, which caused systemic infections in humans [100]. Since the 1990s, both names *Trichosporon cutanem* and *Cryptococcus curvatus* have been used to describe the yeast ATCC 20509 [100, 101, 102]. From 2010 on, the yeast was also described as *Trichosporon oleaginosus* sp., which remained in use in parallel with *Cryptococcus curvatus* in the 2010s and 2020th [103, 104, 105]. Since 2015 it has been re-ordered into the *Cutaneotrichosporon* genus within the family *Trichosporonaceae*, with the name *Cutaneotrichosporon oleaginosus* (HM802135) [106].

### 2.3.2 Characteristics

*C. oleaginosus* belongs to the phylum of *Basidiomycota* and the class *Tremellomycetes* [106]. Tremellomycetes includes both basidiomycetous yeasts and filamentous fungi. At the order level, *Cutaneotrichosporon oleaginosus* belongs to the Tremellales. Tremellales are known for their ability to produce exopolysaccharides and are involved in biodegradation processes [107]. *C. oleaginosus* has an optimal growth temperature of 28°C. The optimal pH for lipid production varies widely in the literature ranging from 4.8 to 7.5. For controlled media composition, the optimal pH is reported to be between 5 and 6.5 [4, 108, 109, 110, 111]. It has been reported that the yeast can metabolize a wide range of sugars, organic acids, and aromatic substances [94, 112, 113, 114]. It metabolizes oligo- and monomeric sugars such as glucose, xylose, fructose, galacturonic acid, maltose, lactose, sucrose, cellobiose, mannose, galactose, N-acetylglucosamine, and with minor growth also trehalose, sorbitol, raffinose, arabinose, and melibiose [112, 115, 116, 117]. For the metabolism of xylose and other pentoses the existence of an additional pathway for pentose metabolism to the pentose phosphate pathway was postulated in 1984 [113]. The detection of a xylulose-5-phosphate phosphoketolase channeling the xylulose 5-phosphate directly to glyceraldehyde 3-phosphate and acetyl-phosphate indicated the presence of another pathway, now called the phosphoketolase pathway [113]. Furthermore, the utilization of other carbon sources such as ethanol, glycerol, acetic acid, and lignin-derived aromatic compounds such as phenol, resorcinol, p-coumarate, and pHBA was demonstrated [4, 112, 113, 114, 118]. The yeast was highly tolerant to potentially toxic compounds, often found in lignocellulosic hydrolysates like furans and phenolic aldehydes [119]. This broad substrate metabolism makes *C. oleaginosus* a suitable host for the bio-conversion of a wide range of lignocellulosic wastes. The lipid production of *C. oleaginosus* depends on the process

conditions, substrates, and the stress method applied [110]. As nutrient stressors, nitrogen, phosphorus, and sulfur limitations have been applied in the past, but most studies focus on nitrogen limitation [56, 120]. More recently, in 2019, a consumption-based acetic acid method was developed that achieved significantly higher lipid titers [4]. With these lipid titers and the ability to metabolize industrial waste streams, *C. oleaginosus* is an ideal host for single-cell oil production.

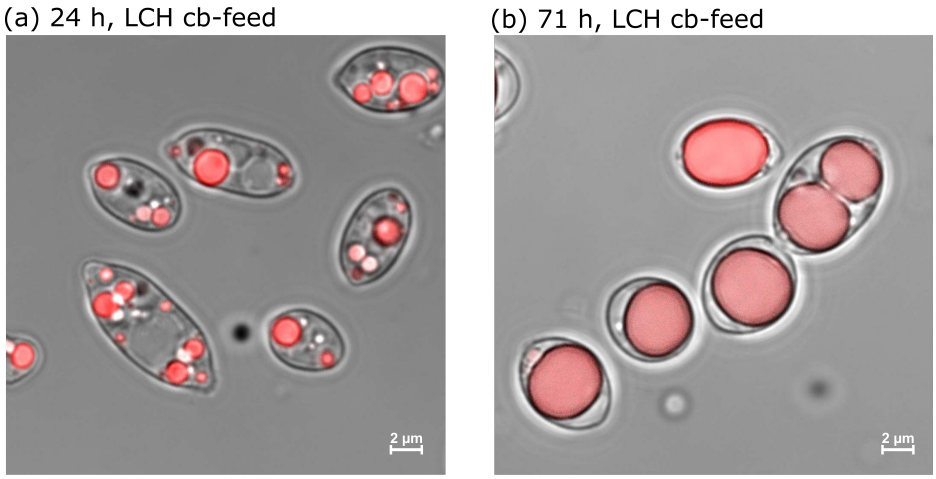


**Figure 2.2.:** *C. oleaginosus* cells from bioreactor fermentation with a LCH from pulping, 24 h (a) and 72 h (b) after fermentation initiation. Lipid bodies are stained with NileRed. The image was taken with a confocal microscope (Carl Zeiss AG, Oberkochen, Germany). LCH, lignocellulosic hydrolysate; cb-feed, consumption-based feed

### 2.3.3 Lipid metabolism and composition

In 2021, Pham et al. published metabolic modeling of *C. oleaginosus* based on genomic data [72]. They proposed that the unconventional yeast uses the central metabolic pathways of glycolysis, the pentose phosphate pathway, and the citric acid (TCA) cycle to catabolize carbon sources [72]. For xylose catabolism, both the pentose phosphate pathway, and the phosphoketolase pathway were identified [113]. Acetic acid is expected to be taken up and converted to acetate and acetyl-CoA [121]. Acetyl-CoA is also one of the products from glycolysis, the TCA cycle, and the phosphoketolase pathway, and is subsequently converted to malonyl-CoA. An overview of the expected metabolism from substrate uptake to lipid droplet formation of *C. oleaginosus* is shown in figure 2.3. Fatty acid production takes place in the cytoplasm and partially in the mitochondria by the fatty acid synthase (FAS) complex, which requires malonyl-CoA and produces fatty acids with a chain length of up to 16 carbon atoms after the carboxyl group (C16:0). The C16-ACP is converted to C16-CoA and transported to the endoplasmic reticulum (ER) for further elongation and desaturation. The fatty acids are then used in the synthesis of triglycerides (TAG). Phospholipids (PE, PC, PS) and sterols, which are also synthesized inside the ER, form lipid bodies that emerge from the ER membrane with a phospholipid monolayer on the outside of the droplet [90, 122]. The latter process has not been investigated for *C. oleaginosus*, but is the standard route for lipid body formation in oleaginous yeasts [90, 122]. The lipid of *C. oleaginosus* is composed of more than 90% TAG with a fatty acid composition that changes over the fermentation time [98]. This is due to lipid droplet formation, which reduces the production of membrane and other functional lipids and increases the proportion of storage lipids.

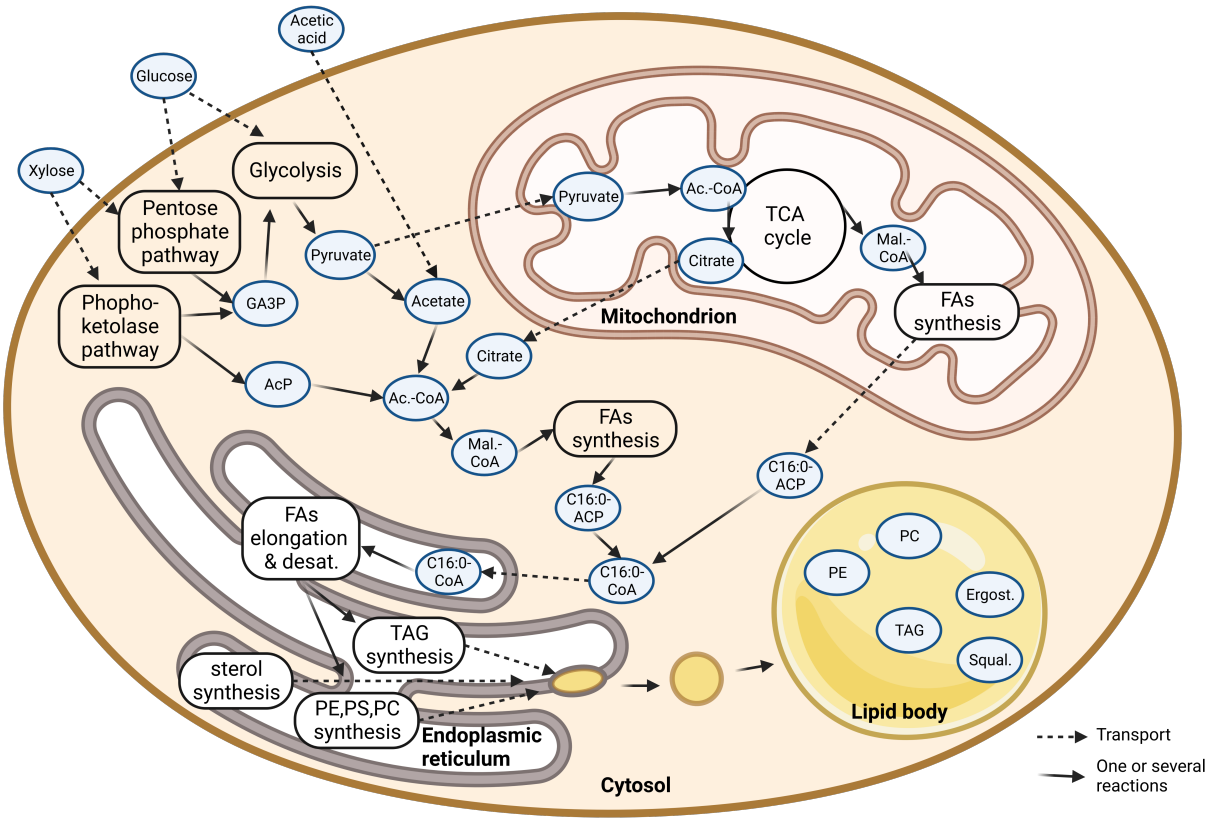


**Figure 2.3.:** Overview of the substrate catabolism and lipid metabolism of *C. oleaginosus*, adapted from Pham et al. [72]. Reactions have been simplified for clarity; the arrow often indicate multiple enzymatic reactions. The dotted arrows indicate transport reactions that may include enzymatic reactions. Created in BioRender.com

### 2.3.4 Genetic engineering

Already in the 1980s and 1990s *C. oleaginosus* was chemically and physically modified by Ykema et al. [98, 108]. They generated several unsaturated fatty acid auxotrophic (Ufa) strains that could be reverted by further mutagenesis. By altering the fatty acid profile, Ykema et al. were able to produce a cocoa butter equivalent [98]. More recently, in 2016, Görner et al. developed a genetic engineering strategy based on *Agrobacterium tumefacines* mediated transformation (ATMT) and random genomic integration of the transferred DNA. This approach allowed for the modification of the fatty acid profile in C. oleaginosus with reduced screening efforts compared to earlier methods [86]. Furthermore, in 2018 a method based on a lithium acetate treatment and electroporation was developed to enhance TAG production in *C. oleaginosus* [123]. This study successfully integrated the genes encoding acetaldehyde dehydrogenase (ALD), pyruvate decarboxylase, acetyl-CoA synthetase, and phospholipid:diacylglycerol acyltransferase in order to bypass the mitochondrial conversion of pyruvate to acetyl-CoA and TAG synthesis inside the cytoplasm [123]. Another study demonstrated the random genomic integration of a *Cryptococcus* adhesin (CFL1) for the flocculation of the yeast cells [124]. Only very recently, in 2023, the first CRISPR-Cas approach was developed, demonstrating different genomic manipulations, such as integration, deletion, and promoter switching. These methods were used to manipulate the fatty acid profile of the yeast [18].

# Part II.

# Material and Methods

# 3 Material and Methods

The essential materials and methods for this work are described in the following sections. Specialized methods are described in the respective publications included in this work. Commonly known methods and producer manuals are not described in detail.

## 3.1 Organisms

The strain *Escherichia coli* DH5$\alpha$ 668369 was used for the molecular construction of DNA and vectors. ATMT was performed with *Agrobacteria tumefaciens* AGL1 ATCC BAA-101, supplied by the Deutsche Sammlung von Mikroorganismen und Zellkultur (DSMZ, Braunschweig, Germany). The lipid-producing cultivations and fermentations were performed with the oleaginous yeast *Cutaneotrichosporon oleaginosus* ATCC 20509 (DSM-11815), supplied by the Deutsche Sammlung von Mikroorganismen und Zellkultur (DMSZ, Braunschweig, Germany).

## 3.2 Chemicals

All chemicals and reagents were perchased from AppliChem GmbH (Darmstadt, Germany), Merck (Darmstadt, Germany), Roth chemicals (Karlsruhe, Germany), Sigma-Aldrich (St. Louis, USA), New England Biolabs (Ipswich, USA), and TH Geyer (Renningen, Germany) if not indicated otherwise. Single-use material was supplied by Carl Roth (Karlsruhe, Deutschland), Eppendorf (Wesseling-Berzdorf, Deutschland), Thermo Fisher Scientific (Schwerte, Deutschland), Sarstedt (Nümbrecht, Deutschland), VWR (Darmstadt, Deutschland) and Greiner (Kremsmünster, Austria).

## 3.3 Enzymes and kits

Enzymes used for molecular biology, like the Taq and Phusion polymerases, restriction enzymes (fast digest), PNK, and DNA ligase, were supplied by Thermo Fisher Scientific (Waltham, USA) and New England Biolabs (Ipswich, USA). For DNA plasmid preparation, the GeneJET Plasmid-Miniprep-Kit from Thermo Fisher Scientific (Waltham, USA), and for Gel-extraction and PCR cleanup, the MONARCH kits from New England Biolabs (Ipswich, USA) were used.

## 3.4 Buffer and media

Buffer and media were prepared with ultra-purified water generated by the Arium pro UV ultrapure water system from Sartorius (Göttingen, Germany); hereafter, this water is referred to as purified water. Standard buffers and media such as TAE, PBS, LB, SOC, and YPD were prepared according

to standard protocols, e.g., from Cold Spring Haber Protocols (CSH, Copyright 2023 by Cold Spring Harbor Laboratory Press). Specific media are listed in Tables 3.3, 3.4, 3.7, and **??**.

## 3.5 Lignocellulosic hydrolysate from pulping

The lignocellulosic hydrolysate was obtained from an industrial pulping process. Beech wood was used for fiber production in an acidic sulfite pulping combined with steam explosion. The concentrated spent liquor was provided and is hereinafter described as lignocellulosic hydrolysate (LCH). It was analyzed with gravimetric, HPLC, GC-MS, chemical analysis of the sulfuric acid and element analysis of the ash. Two batches of LCH were received and analyzed, showing variations in the composition. All experiments in the main publication were performed with the second batch. The total dry mass of the batch utilized for the experiments was 247.7 ± 2.4 g/L. It was stored after sterile filtration at 4-8°C, the solution formed insoluble particles over time.

**Table 3.1.:** Composition of the second batch of lignocellulosic hydrolysate (LCH).

| **Compound** | **Concentration (g/L)** | **Share of total (%)** |
|---|---|---|
| Monomeric sugars | 115.6 ± 5.0 | 46.7 |
| Xylose | 77.1 ± 2.5 | 31.1 |
| Glucose | 11.5 ± 0.4 | 4.6 |
| Mannose | 8.2 ± 0.8 | 3.3 |
| Galactose | 6.5 ± 0.2 | 2.6 |
| Rhamnose | 5.9 ± 0.2 | 2.4 |
| Arabinose | 4.9 ± 0.4 | 2.0 |
| Fucose | 1.6 ± 0.4 | 0.6 |
| Organic acids | 16.8 ± 1.4 | 6.8 |
| Acetic acid | 12.3 ± 1.2 | 5.0 |
| Galacturonic acid | 4.5 ± 0.2 | 1.8 |
| Furans | 5.2 ± 0.6 | 2.1 |
| HMF | 4.5 ± 0.6 | 1.8 |
| Furfural | 0.7 ± 0.1 | 0.3 |
| Sulfates | 19.4 ± 2.0 | 7.8 |
| Sulfuric acid | 19.4 ± 2.0 | 7.8 |
| Ash | 0.7 ± 0.1 | 0.3 |
| Lignin and others | 89.9 ± 30.0 | 36.3 |

### 3.5.1 Pretreatment of LCH

The LCH was pretreated to reduce the containing salts and neutralize the solution. To precipitate sulfates within the lignocellulosic hydrolysate (LCH), 20 g of $CaCO_3$ was added to 1 L. The hydrolysate was thoroughly mixed until complete outgassing of the $CO_2$. Subsequently, the LCH was frozen overnight at -20°C. After defrosting, the LCH was centrifugated at 16000 rcf for 10 minutes. The supernatant was carefully collected for further use. 20 g of $KH_2PO_4$ was added, and the pH was adjusted to 7 with NaOH. The LCH was centrifuged at 16,000 rcf for 10 minutes and subsequently sterile-filtered. The resulting filtrate was then suitable for utilization in cultivation experiments. All LCH utilized for fermentations was pretreated before its addition to the media.

## 3.6 Cultivation on solid media

Solid media on agar plates was used for re-cultivation, selection, or screening. For regular cultivation and screening, YPD media was used with 12 g/L agar. For ATMT IMAS media was used, described in tables 3.7 and 3.8. The plates were usually incubated at 28°C for one to four days and stored at 4-8°C.

**Table 3.2.:** Antibiotic concentration used to select genetically modified *C. oleaginosus* on solid and in liquid media.

| Antibiotic | Resistance gene | Concentration in solid media (µg/mL) | Concentration in liquid media (µg/mL) |
|---|---|---|---|
| Hygromycin B (HygB) | HPH | 70 | 35 |
| Geneticin G418 (Gen) | APH | 50 | 25 |
| Nourseotricin (Nrs) | NAT | 25 | 10 |

## 3.7 Cultivation in liquid media

### 3.7.1 Shake flask cultivation

For initial growth tests, screening, cultivation, and pre-cultures microorganisms were cultivated in shaking flasks. 1/5 of the total flask volume medium was added and the flasks were incubated at 120 rpm. For pre-cultures, growth tests, and screening YPD medium was used. A nitrogen-limited media (NLM), described in table 3.3, was used for lipid analysis. For growth tests on the lignocellulosic hydrolysate (LCH), the LCH (compare table 3.1) was pretreated (3.5.1) and replaced the glucose according to its carbon source content to result in 1% carbon input. A model substrate consisting of 23.2 g/L xylose, 3.4 g/L glucose, and 3.4 g/L acetic acid, short XGA, was used for comparison.

### 3.7.2 24 deep-well-plate cultivation

Screening of *C. oleaginosus* in regard to the growth and lipid composition was performed in 24 deep-well plates (DWPs) instead of shaking flasks to increase the samples throughput. A humidity-enriched shaking system was established with a plastic box containing four shortened 50 mL tubes with 5 mL purified water in each corner of the box and a holding system for max. two 24 DWPs. 2.5 mL media was used in each 10 mL well, and the cultures were inoculated to an OD of 0.1. The incubation was performed inside the humidity-enriched plastic box in an Infors shaking incubator at 28°C and 180 rpm.

## 3.8 Fermentation in Bioreactors

The fermentations were conducted as a fed-batch process, at a pH of 6.5, a temperature of 28°C, and a dissolved oxygen content of 50%. Antifoam 204 (1:10) was used to prevent intensive foaming and added based on a sensor. The stirring velocity was initially set to 200 rpm and then increased to 650 rpm in the first step of the DO cascade. Subsequently, the oxygen ratio was raised from 21% to 100% of the gas supply, and finally, the gas flow rate was increased from 19 - 40 sL/h (DASGIP)

**Table 3.3.:** Nitrogen-limited media for shaking flasks experiments. The resulting C/N ratio is 51.6, with a total carbon intake of 4.21 g and total nitrogen intake of 0.08 g. For some experiments the glucose was replaced with LCH or XGA. n.d. - not defined

| Compound | Molar mass (g/mol) | Concentration (g/L) |
|---|---|---|
| **Carbon sources** | | |
| Glucose | 180 | 10 |
| **Nitrogen sources** | | |
| Urea | 60 | 0.057 |
| **Complex additions** | | |
| Yeast extract | n.d. | 0.5 |
| **Salts** | | |
| $Na_2HPO_4$ | 141 | 0.9 |
| $KH_2PO_4$ | 136 | 2.4 |
| $CaCl_2 \cdot {}_2H_2O$ | 147 | 0.3 |
| $MgSO_4 \cdot {}_7H_2O$ | 246 | 1.5 |
| **Trace elements** | | |
| $FeSO_4 \cdot {}_7H_2O$ | 278 | 0.000027 |
| $CuSO_4 \cdot {}_5H_2O$ | 250 | 0.000025 |
| $ZnSO_4 \cdot {}_7H_2O$ | 288 | 0.00000055 |
| $MnCl_2 \cdot {}_4H_2O$ | 198 | 0.0000242 |
| **Vitamins** | | |
| Thiamin | 337 | 0.0001 |

or 4.75 - 23 sL/h (DASbox). The pH was adjusted with NaOH and acetic acid and before the inoculation, it was raised to pH 8.3 and back to pH 6.5. The p-value for the pump reaction was increased after 24h from 5 to 40.

### 3.8.1 Eppendorf 1 L DASGIP system

The DASGIP® system (Eppendorf AG, Hamburg, Germany) with a total reactor volume of 1.3 L and a maximal working volume of 1 L was employed for the nitrogen-limited and consumption-based (cb) acetic acid fed-batch approaches. In the initial 500 mL medium (Table 3.4), different carbon sources such as LCH, glucose, xylose, or XGA were used, each accounting for 3% of the total content. The nitrogen content was adjusted to achieve a C/N ratio of 15 at the beginning and 65 at the end of the feeding process for the consumption-based approach.

In the case of non-limited cb acetic acid feeding, a 90% acetic acid solution was used for pH regulation. Simultaneously, acetic acid served as feed for the cultivation process. For feeding optimization, the continuous feeding of pretreated and concentrated LCH with a carbon source concentration of 260 g/L, was initiated after 12 hours and maintained at a rate of 10 mL/h and 5 mL/h between 36 and 60 hours. For the combined (co) feeding approach, the consumption-based feed was combined with continuous feeding, utilizing the same medium mentioned above. The C/N ratio was set to 16 at the beginning and reached a maximum of 37 by the end of the fermentation.

**Table 3.4.:** Fermentation media for consumption-based acetic acid fermentations. For some experiments the glucose was replaced with LCH or a model substrate consisting of xylose, glucose, and acetic acid according to the LCH.

| Compound | Molar mass (g/mol) | Concentration (g/L) |
|---|---|---|
| **Carbon sources** | | |
| Glucose | 180 | 30 |
| $CH_3COONa$ | 82 | 4.5 |
| **Nitrogen sources** | | |
| Urea | 60 | 1 |
| **Complex additions** | | |
| Yeast extract | n.d. | 2 |
| Pepton | n.d. | 3 |
| **Salts** | | |
| $Na_2HPO_4$ | 141 | 0.9 |
| $KH_2PO_4$ | 136 | 2.4 |
| $CaCl_2 \cdot 2H_2O$ | 147 | 0.5 |
| $MgSO_4 \cdot 7H_2O$ | 246 | 2 |
| **Trace elemtens** | | |
| $FeSO_4 \cdot 7H_2O$ | 278 | 0.000027 |
| $CuSO_4 \cdot 5H_2O$ | 250 | 0.000025 |
| $ZnSO_4 \cdot 7H_2O$ | 288 | 0.00000055 |
| $MnCl_2 \cdot 4H_2O$ | 198 | 0.0000242 |
| **Vitamins** | | |
| Thiamin | 337 | 0.0001 |

### 3.8.2 Eppendorf 250 mL DASbox system

The feeding strategy was optimized using a DASbox® system (Eppendorf AG, Hamburg, Germany) with a total reactor volume of 350 mL and a maximal working volume of 250 mL. A starting volume of 150 mL medium (Table 3.4) was used. The consumption-based feed consisted of 50% acetic acid and was triggered by the pH increase. For the combined feeding approach, different amounts of LCH were added to 50% (v/v) acetic acid cb-feed, with the two final concentrations of 10% (v/v) and 50% (v/v) LCH. In the continuous feeding method, the feeding rates of pure LCH were set at either 0.5 mL/h or 1 mL/h and initiated 12 hours after inoculation until the maximal working volume was reached.

## 3.9 Genetic engineering of *C. oleaginosus*

### 3.9.1 Genomes

Information about the genome of *C. oleaginosus* was provided by the Genome Data Viewer from NCBI (`https://www.ncbi.nlm.nih.gov/genome/gdv/browser/genome/?id=GCF_001027345.1`) with the genomics and transcriptomics data from [104].

### 3.9.2 Genes and promoter

Endogenous gene and promoter sequences were exported from the genome for *in silico* construction and were amplified from the genomic DNA of *C. oleaginosus* by PCR. For heterologous genes,

the DNA sequences were codon optimized with Geneious Prime (Auckland, New Zealand) to fit the codon usage of *C. oleaginosus*. The sequences were synthesized by Eurofins Genomic GmbH (Ebersberg, Germany).

### 3.9.3 Plasmids

Previously described plasmids were employed from the internal stocks from the Werner Siemens-Chair of Synthetic Biotechnology. New plasmids were constructed by restriction cloning or Gibson assembly method. Table 3.5 lists all plasmids used in this study. Plasmids were constructed based on the `pRF_GAPDHp-HPH` vector described by Görner et al. [86]. Restriction cloning and Gibson assembly were used for the construction of the new plasmids. The exchange of promoters was mainly done by Gibson assembly to prevent unwanted base insertions.

**Table 3.5.:** Plasmids used in this work. Gen, geneticin G418; HygB, hygromycin B; Kana, kanamycin; Nrs, nourseothricin.

| No | Name | Bacterial resistance | Yeast resistance | Application | Reference |
|---|---|---|---|---|---|
| 1 | `pRF_GAPDHp-HPH` | Kana | HygB | Promoter test | [86] |
| 2 | `pRF_D9FADp-HPH` | Kana | HygB | Promoter test | This work [63] |
| 3 | `pRF_UBIp-HPH` | Kana | HygB | Promoter test | This work [63] |
| 4 | `pRF_PPIp-HPH` | Kana | HygB | Promoter test | This work [63] |
| 5 | `pRF_60Sp-HPH` | Kana | HygB | Promoter test | This work [63] |
| 6 | `pRF_PPIp-APH` | Kana | Gen | Marker test | This work [63] |
| 7 | `pRF_PPIp-NAT` | Kana | Nrs | Marker test | This work [63] |

### 3.9.4 Primers

All primers used to construct vectors and sequencing are listed in table 3.6. They were synthesized as double-strand oligo-nucleotides by Eurofins Genomic GmbH (Ebersberg, Germany).

### 3.9.5 *Agrobacterium tumefaciens* mediated transformation

The integration of DNA sequences into the genome of *C. oleaginosus* was accomplished using *Agrobacterium tumefaciens* mediated transformation, following the protocol described by Görner et al. in 2016 [86]. *A. tumefaciens* cells were transformed with the shuttle vector pRF, which harbored the respective genetic construct. The transformation was performed by electroporation, and the transformed cells were selected on LB agar plates supplemented with 30 µg/mL kanamycin. Overnight liquid cultures were prepared from single colonies of the transformed *A. tumefaciens* cells in 5 mL LB medium containing 30 µg/mL kanamycin and incubated with shaking at 28°C. These cultures served as inoculants for 10 mL shaking flasks with IMAS medium (compare tables 3.7 and 3.8) and were incubated at 28°C, 120 rpm for 6 hours. An overnight culture of *C. oleaginosus* in YPD was diluted to an optical density ($OD_{600}$) of 0.5. Subsequently, 50 µl of the *C. oleaginosus* (OD 0.1) and 50 µL of the 6-hour *A. tumefaciens* cultures were mixed. The mixture was plated onto an Amersham Hybond-N+ blotting membrane from GE Healthcare (Chicago, USA), which was placed on top of an IMAS agar plate. The plates were incubated at 24 °C for 48 hours. Following incubation, the membranes were transferred onto YPD agar plates containing elevated

**Table 3.6.:** DNA single strand primers utilized for this work.

| No. | Name | Use | Length | Sequence |
|---|---|---|---|---|
| 1 | pRF_noP_fwd | Constr. pRF_XXp_HPH | 20 | atgaaaaagcctgaactcac |
| 2 | pRF_noP_rev | Construction of pRF_XXp_HPH | 17 | tctagacgtccgcaatg |
| 3 | 60Sp_fwd | Constr. pRF_60Sp_HPH | 33 | cattgcggacgtctagaggcaccggcatcgacg |
| 4 | 60Sp_rev | Constr. pRF_60Sp_HPH | 44 | gagttcaggctttttcatggttagtctggcttctcgaatttctc |
| 5 | PPIp_fwd | Constr. pRF_PPIp_HPH | 33 | cattgcggacgtctagacactatcccccccaccg |
| 6 | PPIp_rev | Constr. pRF_PPIp_HPH | 44 | gagttcaggctttttcattgtaatgaaggagagtgagagtatgg |
| 7 | UBIp_fwd | Constr. pRF_UBIp_HPH | 42 | cattgcggacgtctagactcttctttcttcactctctccatc |
| 8 | UBIp_rev | Constr. pRF_UBIp_HPH | 37 | gagttcaggctttttcattgttgggtgggcaactgttg |
| 9 | D9FADp_fwd | Constr. pRF_D9FADp_HPH | 36 | cattgcggacgtctagacatccatctccctcctccc |
| 10 | D9FADp_rev | Constr. pRF_D9FADp_HPH | 36 | gagttcaggctttttcatgtggcgagatggcctatg |
| 11 | LB_seq_fwd | Sequencing | 21 | gtggtgtaaacaaattgacgc |
| 12 | RB_seq_rev | Sequencing | 23 | ccaatatatcctgtcaaacactg |
| 13 | Gibs-APH_bb_fwd | Constr. pRF_PPIp_APH | 29 | gtttttctgactttctaggttgtagcatg |
| 14 | Gibs-APH_bb_rev | Constr. pRF_PPIp_APH | 29 | ccttacccattgtaatgaaggagagtgag |
| 15 | Gibs-APH_fwd | Constr. pRF_PPIp_APH | 28 | cttcattacaatgggtaaggagaagacc |
| 16 | Gibs-APH_rev | Constr. pRF_PPIp_APH | 28 | acctagaaagtcagaaaaactcgtcgag |
| 17 | NAT_rev | Constr. pRF_PPIp_NAT | 16 | ggggcagggcatggac |
| 18 | NAT_fwd | Constr. pRF_PPIp_NAT | 20 | atgactaccctcgacgacac |

concentrations of the selection antibiotics: 150 µg/mL hygromycin B, 100 µg/mL geneticin G418, 50 µg/mL nourseothricin, or combinations thereof. Additionally, 300 µg/mL cefotaxime was included in the plates to inhibit the growth of *A. tumefaciens*.

After the transformation process, individual colonies were selected from the membrane and streaked onto YPD plates supplemented with 300 µg/mL cefotaxime and the specific antibiotics required for selection: 70 µg/mL hygromycin B, 50 µg/mL geneticin, or 25 µg/mL nourseothricin, or a combination thereof. The plates were then incubated for two to three days until distinct single colonies appeared. Single colonies were picked for cultivation in 5 mL YPD medium supplemented with appropriate concentrations of the antibiotics: 35 µg/mL hygromycin B, 25 µg/mL geneticin G418, 10 µg/mL nourseothricin, or a combination thereof. Transformants capable of growing in liquid cultures were harvested, and genomic DNA was extracted using the Yeast DNA Extraction Kit from Thermo Fisher Scientific™ (Waltham, USA). After PCR amplification of the integrated sequence, the DNA fragments were confirmed by Sanger sequencing at Eurofins Genomics GmbH (Ebersberg, Germany).

**Table 3.7.:** IMAS A media for the *Agrobacterium tumefaciens* mediated transformation. This part was autoclaved and mixed with IMAS B for the complete medium. E.g., 0.5 L medium were prepared with a volume of 400 mL IMAS A and 100 mL IMAS B.

| Compound | End concentration (g/L) | Amount for 0.5 L media (g) |
|---|---|---|
| $K_2HPO_4$ | 2.05 | 1.025 |
| $KH_2PO_4$ | 1.45 | 0.725 |
| NaCl | 0.15 | 0.075 |
| $MgSO_4 \cdot {}_7H_2O$ | 0.5 | 0.25 |
| $FeSO_4 \cdot {}_7H_2O$ | 0.0025 | 0.00125 |
| $(NH_4)_2SO_4$ | 0.5 | 0.25 |
| Glycerol | 5 mL/L | 2.5 mL |
| Agar (only for solid media) | 18 | 9 |

**Table 3.8.:** IMAS B media for the *Agrobacterium tumefaciens* mediated transformation. After preparation, the pH was adjusted to 5.6 with HCl and NaOH and then sterile filtered and mixed with IMAS A for the complete medium. 0.5 L media were prepared with 100 mL IMAS B. Acetosyringone was added immediately before use.

| Compound | End concentration (g/L) | Amount for 0.5 L media (g) |
|---|---|---|
| $CaCl_2$ | 0.06712 | 0.03556 |
| MES | 7.8 | 4.26 |
| Glucose (only for liquid media) | 1.8 | 0.9 |
| Traceelements | 5 mL/L | 2.5 mL |
| Acetosyringone in DMSO | 200 µM | |

# Part III.

# Publications

# 4 Publications

## 4.1 Chapter I: Bioconversion of a Lignocellulosic Hydrolysate to Single Cell Oil for Biofuel Production in a Cost-Efficient Fermentation Process

### 4.1.1 Summary

*The article 'Bioconversion of a Lignocellulosic Hydrolysate to Single Cell Oil for Biofuel Production in a Cost-Efficient Fermentation Process' was published in MDPI Fermentation in February 2023 (https://doi.org/10.3390/fermentation9020189). The authors Zora S. Rerop and Nikolaus I. Stellner contributed equally to this publication. The pretreatment and media formulation was done in close collaboration, as well as the conceptual design, the fermentations, and the feed optimizations. The candidate worked explicitly on data analysis, statistics, and visualization.*

Vegetable oils derived from large-scale monocultures are considered renewable resources; however, they come with several drawbacks. These include extensive land usage, the utilization of pesticides, diminished biodiversity, and frequently the destruction of vast areas of rainforests. Conversely, industrial waste and by-products are often burned or discarded, resulting in the loss of potential carbon sources. A solution to both of these issues lies in the production of single-cell oil from industrial waste streams using the oleaginous yeast *Cutaneotrichosporon oleaginosus* (ATCC 20509). This non-conventional yeast is a highly efficient single-cell oil producer and can be used to metabolize hexoses, pentoses, and organic acids from a wide range of hydrolysates.

In this study, a lignocellulosic hydrolysate (LCH) obtained from a pulping process for cellulose fiber production was used as the starting material for a media formulation suitable for single-cell oil production with *C. oleaginosus*. The hydrolysate was initially analyzed to identify its sugar composition, primarily xylose, lignols, lignans, organic acids as well as sulfuric acids. A chemical pretreatment strategy was developed, including salt removal and neutralization. The pretreated LCH was then formulated into a suitable fermentation medium by adjusting the carbon concentration and adding buffers, salts, trace elements, and nitrogen sources. In a fed-batch fermentation with a consumption-based acetic acid feed, the compounds of the LCH were converted into lipids and biomass. After 40 hours of the 72-hour fermentation, most of the sugars had been consumed. In comparison to the control condition with the model substrate, the hydrolysate fermentation yielded significantly increased biomass and lipid, reaching 55.73 ± 5.20 g/L biomass and 42.1 ± 1.7 g/L lipid (equivalent to 75.5% lipid per biomass). To further optimize the process and maximize LCH uptake, a hybrid approach combining consumption-based and continuous feeding methods

was employed. In addition, a subsequent techno-economic analysis indicated a significant 26% reduction in production costs when using LCH instead of commercial glucose.

In summary, we have successfully developed a comprehensive process that effectively converts pentose-rich industrial waste into valuable single-cell oils. With the achieved high lipid titers, this process shows great potential as an economically viable and industrially relevant process in the future.

### 4.1.2 Full-length publication

*fermentation*

MDPI

*Article*

# Bioconversion of a Lignocellulosic Hydrolysate to Single Cell Oil for Biofuel Production in a Cost-Efficient Fermentation Process

**Zora S. Rerop †, Nikolaus I. Stellner †, Petra Graban, Martina Haack, Norbert Mehlmer, Mahmoud Masri * and Thomas B. Brück ***

Werner Siemens-Chair of Synthetic Biotechnology, School of Natural Sciences, Technical University of Munich, Lichtenbergstraße 4, 85748 Garching bei München, Germany

* Correspondence: mahmoud.masri@tum.de (M.M.); brueck@tum.de (T.B.B.)

† These authors contributed equally to this work.

**Abstract:** *Cutaneotrichosporon oleaginosus* is a highly efficient single cell oil producer, which in addition to hexoses and pentoses can metabolize organic acids. In this study, fed-batch cultivation with consumption-based acetic acid feeding was further developed to integrate the transformation of an industrial paper mill lignocellulosic hydrolysate (LCH) into yeast oil. Employing pentose-rich LCH as a carbon source instead of glucose significantly improved both biomass formation and lipid titer, reaching 55.73 ± 5.20 g/L and 42.1 ± 1.7 g/L (75.5% lipid per biomass), respectively. This hybrid approach of using acetic acid and LCH in one process was further optimized to increase the share of bioavailable carbon from LCH using a combination of consumption-based and continuous feeding. Finally, the techno-economic analysis revealed a 26% cost reduction when using LCH instead of commercial glucose. In summary, we developed a process leading to a holistic approach to valorizing a pentose-rich industrial waste by converting it into oleochemicals.

**Keywords:** fermentation; biotransformations; lipids; single cell oil; biofuel; techno-economic analysis; waste valorization; lignocellulosic hydrolysate; oleaginous yeast



**Citation:** Rerop, Z.S.; Stellner, N.I.; Graban, P.; Haack, M.; Mehlmer, N.; Masri, M.; Brück, T.B. Bioconversion of a Lignocellulosic Hydrolysate to Single Cell Oil for Biofuel Production in a Cost-Efficient Fermentation Process. *Fermentation* **2023**, *9*, 189. https://doi.org/10.3390/fermentation9020189

Academic Editor: Timothy Tse

Received: 6 February 2023
Revised: 15 February 2023
Accepted: 16 February 2023
Published: 18 February 2023



## 1. Introduction

The global energy system is responsible for more than 75% of greenhouse gas (GHG) emissions since it depends primarily on fossil fuels [1]. These emissions accelerate global warming, which impacts our environment, threatens our biodiversity, increases the frequency and intensity of extreme weather events, and damages our economy [2]. In response to these challenges, the UN calls for sustainable and innovative short- and long-term strategies to diversify energy sourcing, accelerate the clean energy transition, and achieve net-zero emissions by 2050 [3,4]. This energy transition demands large-scale deployment of renewable energy sources, such as sustainable advanced biofuels. Furthermore, integrating the up-cycling and end-of-life recycling of urban, agricultural, and industrial wastes into supply chains is a value-adding strategy directed toward the implementation within a truly circular economy. According to the EU's long-term measurement, combining all these approaches can reduce net emissions by around 80% [5]. Such sustainable energy concepts would also reduce dependence on limited resources and disrupted supply chains, the latter of which could be observed during the COVID-19 pandemic. Current biofuel production faces climatic, environmental, and social problems. It relies on globally traded feedstock, such as plant oil or used cooking oil (UCO) [6,7]. The large-scale production of plant oil-based biofuel results in a significant increase in problematic monocultures, increased land use, deforestation, and food competition [6,8–10]. In this respect, biofuel production from domestic biomass waste streams could help lower the external energy dependence

of communities, reduce greenhouse emissions, provide energy storage capability, and implement an efficient route to a circular treatment of waste [8,11].

Oleaginous microorganisms such as the yeast *Cutaneotrichosporon oleaginosus* (ATCC 20509) can utilize these waste streams to produce single cell oil (SCO) as a starting material for advanced biofuel production. As opposed to growing crops for plant oil production, the cultivation of microorganisms is seasonally independent, and biotechnological processes allow for high area efficiency due to vertical scale-up [12,13]. *C. oleaginosus* is one of the most promising oleaginous microorganisms for the production of SCOs as it has been shown to utilize monomers from cellulose, chitin, lignin, and hemicellulose, the most abundant biopolymers on earth [14–16]. The oleaginous yeast displays an excellent ability to grow to very high cell density and to accumulate plant-oil-like lipids with up to 85% of the dry cell weight [8,17]. Moreover, *C. oleaginosus* has a unique ability to simultaneously uptake hexose and pentose sugars, as well as acetic acid, and not follow a typical diauxic cell growth [17]. Furthermore, it shows a high tolerance to inhibitory compounds, such as furans or lignin-derived compounds, such as coumarat and resorcinol, which are major components of depolymerized lignin [15,18,19]. When employed as a high proportion of the carbon source, acetic acid was reported as suitable for *C. oleaginosus*, resulting in high lipid contents of up to 73% but also low biomass generation of only up to 6 g/L [20,21]. Recently, a fermentation process utilizing acetic acid for the cost-efficient production of SCOs with *C. oleaginosus* at high yields was reported [17]. As opposed to other approaches, pure acetic acid was fed to the culture in a consumption-based manner after adding glucose as a starting sugar. To date, this is the process with the highest outcome of SCO, integrating acetic acid as feedstock and using *C. oleaginosus*. Overall, this unconventional yeast is a promising host for the industrial production of SCO as it is efficient, robust, and capable of metabolizing a diverse range of substrates.

The pulp and paper industry is one of the major producers of waste streams, with a high share of biodegradable carbon [22]. The global production of pulp and paper was 188.9 million metric tons in 2020 [23]. Considering that only 30–40% of wood biomass is recovered as cellulose fibers, huge amounts of residual waste are produced. In Europe alone, the pulp and paper industry produces around 11 million tons of waste every year [24]. One of the main processes of pulp production, besides alkaline kraft pulping, is acidic sulfite pulping combined with steam explosion to hydrolyze the plant cells and lignocellulose compounds and separate the valuable cellulose fibers [25]. The pulping waste stream from this process contains high amounts of sugars from hemicellulose (mainly xylose), breakdown compounds from lignin (lignols and lignans), aliphatic carboxylic acids (mainly acetic acid), and furans (mainly furfural and hydroxymethylfurfural) [26,27]. In most industrial plants, the waste stream is heavily concentrated, and the acetic acid therein is evaporated and separated from the rest [28]. To the current date, the released acetic acid is only collected in exceptional cases, such as by the Lenzing AG in Austria [29]. So far, direct combustion for energy production or passing the material into the wastewater is the common strategy to deal with the highly toxic furans, acetic acid, and lignin-derived compounds [30–33]. For these waste streams, specifically for lignin, xylose, and acetic acid, there are no established recovery or valorization systems. However, different lignocellulosic hydrolysates from agriculture residues, such as wheat straw, corn stover, or switch grass, have been applied to produce bioethanol with bacteria or yeasts [34]. Corn steep liquor has been used as a feedstock for lipid production with genetically modified *Rhodosporidium toruloides*, reaching a top-level lipid titer of 39.5 g/L (0.179 g/g yield per sugar) [35]. Moreover, some pilot and demonstration plants have used hard and soft wood chips to produce second-generation bioethanol [36]. Nonetheless, it is important to note that all these examples utilized a lignocellulosic feedstock with a focus on its glucose content, not the pentose sugars or the lignin breakdown products.

For the first time, this study provides an approach for the up-cycling of a crude lignocellulosic hydrolysate, focusing mainly on the valorization of xylose, acetic acid, and lignin-derived compounds. To the best of our knowledge, the fermentative utilization

of a lignocellulosic-rich waste stream directly from a pulping mill and without most of the cellulose and its monomers has never been reported. From this hydrolysate, plant oil-like SCO was produced as a potential domestic feedstock for biofuel or other industrial applications. The current work includes a comprehensive analysis of the hydrolysate, the development of a cost-efficient pretreatment step, and a highly efficient fermentation strategy with the oleaginous yeast *C. oleaginous*. Moreover, the economic viability of the developed process was assessed by a comprehensive techno-economic analysis (TEA).

## 2. Materials and Methods

### *2.1. Analysis of Lignocellulosic Hydrolysate*

#### 2.1.1. Sugar Analysis

The sugars and short organic acids were analyzed with high-performance liquid chromatography (HPLC). All the samples were filtered with a 10 kDa filter. The Agilent 1260 Infinity II LC system with Diode Array (DA) and Refractive Index (RI) detectors was used. For separation, a column Rezex ROA-organic H+ 8% from Phenomenex was used with a mobile phase of 5 mM $H_2SO_4$. An isocratic flow of 0.5 mL/min was applied over 60 min with an oven temperature of 70 °C. The detection in the RID was carried out at 40 °C.

#### 2.1.2. Ash

A neutralized and lyophilized lignocellulose hydrolysate of 2 to 4 g was burned at 1000 °C for 3 h to ash. The amount was determined gravimetrically after cooling overnight in a desiccator.

#### 2.1.3. Elemental Analysis

Elemental analysis was carried out with a Euro EA CHNS elemental analyzer (HEKAtech Ltd., Wegberg, Germany). Dynamic spontaneous combustion in a tin boat at approximately 1800 °C was performed with subsequent gas chromatographic separation and was detected using a thermal conductivity detector (TCD).

#### 2.1.4. Quantification of Sulfates

The quantification of sulfates in the hydrolysate was performed chemically with treatment with $CaCO_3$ and $BaCl_2$. The resulting $BaSO_4$ precipitate was quantified gravimetrically.

### *2.2. Strain and Media Composition*

#### 2.2.1. Strain

The oleaginous yeast *Cutaneotrichosporon oleaginosus* ATCC 20509 (DSM-11815), supplied by the Deutsche Sammlung von Mikroorganismen und Zellkultur (DMSZ, Braunschweig, Germany), was used for all cultivation and fermentation experiments.

#### 2.2.2. Pretreatment of the Lignocellulosic Hydrolysate

For the precipitation of sulfates within the hydrolysate, 20 g of $CaCO_3$ was added to 1 L of lignocellulosic hydrolysate (LCH) in a 5 L beaker while constantly stirring. The hydrolysate was mixed until the complete outgassing of $CO_2$. Next, the LCH was frozen at −20 °C overnight. After defrosting, the LCH was centrifuged at 16000 rcf for 10 min and the supernatant was collected. Twenty grams of $KH_2PO_4$ was added to the remaining liquid for the removal of excess calcium, and the pH was adjusted with 3 M NaOH to 7. The LCH was centrifuged at 16000 rcf for 10 min and sterile-filtered to be used in the cultivation experiments. All the LCH used for the fermentations was pretreated before its addition to the media.

#### 2.2.3. Pre-Culture

Fifty milliliters of YPD medium (10 g/L yeast extract, 20 g/L peptone, and 20 g/L glucose) in an Erlenmeyer flask containing antibiotics (0.05 g/L kanamycin and 0.1 g/L

ampicillin) was inoculated with a single colony of *C. oleaginosus* (ATCC 20509) from a YPD plate. Antibiotics in fermentation pre-cultures were added to prevent contaminations. The flasks were incubated at 28 °C under constant shaking at 120 rpm for 2 days.

#### 2.2.4. Medium Composition for Bioreactor Cultivation

Different media were used for either nitrogen limitation or consumption-based cultivation with acetic acid. The base medium was composed of 0.9 g/L $Na_2HPO_4$, 2.4 g/L $KH_2PO_4$, 4.5 g/L $CH_3COO{\cdot}Na$, 2 g/L $MgSO_4{\cdot}7H_2O$, 0.5 $CaCl_2{\cdot}2H_2O$, 0.00055 mg/L $ZnSO_4{\cdot}7H_2O$, 0.024 mg/L $MnCl_2{\cdot}6H_2O$, 0.025 mg/L $CuSO_4\ {\cdot}5H_2O$, 0.027 mg/L $C_6H_8O_7{\cdot}Fe{\cdot}H_3N$, 1 g/L urea, 3 g/L peptone, and 2 g/L yeast extract. For nitrogen limitation, the medium above was adjusted to 1.74 g/L urea, 0.5 g/L yeast extract, and no peptone and $CH_3COO{\cdot}Na$. The C/N ratio was calculated based on the elemental carbon and nitrogen content, using the information provided by the suppliers of the chemicals. As carbon sources, either glucose, pretreated LCH, or a mix of xylose, glucose, and acetic acid (XGA) was used.

### *2.3. Fermentation*

#### 2.3.1. Fermentation in 1.3 L Bioreactor

The fermentations were carried out at pH 6.5, at 28 °C, and with a dissolved oxygen content of 50% in a fed-batch process. For the nitrogen-limited and consumption-based acetic acid approaches, a scale of 1 L maximal working volume in the DASGIP® system (Eppendorf AG, Hamburg, Germany) with a total reactor volume of 1.3 L was utilized. In the 500 mL starting medium, the sugar content of 3% from either LCH, glucose, xylose, or XGA was used. The nitrogen content was adjusted to accomplish a C/N ratio of 15 at the start and 65 at the end of the feeding. Pretreated pure and concentrated LCH or XGA with a carbon source content of 260 g/L was continuously fed, starting after 12 h, at a rate of 10 mL/h and 5 mL/h between 36 and 60 h. For non-limited consumption-based (cb) acetic acid feeding, a feed of 90% acetic acid solution was used for the pH regulation. At the same time, the acetic acid functioned as feed for the cultivation. For the combined (co) feeding, the cb-feed was combined with a continuous feed, with the medium mentioned above and a C/N ratio of 16 at the start and a maximum of 37 at the end of the fermentation.

#### 2.3.2. Fermentation in 350 mL Bioreactor

The feeding strategy optimization was performed in a maximal working volume of 250 mL in the DasBOX® system (Eppendorf AG, Hamburg, Germany) with a 350 mL total reactor volume. Fifty percent acetic acid was used as consumption-based feed, controlled by the pH change. In the combined feeding condition, LCH was added to 50% (*v*/*v*) acetic acid to a final concentration of either 10% (*v*/*v*) and 50% (*v*/*v*) (50:10 and 50:50 mix of acetic acid:LCH). In the case of continuous feeding, the feeding rates were either 0.5 mL/h or 1 mL/h, starting from 12 h after inoculation, by maintaining a consumption-based acetic acid feed with 50% acetic acid.

### *2.4. Monitoring of Fermentation*

#### 2.4.1. $OD_{600}$ Measurement

Cell growth was monitored by measuring the optical density at 600 nm ($OD_{600}$). The samples were diluted in the respective cultivation media to an $OD_{600}$ between 0.1 and 1.

#### 2.4.2. Dry Weight

The dry weight of the substrate solutions and biomass samples was determined gravimetrically. To measure the dry cell weight, 4 mL of fermentation culture was transferred to pre-weighed reaction tubes, centrifuged (4500 rcf, 20 min), and washed two times with an equal amount of purified water or 50% ethanol in the case of lipid-rich cells. Alternatively, 0.5 mL of a lipid-rich culture was filtered through a pre-weighed 0.2 µm filter paper and washed three times with 2 mL water. The samples were frozen and lyophilized. For each biological replicate, the technical duplicates at least were measured. Growth curve fitting

was performed by the Gompertz function, as shown in Equation (1); here, A is the upper asymptote, $k_G$ is the growth-rate coefficient, and $T_i$ is the time of inflection [37].

$$W(t) = A \times \exp(-\exp(-k_G(t - T_i))) \quad (1)$$

2.4.3. Lipid Content

For the lipid content analysis, the cells from the fermentation were centrifuged and washed two times with 50% ethanol and resolved in water. The cells were disrupted mechanically with a High-Pressure Homogenizer Type HPL6 from Maximator. Triplicates of the 7 mL disrupted cell solution were frozen and lyophilized. The chloroform-methanol lipid extraction was carried out after modifying with the Bligh and Dyer method [38]. Briefly, 100–200 mg biomass was weighed in a glass tube, and 4 mL $Cl_3CH$: methanol (2:1) and and 1 mL $H_2O$ (0.58% NaOH) were added. After 60 min shaking at 120 rpm, it was centrifuged for 10 min at 2000 rcf, and the bottom layer was transferred to a new glass tube. An additional 3 mL $Cl_3CH$: methanol (2:1) was added to the upper phase in the first tube and quickly mixed. After centrifugation, the bottom layer was combined with the lower phase from the first extraction step, and 2 mL of $H_2O$ (0.58% NaOH): methanol (1:1) was added. After mixing and centrifugation, the bottom phase was transferred to a fresh pre-weighed glass tube, and the solvents were evaporated under a nitrogen flow. The lipid amount was determined gravimetrically.

2.4.4. Fatty Acid Profile

The fatty acid profile was measured through gas chromatography. Therefore, fatty acid methyl esterification (FAME) of the lyophilized cells was performed; the biomass was not washed, to avoid the loss of very fat cells. Three to ten milligrams of the biomass was weighed in glass vials; all further steps were automated with the Multi-Purpose Sampler MPS robotic from Gerstel. An internal standard of 10 g/L C19 TAG in toluene was used for quantification. First, 490 µL toluene and 10 µL internal standard were added and mixed for 1 min at 1000 rpm, followed by the addition of 1 mL 0.5 M sodium methoxide in methanol, and the solution was heated to 80 °C and shaken at 750 rpm for 20 min. After cooling to 5 °C, 1 mL of 5% HCl in methanol was added, and the mixture was heated to 80 °C while shaking at 800 rpm for 20 min and cooled to 5 °C afterwards. Four hundred microliters of de-ionized $H_2O$ was added and mixed for 30 s at 1000 rpm before 1 mL hexane was added. Extraction was performed by shaking three times for 20 s at 2000 rpm in a quickMix device. The samples were centrifuged for 3 min at 1000 rpm and cooled at 5 °C before a 200 µL sample of the organic phase was transferred to a 1.5 mL vial for chromatography. Gas chromatograph flame ionization detection (GC-FID) was used to quantify the fatty acids. GC-MS was carried out to identify the acids, with the TRACE™ Ultra Gas Chromatograph from Thermo Scientific coupled to a Thermo DSQ™ II mass spectrometer and a Triplus™ Autosampler injector in positive ion mode. A Stabilwax® fused silica capillary column (30 m × 0.25 mm, film thickness 0.25 µm) was used for separation. The temperature profile for the analysis was set to an initial column temperature of 50 °C, increasing at a rate of 4 °C/min up to a final temperature of 250 °C. Hydrogen was used as a carrier gas at a constant flow rate of 35 mL/min. Standardization was performed with the FAMEs Marine Oil Standard (20 components, from C14:0 to C24:1).

2.4.5. Statistical Analysis

For statistical analysis of the significant differences in the analysis outcomes, first an ANOVA test was performed. When the ANOVA test showed a test value of $p < 0.001$, and thereby indicated a significant difference, in the next step a Duncan test was applied. The Duncan tests were performed with a test value of $p < 0.01$, and they detected differences and similarities between the test conditions by grouping the results.

### *2.5. Techno-Economic Analysis*

To estimate the total capital investment and operation cost for the production of oil from LCH using *C. oleaginosus*, a techno-economic analysis (TEA) was performed. The process was designed with a consequential approach in silico, according to previous laboratory results and available data from the literature [39]. SuperPro Designer (SPD) version 10 (Intelligen, Inc., Scotch Plains, NJ, USA) was used, and the functions describing the biochemical processes were integrated [39]. In the process simulation, a production plant was created with a lipid production capacity of 0.81 metric tons per hour (t/h). The feedstock requirements and the chemicals needed for the LCH pretreatment were estimated based on the media components used in the current work. The mathematical equations and parameters for simulating yeast biomass generation, lipid formation, and enzymatic hydrolysis were based on the results generated in this work or previous experiments [17]. To calculate energy balance, equipment sizing, and purchasing prices, the values from the SPD database were completed with publicly available current prices and data from the literature. The in silico plant featured several operations for LCH pretreatment, fermentation, and downstream processing, including recovery of SCO and recycling of waste streams and side products. The list of modules used in the SPD for the different fermentation conditions (glucose and LCH with acetic acid co-feeding and combination of continuous and consumption-based feeding) is included in the supplements. Lipid productivity was deduced from the lipid titers from the fermentations performed in the 1 L DASGIP® system after 71 h.

$$\text{Lipid productivity (g/L/h)} = \text{lipid titer (g/L)/time (h)} \quad (2)$$

The lipid productivities were calculated for three conditions: glucose with acetic acid co-feeding, LCH with acetic acid co-feeding, and the combination of continuous feed and consumption-based acetic acid co-feeding. The equipment purchase cost (PC) was calculated with an internal SPD function based on the size of the equipment. The installation cost factors relative to the PC were included with values between 1.1 and 1.3 [40]. The cost factors for storage (4%), piping (9%), and site development (5%) were included [41]. The indirect capital costs consisted of insurance (5%), field expenses (5%), construction (10%), contingency (10%), and other expenses (10%). Capital interest was included as 6% of the total investment. Utility and labor costs, as well as waste disposal, were estimated based on the current prices in Germany [42]. The costs for consumables and raw materials were set according to current market prices. Maintenance and insurance were included as faculty-dependent costs at 3% and 0.7% [41].

## 3. Results

### *3.1. Analysis of the Lignocellulosic Hydrolysate*

The lignocellulosic hydrolysate (LCH), coming from the spent liquor of the pulping process, was comprehensively analyzed to gain a better understanding of its composition and to set up a pretreatment strategy. The pH was 1.7, with a dry mass of 247.7 ± 13.9 g/L and a high sulfate content of 19.4 ± 2.0 g/L. HPLC analysis was used to quantify the sugar, organic acids, and furans. It showed that the primary sugar of the hydrolysate was xylose, with 77.05 ± 2.46 g/L, and smaller amounts of other sugars, such as glucose (11.51 ± 0.39 g/L), mannose (8.21 ± 0.84 g/L), galactose (6.47 ± 0.21 g/L), and others (12.37 ± 1.10 g/L), resulting in a total sugar content of 115.60 ± 4.99 g/L. The organic acids had a total concentration of 16.83 ± 1.43 g/L, acetic acid being the major one with 12.34 ± 1.20 g/L. A considerable amount of hydroxymethylfurfural (HMF), with 4.53 ± 0.59 g/L, and furfural, with 0.68 ± 0.04 g/L, was detected. The hydrolysate is a waste stream from the industrial production of cellulose fibers using hardwood as a source material in an acidic sulfite pulping process. The chemical hydrolysis of lignocellulose results in the detected sugar monomers, organic acids, and breakdown compounds from lignin. The total ash was 0.70 ± 0.01 g/L, with low concentrations of phosphorus (0.035 g/L) and no detectable nitrogen. The rest of the material derives from lignols and

lignans as well as other plant metabolites, resulting in a total amount of 89.95 ± 22.97 g/L. Table S1 gives a summarized overview of the composition.

### *3.2. Pretreatment of the Lignocellulosic Hydrolysate*

To transform the waste stream LCH into a suitable carbon source for yeast fermentation, the challenges of low pH and the lack of essential nutrients needed to be addressed with a suitable pretreatment strategy. However, the formation of insoluble particles was observed after the addition of the other medium compounds such as buffering salts, vitamins, nitrogen, and trace elements, as well as during the cultivation. To address this problem, some simple pretreatment steps were taken. As a result of the chemical hydrolysis from the industrial pulping process, the LCH has a high sulfate content and a highly acidic pH. To reduce the amount of residual sulfate, overliming was performed using $CaCO_3$. Nevertheless, particle formation could still be observed. Titration of the overlimed LCH with $H_2PO_4^-$ or $HPO_4^{2-}$ salts was empirically found to prevent this particle formation. As this process still results in an acidic pH, a final neutralization with NaOH was performed after the $KH_2PO_4$ treatment. The details of the different tested pretreatment conditions are provided in the Table S2. The reduction in the overall bioavailable carbon by the pretreatment (159.85 ± 2.80 g/L) was negligible compared to the starting material (162.05 ± 1.44 g/L). This qualifies the LCH pretreatment as a suitable step in the preparation of the waste stream as a carbon source for bioreactor fermentations. This optimized pretreatment strategy was applied to all the LCH used for fermentation in this study.

### *3.3. Nitrogen-Limited Fermentation*

Fermentation under nutrient limitation, such as with phosphate or nitrogen, is a common strategy to trigger lipid accumulation in oleaginous yeast [43]. Therefore, nitrogen-limited fermentation was performed using LCH as a carbon source (Figure 1a). To understand the effect of the lignocellulose-derived compound on the yeast metabolism, a further control medium was composed. The control medium contained only the main sugars from the LCH in their respective ratios: xylose (8.28%), glucose (1.03%), and acetic acid (0.69%), and it is therefore abbreviated with xylose, glucose, and acetic acid (XGA). The fermentations resulted in a biomass formation of 7.02 ± 0.88 g/L and 16.65 ± 0.24 g/L for LCH and XGA, respectively, showing better growth performance on the XGA medium.

### *3.4. Acetic Acid-Based Fermentation with Commercial Sugars as Carbon Source*

The successful production of SCO from refined sugars with acetic acid-based fermentation was shown previously [17]. In this work, LCH was integrated as a carbon source for fed-batch fermentation with consumption-based acetic acid feeding. As controls, glucose and xylose, as well as the XGA mix, as starting sugars were tested. The analysis showed that the concentration of acetic acid remained constant due to the consumption-based feeding; the sugars were consumed within the first 40 h after inoculation, as shown in Figure 1b–d. The biomass increased further after the full consumption of the sugar and reached 35.11 ± 1.11 g/L, 39.95 ± 4.59 g/L, and 39.00 ± 0.76 g/L for glucose, xylose, and XGA by 71 h, with lipid titers of 18.5 ± 3.6 g/L, 23.6 ± 0.5 g/L, and 21.6 ± 2.8 g/L for glucose, xylose, and XGA, respectively (Figure 2a). The same applied to the carbon-to-lipid conversion yield of lipid carbon from substrate carbon, which was 0.204 ± 0.003 g/g, 0.230 ± 0.001 g/g, and 0.235 ± 0.001 g/g for glucose, xylose, and XGA, respectively (Figure 2b). The fatty acid profile of the oil is shown in Figure 2c; the most abundant fatty acid was C18:1 with around 54%, followed by C16:0 (~24%), 18:0 (~15%), and C18:2 (~6%) and by traces of C18:3, C16:1, and C22:0 with less than 0.3% each.

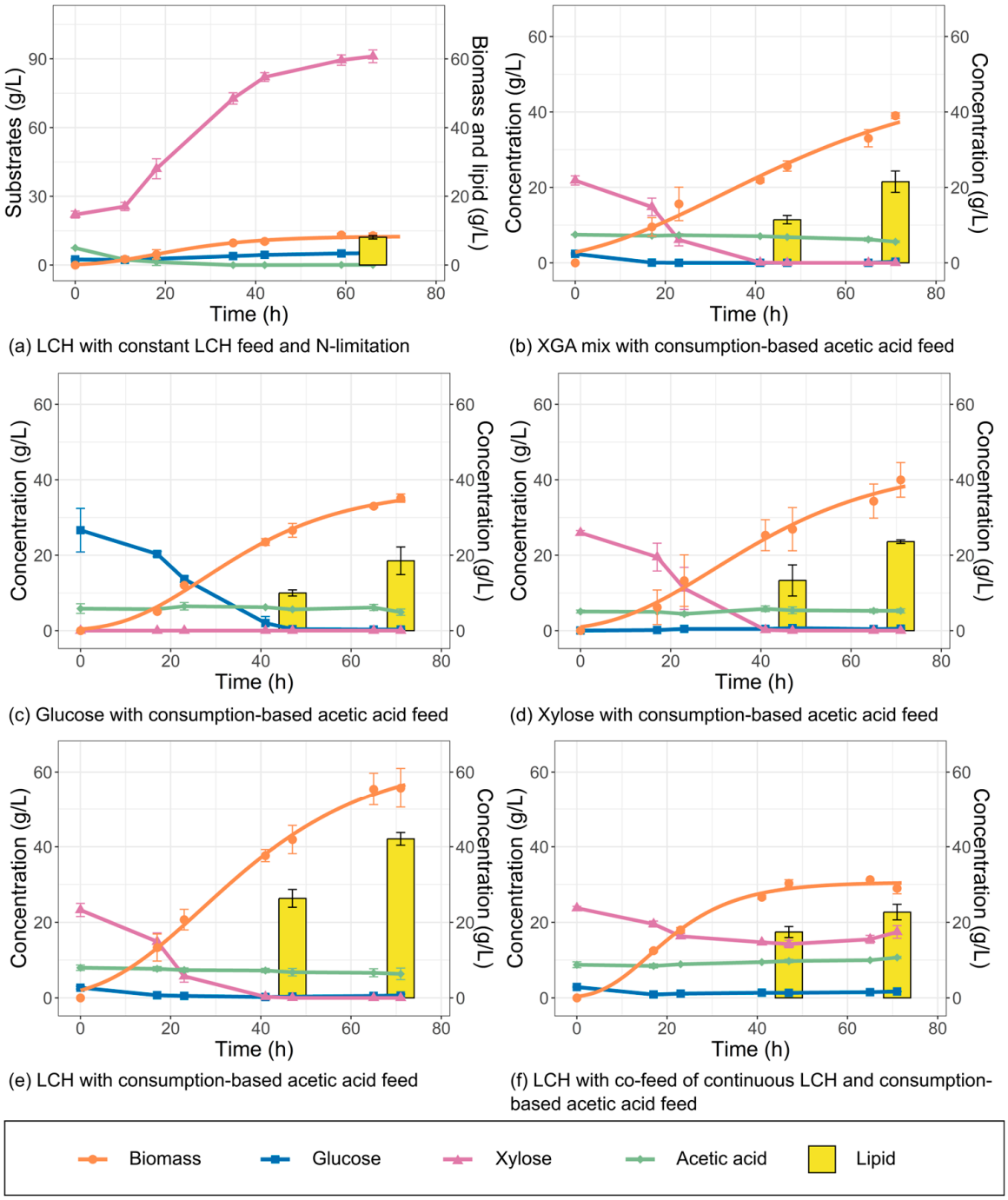


**Figure 1.** Biomass, substrate—namely glucose, xylose, and acetic acid—concentration, and lipid titer for different fermentation conditions. (**a**) LCH with constant feed and N-limitation; (**b**) XGA mix with consumption-based acetic acid feed; (**c**) Glucose with consumption-based acetic acid feed; (**d**) Xylose with consumption-based acetic acid feed; (**e**) LCH with consumption-based acetic acid feed; (**f**) LCH with co-feed of continuous LCH and consumption-based acetic acid feed. Fermentations were performed in triplicates (except for glucose and xylose, which were performed in duplicates). Error bars display two times the standard deviation. LCH—lignocellulosic hydrolysate, XGA—xylose, glucose, and acetic acid mix as model substrate.

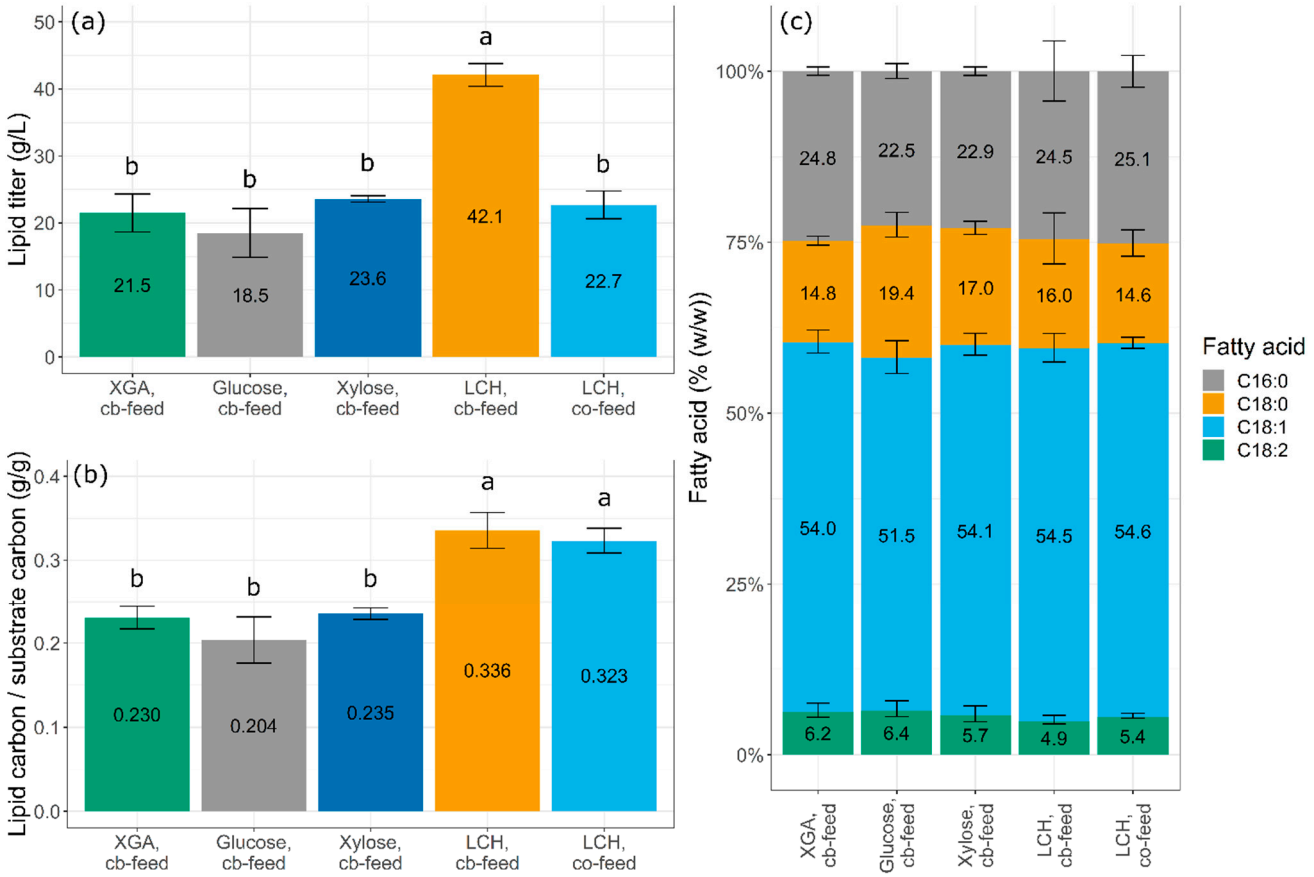


**Figure 2.** Lipid analysis of the four most important fermentation conditions. (**a**) Lipid titers after 71 h fermentation in 1 L scale. (**b**) Carbon conversion yield from substrate carbon to lipid carbon. (**c**) fatty acid profile of the main fatty acids quantified with GC-FID. Error bars display two times standard deviation; Duncan tests were performed with $p < 0.01$ to determine statistical groups a and b for lipid titer and carbon conversion, Duncan results for the fatty acid profile are shown in the Table S3. cb-feed—consumption-based acetic acid feed; LCH—lignocellulosic hydrolysate; LCH co-feed—lignocellulosic hydrolysate as starting carbon, and constant feed with cb-feed.

### *3.5. Acetic Acid-Based Fermentation of Lignocellulosic Hydrolysate at Different Starting Concentrations*

The LCH used in this study is the spent liquor from acidic hardwood pulping, containing sugars, mainly xylose, as well as acetic acid. LCH further contains furans and lignin breakdown products that can have an inhibitory effect on microorganisms. To assess the optimal balance between carbon supply and the toxic level of inhibitory compounds, fermentations with three different starting concentrations of LCH were performed. The amount of hydrolysate corresponded to the concentrations of 3%, 5%, and 7% of the bioavailable carbon in the starting medium. The fermentation with the highest LCH concentration of 7% showed a slower overall growth with a growth-rate coefficient of 1.21 compared with 1.33 for 3%. The dry biomass formations were 39.64 ± 6.30 g/L and 51.92 ± 0.18 g/L for 7% and 5%, compared to 55.73 ± 5.20 g/L in the case of 3%. Accordingly, an increase in the concentration to 5% resulted in a slightly longer lag phase and a slightly lower biomass accumulation after three days of fermentation. The lipid titer was lower for 7% LCH (19.83 ± 1.38 g/L) and 5% (25.75 ± 2.02 g/L) and much higher for 3% (42.1 ± 1.7 g/L). The starting carbon source concentration of 3% resulted in the shortest lag phase, the best growth rate, and the overall biomass formation, as shown in Figure S1.

### *3.6. Acetic Acid-Based Fermentation on Lignocellulosic Hydrolysate with Optimized Conditions*

The optimized conditions for the fed-batch fermentation of *C. oleaginosus* on LCH were carried out in three biological replicates. The starting carbon content of the hydrolysate corresponding to 3% sugar and acetic acid was used. A high biomass formation of 55.73 ± 5.20 g/L was achieved after 71 h, which is a seven-fold increase compared to the nitrogen-limited fermentation of LCH. Moreover, the biomass formation was about 50% higher with LCH as a carbon source compared to glucose or xylose under equivalent reaction conditions (Figure 1b,c). However, the sugar consumption showed a similar profile to that of the fermentation processes using sole sugars. The lipid titer after 71 h was, with 42.1 ± 1.7 g/L (lipid productivity 0.593 g/L/h), twice as high as that from the glucose fermentation (18.5 ± 3.6 g/L, productivity 0.261 g/L/h) (Figure 2a). The carbon conversion was 0.336 g/g lipid carbon from substrate carbon (Figure 2b) with 76.05 ± 9.04% lipid per dry biomass. The fatty acid profile did not show significant changes compared to the lipid profile of the fermentation on xylose or XGA and slight changes compared to the fermentation on glucose (Figure 2c and Table S3).

Furthermore, lignin breakdown products were shown to be metabolized by *C. oleaginosus*, in a range of 91.6% of the initial compound amount (Figure S2 and Table S4).

### *3.7. Screening of Different Strategies for Feeding Lignocellulosic Hydrolysate*

In several fermentation approaches, the combined feeding of a mix of LCH and acetic were tested. The biomass of the cells fed with a 50:10 (50% acetic acid, 10% LCH, 40% purified water) and a 50:50 (50% acetic acid, 50% LCH) mix of acetic acid:LCH were 51.5 ± 3.7 g/L and 59.6 ± 1.2 g/L. Those solely fed with acetic acid after 65 h (50.8 ± 0.1 g/L), with 50:50 co-feeding, resulted in the highest biomass (Figure 3). The lipid titers after 65 h were 28.4 ± 0.4 g/L and 30.4 ± 1.4 g/L for the 50:10 and 50:50 feeding, respectively, while 25.2 ± 3.1 g/L was measured for the control settings (Figure 3). As an alternative feeding strategy, the pure pretreated LCH was continuously fed into the reactor throughout the fermentation process at two feeding rates: 0.5 mL/h or 1 mL/h, in addition to the consumption-based feeding of acetic acid. The dry biomass accumulated after 65 h was 50.4 ± 2.2 g/L and 50.4 ± 4.6 g/L for 0.5 mL/h and 1 mL/h, respectively. The maximum lipid titers were 0.5 ± 2.4 g/L for 0.5 mL/h and 26.3 ± 2.7 g/L for 1 mL/h and were therefore above the control (25.2 ± 3.1 g/L). The control and the two best feeding strategies are visualized in Figure 3; a comparison of all five strategies can be found in the Figure S3.

To select the setup with the highest LCH turnover, the share of LCH in the overall consumed carbon was calculated. The strategy using 1 mL/h of continuous feeding resulted in the highest percentage of LCH consumed (21.3 ± 2.9%), followed by 50:50 acetic acid:LCH (12.5%) and continuous feed with 0.5 mL/h (10.4 ± 1.2%). For the differences between the duplicates continuously fed with LCH results and the different consumed quantities of acetic acid, see Table S6. As the share of LCH using 50:50 acetic acid:LCH stayed constant over the fermentation, no standard deviation could be calculated. In addition, the carbon conversion rate of fed carbon to lipid was calculated for all conditions. In comparison, the setups using continuous feed had the highest carbon conversion yield, with 0.198 ± 0.002 g/g for 0.5 mL/h and 0.188 ± 0.0002 g/g for 1 mL/h. The control showed a conversion yield of 0.164 ± 0.0002 g/g, and co-feeding with the acetic acid:LCH mix resulted in 0.167 ± 0.0001 g/g, for a ratio of 50:10 and 0.167 ± 0.0005 g/g for 50:50.

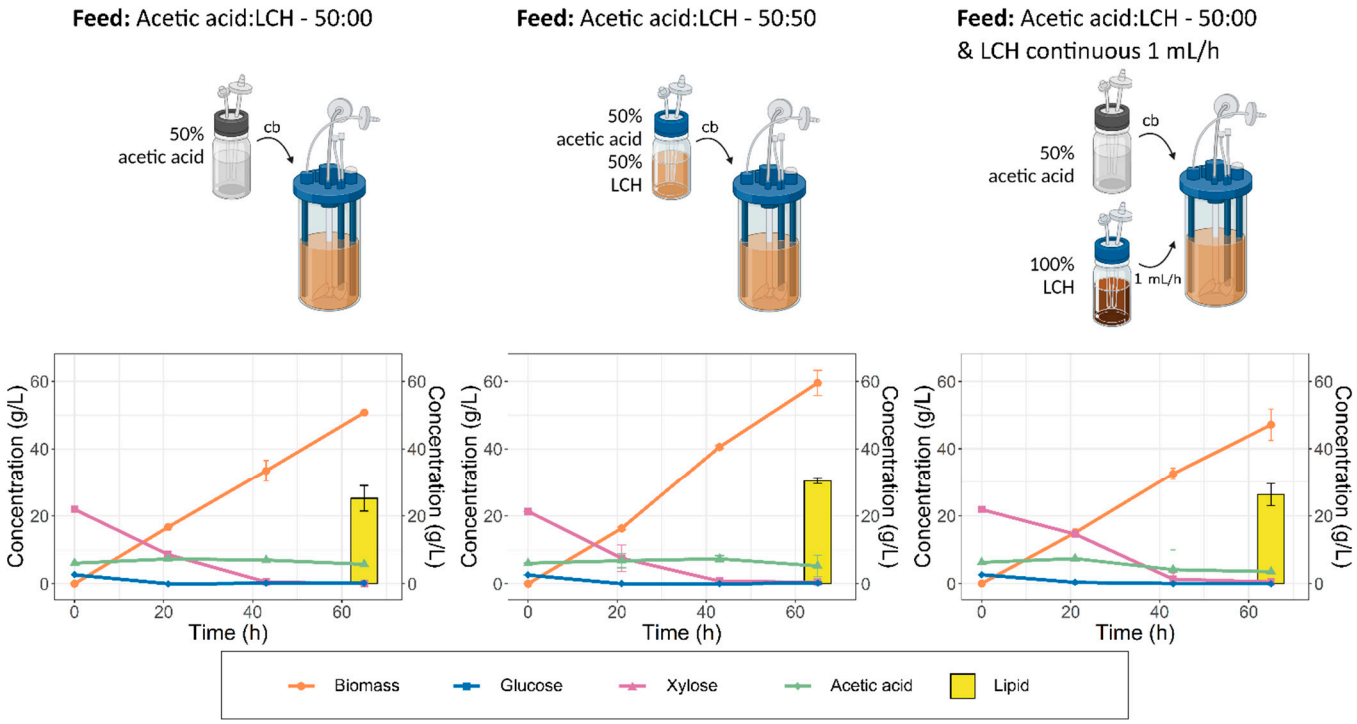


**Figure 3.** Comparison of the different feeding strategies in 0.25 L scale in the DASbox® system. Below each schema, the biomass accumulation, substrate concentration, and total lipid titer after 65 h are shown. On the left side, the consumption-based acetic acid feed with a 50% acetic acid solution is displayed (acetic acid:LCH 50:00), in the middle the consumption-based feed mixture of LCH and acetic acid (acetic acid:LCH—50:50), and on the right side the combination of continuous feeding with LCH at 1 mL/h and consumption-based acetic acid feeding (acetic acid:LCH 50:00 and LCH continuous). Fermentations were performed in duplicates at least. Error bars display two times standard deviation. LCH—Lignocellulosic hydrolysate, cb—consumption-based acetic acid feed.

### *3.8. Fermentation with Co-Feeding of Acetic Acid and Lignocellulosic Hydrolysate*

Using 1 mL/h continuous feed of LCH (LCH co-feed) led to the highest share of LCH consumed of the overall carbon source and had the second highest carbon conversion yield among all the tested conditions. Therefore, this condition was selected for the 1 L DASGIP® system. The slight scale-up also allowed a better direct comparison of the fermentation output with the other conditions tested in the DASGIP® system. A consumption-based feed with 90% acetic acid was used in combination with a continuous LCH feed of 3.3 mL/h. The biomass accumulation reached 29.0 ± 5.87 g/L after 71 h, with a lipid titer of 22.7 ± 1.95 g/L (lipid productivity 0.320 g/L/h). HPLC analysis showed that the sugars and acetic acid were evenly consumed throughout the fermentation, and only xylose accumulated slightly from 15.5 ± 1.11 g/L at 65 h to 17.44 ± 1.85 g/L at 71 h, as shown in Figure 1f. The xylose accumulation could presumably be solved by using a slightly lower feeding rate, resulting in a steady supply of sugar and fewer inhibitory compounds. When compared to the other conditions tested in the DASGIP® system, biomass accumulation with LCH co-feed was only approximately 17% less than that with glucose as the starting sugar. The lipid titers were comparable to the titers reached with glucose or xylose, with the LCH co-feed performing only 4% worse than the titers reached with xylose.

### *3.9. Techno-Economic Analysis*

Aside from the experimental results in this study, a consequential TEA was performed to assess the economic feasibility of a commercial-scale production plant using LCH as an industrially relevant feedstock. Two different modes of LCH fermentation from the 1 L

scale DASGIP® experiments were implemented and compared to the setup with glucose as a carbon source, as shown in Figure S4. Firstly, there was the consumption-based acetic acid feeding using LCH as a starting carbon source, and secondly, there was the combination of consumption-based acetic acid and the continuous feeding of LCH. Both fermentation modes were compared to an operation setup, where glucose was used as the starting carbon source for consumption-based acetic acid feeding. According to the simulation, the capital expenditure (CAPEX) was lowest for the LCH cb-feed at USD 30.1 M. In comparison, the CAPEX in the glucose cb-feed was USD 42.5 M and USD 41.8 M for the LCH co-feed. The increased capital cost was mainly caused by the different amounts and the vessel volumes of the fermentation vessels in the respective model. Different vessel combinations had to be used for the different fermentation strategies because of differences in the dwell times to simulate comparable lipid productivities. Other than the vessel amounts and the volumes, the equipment costs were the same. Depreciation was calculated as 10% over ten years, resulting in USD 4.2 M, USD 3.0 M, and USD 4.2 M for glucose cb-feed, LCH cb-feed, and LCH co-feed, respectively. The quantity and volumes of the vessels also resulted in differences in the operating costs, especially the costs for power (glucose cb-feed: USD 4.8 M, LCH cb-feed: USD 2.3 M, LCH co-feed: USD 4.0 M), cooling water (glucose cb-feed: USD 1.0 M, LCH cb-feed: USD 0.5 M, LCH co-feed: USD 0.9 M), labor cost (glucose cb-feed: USD 2.2 M, LCH cb-feed: USD 1.5 M, LCH co-feed: USD 1.8 M), maintenance (glucose cb-feed: USD 0.8 M, LCH cb-feed: USD 0.6 M, LCH co-feed: USD 0.8 M). Raw materials were a major expense, dominated by the acetic acid price. For the main analysis, an acetic acid price of 600 USD/t was used, resulting in a raw material cost of USD 8.5 M for glucose cb-feed, USD 7.7 M for LCH cb-feed, and USD 7.2 for LCH co-feed. The final costs for the yeast oil calculated from the in silico model were 3985 USD/t (glucose cb-feed), 2938 USD/t (LCH cb-feed), and 3576 USD/t (LCH co-feed), respectively (Figure 4a).

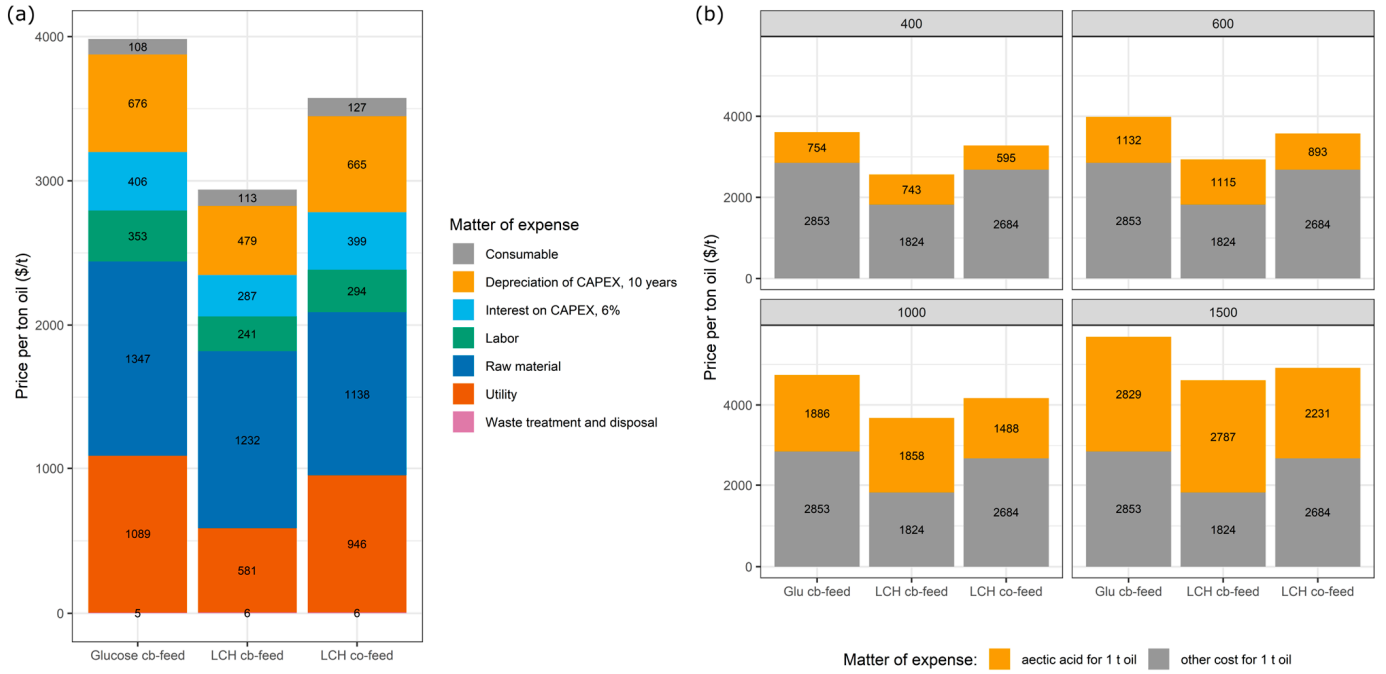


**Figure 4.** (**a**) Annual production cost of yeast oil in USD/Mt for the three fermentation strategies analyzed with the TEA. The respective amount of feedstock was set to produce yeast oil at a rate of 0.81 Mt/h (LCH cb-feed: 1 Mt/h, glucose cb-feed: 0.151 Mt/h, LCH co-feed: 2.1 Mt/h). (**b**) Annual production costs in a sensitivity analysis of the influence of the acetic acid prices 400, 600, 1000, and 1500 USD/t. LCH—lignocellulosic hydrolysate; cb-feed—consumption-based acetic acid feed; co-feed—lignocellulosic hydrolysate as starting carbon and constant feed with cb-feed.

In addition, a sensitivity analysis was performed considering different acetic acid prices, as it accounted for the major part of the raw material costs (glucose cb-feed: 84%, LCH cb-feed: 90%, LCH co-feed: 78%). Acetic acid prices in Western Europe fluctuated between 400 USD/t and 1500 USD/t between 2012 and 2023; so, the cost of yeast oil per t is largely dependent on the current acetic acid price [44,45]. Therefore, acetic acid costs of 400 USD/t, 600 USD/t, 1000 USD/t, and 1500 USD/t were assumed for the sensitivity analysis. The scenario using LCH cb-feed responded strongest to the price changes, as shown in Figure 4b. The price decrease to 400 USD/t led to a 12.6% decrease in the cost to 2567 USD/t oil. The rise to 1000 USD/t led to a 25.3% increase in production costs (3682 USD/t), and an elevated acetic acid price of 1500 USD/t resulted in a 56.9% increase (4611 USD/t). These tendencies were similar for the glucose cb-feed and LCH co-feed. Overall though, LCH cb-feed still showed the cheapest production costs for a decrease or increase in acetic acid prices.

## 4. Discussion

The lignocellulosic hydrolysate from acidic hardwood pulping mainly consisted of xylose, glucose, and other sugars, as well as acetic acid and lignin breakdown products, as expected and described by the literature [26,27]. This composition makes LCH an ideal carbon source for *C. oleaginosus*, which has been shown to efficiently metabolize both hexose and pentose sugars as well as acetic acid [17]. Waste streams with a high content of xylose and lignin-derived compounds are of special research interest because only a few commercial valorization strategies are available [46,47].

Due to the low amounts of nitrogen, phosphorus, and other elements, such as sulfur, magnesium, or calcium, additional nutrient supplementation is required before using the hydrolysate in a fermentation medium. Without pretreatment the LCH formed insoluble particles when combined with the other media components, which was presumably the result of sulfate and phosphate salt formation.

The pretreatment strategy established in this study produced a neutral LCH that did not form insoluble material when buffering salts or trace elements were added. As the sugar content was maintained, it could be efficiently applied as a carbon source for *C. oleaginosus*.

Primarily, the conventional nitrogen-limited fermentation approach was applied for the comparison of the LCH-containing medium with the XGA model. The reduced growth in LCH conditions was presumably caused by the high concentration of inhibitory furans and phenolic compounds in the medium. However, the contained phenolic and other lignin-derived compounds, did not inhibit growth completely. Furthermore, *C. oleaginosus* has already been shown before to metabolize some of the lignin breakdown compounds [16]. Generally, nitrogen limitation induces lipid formation but may restrict biomass formation at the same time, as nitrogen is required for protein synthesis and other metabolic processes [48]. Due to these drawbacks, nutrient limitation strategies are difficult for the production of SCO with the high yields required for commercial production.

The successful production of SCO with *C. oleaginosus* from refined sugars with acetic acid-based fermentation was shown previously. This approach combines a non-limiting sugar-containing starting medium with a consumption-based acetic acid feeding strategy [17]. For a commercially more attractive process, the LCH as a waste product was applied as a starting carbon source in this study, in place of costly sugars. This was further advanced in the fed-batch fermentations of this study. Xylose and glucose as sole carbon sources showed a similar growth behavior to the fermentation using XGA, which indicates a good and simultaneous uptake of both glucose and xylose. This is a considerable advantage of *C. oleaginosus* as a fermentation strain because the full potential of the biomass as a carbon source can be exploited. Moreover, the acetic acid can theoretically be directly channeled into the metabolism of lipid synthesis by acetyl-CoA synthetase. Therefore, a more efficient method of lipid biosynthesis in *C. oleaginosus*, compared to nutrient limitation conditions, can be employed [17]. Fortunately, acetic acid is part of the pulp and paper

waste streams and hence represents an industrially more promising carbon source than refined sugars, as it is a byproduct of hardwood pulping alongside the LCH [29,49].

The fatty acid profile of the SCO produced showed a typical composition of oleaginous yeasts, mainly consisting of C16 to C18 fatty acids, which is favorable for biodiesels [50]. Bio-based diesel from plant oils is used in the form of fatty acid esters. One main factor in evaluating the suitability of the fatty acids for biodiesel is the cetane number. This number indicates the combustion speed; it increases with chain length and decreases with saturation. The minimal overall values for use as biodiesel are 47 (U.S. American specification) and 51 (European specification). Examples of cetane ranges of biodiesels are 48–67 (soy oil) and 60–63 (palm oil) [51,52]. Among the unsaturated fatty acids, oleic acid has the greatest cetane number of 56 and is most prominent in the fatty acid profile of *C. oleaginosus* [53]. The cetane numbers of the other dominating fatty acids are 75 (palmitic acid) and 76 (stearic acid) [53]. As C16:0, C18:0, and C18:1 compose around 93% of the fatty acids, based on its composition the oil of *C. oleaginosus* fits well as a raw material for biodiesel.

The starting carbon source concentration of 3% resulted in the shortest lag phase, the best growth rate, and the overall biomass formation, demonstrating that the combination of monomeric sugars and acetic acid in the LCH can be metabolized efficiently and simultaneously by *C. oleaginosus*. Higher concentrations resulted in higher concentrations of inhibitory furans and lignin breakdown products, explaining the longer lag phase and decreased growth rates. Therefore, the starting carbon concentration of 3% was used for all further experiments.

The optimized fermentation strategy of *C. oleaginosus* on LCH with acetic acid consumption-based feeding showed the best performance in biomass accumulation, lipid titer, and lipid yield, with minor changes in the lipid profile. The increased performance of LCH as a substrate might be attributed to the contained lignol and lignan compounds that can partly be metabolized by *C. oleaginosus* [16]. In summary, this combination of the waste stream and oleaginous yeast is promising for a sustainable new process of SCO production. It combines the application of a waste stream rich in xylose, lignols, and lignans with a fermentation strategy resulting in high lipid yields. The lipid titer of 42.1 $\pm$ 1.7 g/L with a wild-type *C. oleaginosus* from this study is higher than the top yields from the literature of 39.5 $\pm$ 0.49 g/L with a genetically modified *R. toruloides* [35]. In the measured lipid carbon conversion, both sugars and acetic acid were considered but not the lignols and lignans from the hydrolysate. Nevertheless, the conversion yield of 0.336 g/g per carbon source is close to the theoretical maximum for xylose of 0.34 g/g [54]. Furthermore, efficient metabolization of the lignin breakdown products was shown, which can explain the high conversion yield and demonstrates the potential of *C. oleaginosus* for the valorization of waste streams from the pulp and paper industry.

Consumption-based acetic acid feeding results in a high lipid productivity of over 80%, as shown in the literature [17]. However, compared to acetic acid or commercially available sugars, LCH is a cheap feedstock as it is a waste product with limited options for value creation. To increase LCH uptake by the oleaginous yeast relative to the consumption of acetic acid and to better balance the two waste streams, different fermentation modes were compared. For the overall evaluation of the feeding strategies, the focus was set on the share of the consumed LCH and the lipid titer. With regard to this, the two best feeding strategies were cb-feed with 50:50 acetic acid:LCH as well as a co-feed with a continuous feed of 1 mL/h LCH. Providing more LCH during the fermentation process, these strategies could significantly increase the share of LCH. At the same time, the starting concentration of inhibitory compounds was not increased, which prevents an elongated lag phase, as observed for higher LCH concentrations.

The consequential TEA revealed a price reduction of 26% using LCH instead of glucose. Looking forward, the price points for the LCH processes could potentially be reduced by the further optimization of the fermentation processes and the resulting lipid conversion yields. All the calculated price regimes are in the current price range for organic palm oil (2500–3000 USD/t) [55]. Nevertheless, the consequential TEA, as applied in this study,

focuses mainly on the changes in the input and output conditions relative to each other [56]. The calculated prices per t should therefore be considered as an estimate of magnitude. Other plant oils used for biofuel production, such as canola oil, are priced well below 1000 USD/t [57]. However, utilizing an industrial waste stream circumvents the competition for edible oils, thus enhancing the sustainability aspect of the LCH-based oil production processes presented in this study. Furthermore, vertical fermentation setups are seasonally independent compared to their agricultural counterparts, and in contrast to conventional agriculture, do not require fertilizers and pesticides [58]. Moreover, fermentative SCO production is not heavily affected by climate change and represents an area-efficient alternative to plant oils.

A main factor for the production cost of the SCO is the price of acetic acid, as it is one of the main carbon sources in this process. The high recent fluctuation in acetic acid prices can be explained by the limited number of suppliers, namely the USA and China, which supply the majority of the acetic acid, with the market shares of 17% and 55%, respectively [59]. Therefore, problems or even disruptions in the supply chains of these two countries have a profound impact on the pricing as the availability can be drastically decreased [44,60]. Local or even on-site production and supply of acetic acid would be the best route to avoid such dependencies and price fluctuations. In that context, up to 5% of wood weight is acetate esters, which could potentially be separated and used directly from pulp and paper waste streams as an acetic acid source [27,61].

In Europe alone, the pulp and paper industry produces around 11 million tons of waste every year [24]. Wood is mainly composed of 40–44% cellulose, 18–32% lignin, and 15–35% hemicelluloses [27,61]. The hemicellulose consists of xylan with 10–35% and acetate esters with 3–5% of the total wood [62,63]. Extrapolating these numbers to the actual biomass volume results in waste material of 85–151, 47–151, and 14–24 million metric tons of lignin, xylan, and acetate, respectively. Even a small proportion of these waste amounts would be enough to supply a biotechnological plant, as described here.

In the TEA, our lab-scale experiments for the biotechnological valorization of an industrial waste stream using *C. oleaginosus* were validated in an in silico industrial fermentation plant model. It was performed with a focus on the comparison of different conditions and raw material costs. Compared to glucose, the cost efficiency of LCH was demonstrated for the production of SCO on an industrially relevant scale. SCO can be used as a starting material for similar applications to those of plant-based oils in the biofuel sector as well as for the production of polymeric materials, lubricants, and other oleochemicals [64,65]. Such resource-efficient approaches could lead to more independent, circular, and sustainable economies in the future.

## 5. Conclusions

Single cell oils are a promising alternative to plant-based oils for the production of sustainable biofuels. This study provides a novel strategy to produce SCOs with the oleaginous yeast *C. oleaginosus*, utilizing lignocellulosic hydrolysate, a biogenic waste stream from the pulp and paper industry. To this end, fermentations were performed, and a maximal lipid titer of 42.1 $\pm$ 1.7 g/L (75.5% lipid per biomass) and a carbon conversion to lipid of 0.336 g/g were reached with optimized conditions. Furthermore, feeding strategies were tested to enhance the share of LCH in the total amount of fed carbon, where acetic acid has the main share. The most effective feeding strategy utilized a mix of acetic acid and LCH as the main carbon sources, both of which account for the main part of the waste stream from the pulp and paper industry. In summary, our data indicate that the xylose-rich LCH is a highly suitable substrate for the efficient bioconversion to SCO. By adding continuous feeding to the established consumption-based approach, the LCH share of consumed carbon was increased. The economic advantages of the use of LCH over glucose were shown in a techno-economic analysis. The predicted prices for the SCO produced moved in a range (2900 USD/t) that was competitive with sustainably produced organic plant oils (1000–3000 USD/t) [55,57]. At the same time, vertical fermentation

setups can be run in a seasonally independent manner, without the use of fertilizers and pesticides, and offer options for land-efficient scale-up. Our further research will continue in the direction of maximizing the reuse of industrial waste streams in an economically feasible way to close the remaining gaps for a circular bioeconomy and to contribute to the environmental challenges the world faces today. In conclusion, we present a sustainable and economical strategy to produce SCOs as an alternative platform to produce advanced biofuels, lubricants, and other oleochemical products.

## 6. Patents

Thomas B. Brueck, Mahmoud Masri, Nikolaus I. Stellner, and Zora S. Rerop have a European patent field with the Technical University of Munich involving the methodology described in this work.

**Supplementary Materials:** The following supporting information can be downloaded at: https://www.mdpi.com/article/10.3390/fermentation9020189/s1, Table S1: composition of the LCH, Table S2: pretreatment strategies, Table S3: sugar and organic acid composition of LCH before and after pretreatment, Figure S1: comparison between three different starting concentration of LCH, Table S4: Duncan groups of the statistical analysis of the fatty acid profile, Figure S2: GC-MS chromatograms of fermentation medium before and after fermentation, Table S5: share of LCH from the overall consumed carbon for the different feeding strategies, Figure S3: comparison of all five different feeding strategies as well as respective carbon conversion rates, Table S6: GC-FID relative quantification of LCH-derived lignin breakdown products before and after the fermentation, Figure S4: Super Pro Designer model for the TEA of SCO production on the basis of LCH and acetic acid.

**Author Contributions:** Conceptualization, T.B.B., M.M., N.I.S. and Z.S.R.; methodology, M.H., P.G., M.M., N.I.S. and Z.S.R.; software, M.M., N.I.S. and Z.S.R.; validation, T.B.B., M.M. and N.M.; investigation, P.G., M.M., N.I.S. and Z.S.R.; resources, T.B.B.; data curation, P.G., M.M., N.I.S. and Z.S.R.; writing—original draft preparation, N.I.S. and Z.S.R.; writing—review and editing, T.B.B. and M.M.; visualization, N.I.S. and Z.S.R.; supervision, T.B.B., N.M. and M.M.; project administration, M.M.; funding acquisition, T.B.B. All authors have read and agreed to the published version of the manuscript.

**Funding:** This research was funded by: The German Federal Ministry of Education and Research (Bundesministerium für Bildung und Forschung), grant number: FKZ 031B0662B; European Union's Horizon Europe research and innovation program, grant number: 101059786; Werner Siemens Foundation.

**Institutional Review Board Statement:** Not applicable.

**Informed Consent Statement:** Not applicable.

**Data Availability Statement:** The data presented in this study are available on request from the corresponding author. The data are not publicly available due to privacy protection.

**Acknowledgments:** We would like to thank Jeremias Widmann for his outstandingly diligent and dependable help with the sample preparation and analysis throughout our work. We also very much appreciate the expert knowledge and advice of Uwe Arnold, managing director of AHP Group GmbH, which led to the optimization of our techno-economic analysis setup. Finally, we express our thanks to Gülnaz Celik for her reliable support and advice in the fermentations performed for this study.

**Conflicts of Interest:** Thomas B. Brueck and Mahmoud Masri are board members at Global Sustainable Transformation GmbH.

## References

1. Ge, M.; Friedrich, J.; Vigna, L. *5 Facts about Country & Sector GHG Emissions*; World Resources Institute: Washington, DC, USA, 2022; pp. 1–9.
2. Pörtner, H.-O.; Roberts, D.C.; Adams, H.; Adelekan, I.; Adler, C.; Adrian, R.; Aldunce, P.; Ali, E.; Begum, R.A.; Friedl, B.B.; et al. *2022: Technical Summary*; Cambridge University Press: Cambridge, UK; New York, NY, USA, 2022; ISBN 9781009157896.

3. United Nations. "17 Sustainable Development Goals (SDGs)", Sustainable Development Goals (SDGs), 2022. Available online: https://sdgs.un.org/goals (accessed on 29 September 2022).
4. European Commission. *REPowerEU Plan*; European Commission: Brussels, Belgium, 2022.
5. European Commission. *A Strategic Long-Term Vision for a Prosperous, Modern, Competitive & Climate-Neutral Economy EU Vision for 2050—"A Clean Planet for All"*; European Commission: Brussels, Belgium, 2018.
6. Flach, B.; Lieberz, S.; Bolla, S. *EU Biofuels Annual 2019*; USDA: Washington, DC, USA, 2019.
7. Irena & Ace. *Renewable Energy Outlook for ASEAN*; Irena & Ace: Masdar City, Abu Dhabi, 2022; ISBN 9789295111288.
8. Abeln, F.; Chuck, C.J. The history, state of the art and future prospects for oleaginous yeast research. *Microb. Cell Fact.* **2021**, *20*, 221. [CrossRef] [PubMed]
9. Huang, C.; Chen, X.-F.; Xiong, L.; Chen, X.-D.; Ma, L.L.; Chen, Y. Single cell oil production from low-cost substrates: The possibility and potential of its industrialization. *Biotechnol. Adv.* **2013**, *31*, 129–139. [CrossRef] [PubMed]
10. Agricultural Market Information Company (AMI). *Report on Global Market Supply: 2020/2021*; Agricultural Market Information Company (AMI): Las Vegas, NV, USA, 2020.
11. Brandenburg, J. Lipid Production from Lignocellulosic Material by Oleaginous Yeasts. Doctoral Thesis, Swedish University of Agricultural Sciences Uppsala, Uppsala, Sweden, 2021.
12. Shaigani, P.; Awad, D.; Redai, V.; Fuchs, M.; Haack, M.; Mehlmer, N.; Brueck, T. Oleaginous yeasts- substrate preference and lipid productivity: A view on the performance of microbial lipid producers. *Microb. Cell Fact.* **2021**, *20*, 220. [CrossRef] [PubMed]
13. Vasconcelos, B.; Teixeira, J.C.; Dragone, G.; Teixeira, J.A. Oleaginous yeasts for sustainable lipid production—From biodiesel to surf boards, a wide range of "green" applications. *Appl. Microbiol. Biotechnol.* **2019**, *103*, 3651–3667. [CrossRef] [PubMed]
14. Banwell, M.G.; Pollard, B.; Liu, X.; Connal, L.A. Exploiting Nature's Most Abundant Polymers: Developing New Pathways for the Conversion of Cellulose, Hemicellulose, Lignin and Chitin into Platform Molecules (and Beyond). *Chem.-Asian J.* **2021**, *16*, 604–620. [CrossRef] [PubMed]
15. Lee, S.; Monnappa, A.K.; Mitchell, R.J. Biological activities of lignin hydrolysate-related compounds. *BMB Rep.* **2012**, *45*, 265–274. [CrossRef] [PubMed]
16. Yaguchi, A.; Robinson, A.; Mihealsick, E.; Blenner, M. Metabolism of aromatics by Trichosporon oleaginosus while remaining oleaginous. *Microb. Cell Fact.* **2017**, *16*, 206. [CrossRef]
17. Masri, M.; Garbe, D.; Mehlmer, N.; Brück, T. A sustainable, high-performance process for the economic production of waste-free microbial oils that can replace plant-based equivalents. *Energy Environ. Sci.* **2019**, *12*, 2717–2732. [CrossRef]
18. Yaguchi, A.; Franaszek, N.; O'Neill, K.; Lee, S.; Sitepu, I.; Boundy-Mills, K.; Blenner, M. Identification of oleaginous yeasts that metabolize aromatic compounds. *J. Ind. Microbiol. Biotechnol.* **2020**, *47*, 801–813. [CrossRef]
19. Yu, X.; Zheng, Y.; Dorgan, K.M.; Chen, S. Oil production by oleaginous yeasts using the hydrolysate from pretreatment of wheat straw with dilute sulfuric acid. *Bioresour. Technol.* **2011**, *102*, 6134–6140. [CrossRef]
20. Gong, Z.; Shen, H.; Zhou, W.; Wang, Y.; Yang, X.; Zhao, Z.K. Efficient conversion of acetate into lipids by the oleaginous yeast *Cryptococcus curvatus*. *Biotechnol. Biofuels* **2015**, *8*, 189. [CrossRef]
21. Gong, Z.; Zhou, W.; Shen, H.; Yang, Z.; Wang, G.; Zuo, Z.; Hou, Y.; Zhao, Z.K. Co-fermentation of acetate and sugars facilitating microbial lipid production on acetate-rich biomass hydrolysates. *Bioresour. Technol.* **2016**, *207*, 102–108. [CrossRef] [PubMed]
22. Saxena, G.; Bharagava, R.N. *Bioremediation of Industrial Waste for Environmental Safety*; Springer: Singapore, 2020; Volume I, ISBN 9789811318900.
23. Tiseo, I. Annual production of plastics worldwide from 1950 to 2020 (in million metric tons). *Statista* **2022**, *2020*, 22–24.
24. European Commission. New market niches for the Pulp and Paper Industry waste based on circular economy approaches. In *H2020-Eu*; European Commission: Brussels, Belgium, 2017; pp. 1–4.
25. Gottumukkala, L.D.; Haigh, K.; Collard, F.X.; van Rensburg, E.; Görgens, J. Opportunities and prospects of biorefinery-based valorisation of pulp and paper sludge. *Bioresour. Technol.* **2016**, *215*, 37–49. [CrossRef] [PubMed]
26. Luo, H.; Liu, Z.; Xie, F.; Bilal, M.; Peng, F. Lignocellulosic biomass to biobutanol: Toxic effects and response mechanism of the combined stress of lignin-derived phenolic acids and phenolic aldehydes to Clostridium acetobutylicum. *Ind. Crops Prod.* **2021**, *170*, 113722. [CrossRef]
27. Jönsson, L.J.; Martín, C. Pretreatment of lignocellulose: Formation of inhibitory by-products and strategies for minimizing their effects. *Bioresour. Technol.* **2016**, *199*, 103–112. [CrossRef] [PubMed]
28. Koutinas, A.A.; Vlysidis, A.; Pleissner, D.; Kopsahelis, N.; Garcia, I.L.; Kookos, I.K.; Papanikolaou, S.; Kwan, T.H.; Lin, C.S.K. Valorization of industrial waste and by-product streams via fermentation for the production of chemicals and biopolymers. *Chem. Soc. Rev.* **2014**, *43*, 2587–2627. [CrossRef] [PubMed]
29. Sixta, H. Lenzinger AG Zellstoffherstellung und Recycling von Roh- und Hilfsstoffen nach dem Lenzinger Mg- Bisulfitverfahren. *Lenzing. Ber.* **1986**, *61*, 5–11.
30. Singh, A.K.; Bilal, M.; Iqbal, H.M.N.; Meyer, A.S.; Raj, A. Bioremediation of lignin derivatives and phenolics in wastewater with lignin modifying enzymes: Status, opportunities and challenges. *Sci. Total Environ.* **2021**, *777*, 145988. [CrossRef]
31. Koul, B.; Yakoob, M.; Shah, M.P. Agricultural waste management strategies for environmental sustainability. *Environ. Res.* **2021**, *206*, 112285. [CrossRef]
32. Nitsos, C.K.; Matis, K.A.; Triantafyllidis, K.S. Optimization of hydrothermal pretreatment of lignocellulosic biomass in the bioethanol production process. *ChemSusChem* **2013**, *6*, 110–122. [CrossRef]

33. Almeida, J.R.M.; Wiman, M.; Heer, D.; Brink, D.P.; Sauer, U.; Hahn-Hägerdal, B.; Lidén, G.; Gorwa-Grauslund, M.F. Physiological and Molecular Characterization of Yeast Cultures Pre-Adapted for Fermentation of Lignocellulosic Hydrolysate. *Fermentation* **2023**, *9*, 72. [CrossRef]
34. Duwe, A.; Tippkötter, N.; Ulber, R. Lignocellulose-biorefinery: Ethanol-focused. *Adv. Biochem. Eng. Biotechnol.* **2017**, *166*, 177–215.
35. Díaz, T.; Fillet, S.; Campoy, S.; Vázquez, R.; Viña, J.; Murillo, J.; Adrio, J.L. Combining evolutionary and metabolic engineering in Rhodosporidium toruloides for lipid production with non-detoxified wheat straw hydrolysates. *Appl. Microbiol. Biotechnol.* **2018**, *102*, 3287–3300. [CrossRef] [PubMed]
36. Nigam, J.N. Ethanol production from hardwood spent sulfite liquor using an adapted strain of Pichia stipitis. *J. Ind. Microbiol. Biotechnol.* **2001**, *26*, 145–150. [CrossRef] [PubMed]
37. Tjørve, K.M.C.; Tjørve, E. The use of Gompertz models in growth analyses, and new Gompertz-model approach: An addition to the Unified-Richards family. *PLoS ONE* **2017**, *12*, e0178691. [CrossRef] [PubMed]
38. Bligh, E.G.; Dyer, W.J. A rapid method of total lipid extraction and purification. *Can. J. Biochem. Physiol.* **1959**, *37*, 911–917. [CrossRef] [PubMed]
39. Intelligen Inc. *SuperPro® Designer V10*; Intelligen, Inc.: Medford, MA, USA, 2019.
40. Walas, S.M. *Chemical Process Equipment: Selection and Design*; Butterworth-Heinemann Reed Publ. Inc.: Oxford, UK, 1990; pp. 1–755.
41. Humbird, D.; Davis, R.; Tao, L.; Kinchin, C.; Hsu, D.; Aden, A. *Process Design and Economics for Biochemical Conversion of Lignocellulosic Biomass to Ethanol*; National Renewable Energy Lab.: Golden, CO, USA, 2011; pp. 153–170.
42. Eurostat Industriestrompreise in Deutschland in den Jahren 2001 bis 2021. *Statista*. 2022. Available online: https://de.statista.com/statistik/daten/studie/155964/umfrage/entwicklung-der-industriestrompreise-in-deutschland-seit-1995/ (accessed on 18 October 2022).
43. Ageitos, J.M.; Vallejo, J.A.; Veiga-Crespo, P.; Villa, T.G. Oily yeasts as oleaginous cell factories. *Appl. Microbiol. Biotechnol.* **2011**, *90*, 1219–1227. [CrossRef] [PubMed]
44. Bann, W. *Acetic Acid/Vinyl Acetate—The Waiting Is The Hardest Part*; ResourceWise: Charlotte, NC, USA, 2021.
45. Alibaba.com. Acetic Acid. 2022. Available online: https://www.alibaba.com/trade/search?fsb=y&IndexArea=product_en&CatId=&tab=all&SearchText=acetic+acid (accessed on 18 October 2022).
46. Broda, M.; Yelle, D.J. Bioethanol Production from Lignocellulosic Biomass—Challenges and Solutions. *Molecules* **2022**, *27*, 8717. [CrossRef]
47. Sharma, S.; Tsai, M.L.; Sharma, V.; Sun, P.P.; Nargotra, P.; Bajaj, B.K.; Chen, C.W.; Dong, C. Di Environment Friendly Pretreatment Approaches for the Bioconversion of Lignocellulosic Biomass into Biofuels and Value-Added Products. *Environments* **2023**, *10*, 6. [CrossRef]
48. Chopra, J.; Sen, R. Process optimization involving critical evaluation of oxygen transfer, oxygen uptake and nitrogen limitation for enhanced biomass and lipid production by oleaginous yeast for biofuel application. *Bioprocess Biosyst. Eng.* **2018**, *41*, 1103–1113. [CrossRef] [PubMed]
49. Schneider, H. Selective removal of acetic acid from hardwood-spent sulfite liquor using a mutant yeast. *Enzym. Microb. Technol.* **1996**, *19*, 94–98. [CrossRef]
50. Singh, S.; Pandey, D.; Saravanabhupathy, S.; Daverey, A.; Dutta, K.; Arunachalam, K. Liquid wastes as a renewable feedstock for yeast biodiesel production: Opportunities and challenges. *Environ. Res.* **2022**, *207*, 112100. [CrossRef] [PubMed]
51. Van Gerpen, J. Cetane Number Testing of Biodiesel. In *Third Liquid Fuel Conference: Liquid Fuel and Industrial Products from Renewable Resources*; American Society of Agricultural Engineers: St. Joseph, MI, USA, 1996; pp. 197–206.
52. Zahan, K.A.; Kano, M. Biodiesel production from palm oil, its by-products, and mill effluent: A review. *Energies* **2018**, *11*, 2132. [CrossRef]
53. Tamilselvan, P.; Sassykova, L.; Bhaskar, K.; Subramanian, S.; Gomathi, K.; Prabhahar, M.; Prakash, S. Effect of Saturated Fatty Acid Composition of Biodiesel on Oxides of Nitrogen and Smoke Emissions. *J. Chem. Technol. Metall.* **2023**, *58*, 167–177.
54. Papanikolaou, S.; Aggelis, G. Lipids of oleaginous yeasts. Part I: Biochemistry of single cell oil production. *Eur. J. Lipid. Sci. Technol.* **2011**, *113*, 1031–1051. [CrossRef]
55. Alibaba_Palm-Oil. 2022. Available online: https://www.alibaba.com/product-detail/Best-Quality-cheap-organic-refined-Crude_60360488487.html?spm=a2700.galleryofferlist.normal_offer.d_title.56f1cfd5ZqfiRs&s=p (accessed on 18 October 2022).
56. Brander, M.; Tipper, R.; Hutchison, C.; Davis, G. Consequential and attributional approaches to LCA: A Guide to policy makers with specific reference to greenhouse gas LCA of biofuels. *Econ. Press* **2008**, *44*, 1–14.
57. Alibaba2_Canola-Oil. 2022. Available online: https://www.alibaba.com/trade/search?fsb=y&IndexArea=product_en&CatId=&SearchText=canola+oil&selectedTab=product_en (accessed on 20 October 2022).
58. Ullmann, J.; Grimm, D. Algae and their potential for a future bioeconomy, landless food production, and the socio-economic impact of an algae industry. *Org. Agric.* **2021**, *11*, 261–267. [CrossRef]
59. Acetic Acid. *Chemical Economics Handbook*; IHS Markit, S&P Global: London, UK, 2021. Available online: https://ihsmarkit.com/products/acetic-acid-chemical-economics-handbook.html (accessed on 5 April 2022).
60. Helmlinger, E. Celanese Corporation Berichtet Ergebnisse für das Erste Quartal 2021. 2021. Available online: https://www.celanese.de/News-And-Media/2021/April/ergebnisse-fur-das-erste-quartal-2021 (accessed on 17 February 2023).

61. Doelle, K.; Bajrami, B. Sodium Hydroxide and Calcium Hydroxide Hybrid Oxygen Bleaching with System. *IOP Conf. Ser. Mater. Sci. Eng.* **2018**, *301*, 12136. [CrossRef]
62. Patil, R.; Genco, J.; Pendse, H.; Van Heiningen, A. Process for producing acetic acid in hardwood kraft pulp mills. *Tappi J.* **2017**, *16*, 287–300. [CrossRef]
63. Kobetičová, K.; Nábělková, J. Effect of wood hemicellulose composition on binding interactions with caffeine. *Buildings* **2021**, *11*, 515. [CrossRef]
64. Sivasamy, A.; Cheah, K.Y.; Fornasiero, P.; Kemausuor, F.; Zinoviev, S.; Miertus, S. Catalytic applications in the production of biodiesel from vegetable oils. *ChemSusChem* **2009**, *2*, 278–300. [CrossRef] [PubMed]
65. Nurchi, C.; Buonvino, S.; Arciero, I.; Melino, S. Sustainable Vegetable Oil-Based Biomaterials: Synthesis and Biomedical Applications. *Int. J. Mol. Sci.* **2023**, *24*, 2153. [CrossRef] [PubMed]

## 4.2 Chapter II: Expanding the genetic toolbox for *Cutaneotrichosporon oleaginosus* employing newly identified promoters and two novel antibiotic resistance markers

### 4.2.1 Summary

*The article 'Expanding the genetic toolbox for Cutaneotrichosporon oleaginosus employing newly identified promoters and two novel antibiotic resistance markers' has been published in xxx 2023 (https://doi.org/xxx). The authors Zora S. Rerop and Nikolaus I. Stellner contributed equally to this publication. The candidate performed promoter analysis and motif discovery, as well as the selection of endogenous promoters and their in vivo validation. Additionally, the candidate worked on the establishment of the aminoglycoside 3'-phosphotransferase marker. The combination of the markers was done in close collaboration with Nikolaus I. Stellner.*

The research on the genetic accessibility of *Cutaneotrichosporon oleaginosus* has been limited to a few studies worldwide. Manipulating this oleaginous yeast is challenging, and many aspects of its composition, metabolism, and regulation are not yet understood. However, genetic adaptation of the microorganism can enable targeted optimization of nutrient uptake, product specifications, and overall yield, and other desirable traits. To facilitate genetic modification of *C. oleaginosus*, basic elements such as promoters and dominant makers are needed.

In this study, we analyzed the structure of putative endogenous promoter sequences by analyzing the genes of more than 280 highly expressed proteins. We identified a potential regulatory element, the CT-motif, and discovered a translation initiation site, which is related to the known Kozak-sequence. Based on these findings, four endogenous putative promoter sequences were annotated, namely D9FADp, UBIp, PPIp, and 60Sp. These promoter sequences were used to express the known dominant marker hygromycin B phosphotransferase. All newly described promoters along with the previously established GAPDHp showed successful expression of the resistance gene. Among the four promoters, the shortest promoter, PPIp, was selected to establish two dominant markers: Aminoglycoside 3'-phosphotransferase (APH) which mediates geneticin G418 resistance, and N-acetyltransferase (NAT) which carries the nourseothricin resistance gene. Both dominant markers exhibited high transformation efficiency and rapid growth rates. Compatibility testing showed no cross-activity, indicating a successful sequential and simultaneous genomic integration of the two markers. Successive integration did not affect the transformation efficiency, but simultaneous integration significantly reduced the transformation efficiency.

The four newly described promoters can further expand the options for gene expression in *C. oleaginosus*, solving issues related to the use of a single known promoter for multiple genetic constructs, resulting in, among other things, transcription factor competition. In addition, the two novel dominant markers allow the genomic integration of two separate constructs, offering more flexibility for genetic engineering. In particular, the compatible use of the two markers makes the metabolic manipulation of a target strain much more versatile. In conclusion, the described genetic tools

enable a more flexible and versatile metabolic and genetic manipulation of *C. oleaginosus*.

### 4.2.2 Full-length publication

Stellner *et al. BMC Biotechnology* (2023) 23:40
https://doi.org/10.1186/s12896-023-00812-7

BMC Biotechnology

RESEARCH Open Access

# Expanding the genetic toolbox for *Cutaneotrichosporon oleaginosus* employing newly identified promoters and a novel antibiotic resistance marker

Nikolaus I. Stellner[1,2†], Zora S. Rerop[1†], Norbert Mehlmer[1], Mahmoud Masri[1], Marion Ringel[1] and Thomas B. Brück[1*]

## Abstract

**Background** *Cutaneotrichosporon oleaginosus* is an oleaginous yeast that can produce up to 80% lipid per dry weight. Its high capacity for the biosynthesis of single cell oil makes it highly interesting for the production of engineered lipids or oleochemicals for industrial applications. However, the genetic toolbox for metabolic engineering of this non-conventional yeast has not yet been systematically expanded. Only three long endogenous promoter sequences have been used for heterologous gene expression, further three dominant and one auxotrophic marker have been established.

**Results** In this study, the structure of putative endogenous promoter sequences was analyzed based on more than 280 highly expressed genes. The identified motifs of regulatory elements and translational initiation sites were used to annotate the four endogenous putative promoter sequences D9FADp, UBIp, PPIp, and 60Sp. The promoter sequences were tested in a construct regulating the known dominant marker hygromycin B phosphotransferase. The four newly described promoters and the previously established GAPDHp successfully initiated expression of the resistance gene and PPIp was selected for further marker development. The geneticin G418 resistance (aminoglycoside 3′-phosphotransferase, APH) and the nourseothricin resistance gene N-acetyl transferase (NAT) were tested for applicability in *C. oleaginosus*. Both markers showed high transformation efficiency, positive rate, and were compatible for combined use in a successive and simultaneous manner.

**Conclusions** The implementation of four endogenous promoters and one novel dominant resistance markers for *C. oleaginosus* opens up new opportunities for genetic engineering and strain development. In combination with recently developed methods for targeted genomic integration, the established toolbox allows a wide spectrum of new strategies for genetic and metabolic engineering of the industrially highly relevant yeast.

**Keywords** *Cutaneotrichosporon oleaginosus*, Promoter, Dominant marker, Oleaginous yeast, Antibiotic resistance, Aminoglycoside 3′-phosphotransferase, N-acetyl transferase

†Nikolaus I. Stellner, Zora S. Rerop contributed equally to this work.

*Correspondence:
Thomas B. Brück
brueck@tum.de

[1]TUM School of Natural Sciences, Department of Chemistry, Werner Siemens-Chair for Synthetic Biotechnology, Technical University of Munich, Lichtenbergstr. 4, 85748 Garching, Germany
[2]TUM CREATE Ltd, 1 Create Way, #10-02 CREATE Tower, Singapore 138602, Singapore

## Background

*Cutaneotrichosporon oleaginosus* is an oleaginous yeast with the ability to metabolize a variety of both hexoses and pentoses and to produce high amounts of intracellular lipids. Among the known and described oleaginous yeasts it is one of the most efficient producers of single cell oils. Further, it has been shown to grow on a diverse range of industrial side streams like lignocellulosic hydrolysates [1, 2]. It can catabolize sugars without diauxic preferences and therefore generally shows a consistent growth behavior in the presence of several different carbon sources [3]. Further, in comparison to other yeasts, it is more resistant to toxic by-products of acidic hydrolysis, like furfural, HMF, organic acids, and phenols [4–6]. *C. oleaginosus* is capable of producing more than 80% lipid per dry cell weight and reaching lipid titers over 42 g/L in bioreactor fermentations [2, 7]. These qualities make it an ideal host organism for the conversion of side streams into valuable single cell oils and oleochemicals that can be used e.g., for biofuel, lubricant, cosmetic, and food applications.

Its unique properties make *C. oleaginosus* an attractive target for metabolic engineering to enhance triglyceride productivity, generate altered lipid profiles, change its ability for carbon substrate utilization, or implement lipid secretion [8–11]. Beyond triglyceride production, *C. oleaginosus* can be used as a cell factory platform to generate structurally diverse, high-value compounds [12]. *C. oleaginosus* is one of the most studied oleaginous yeasts, next to *Rhodotorula toruloides*, *Yarrowia lipolytica*, and *Lipomyces starkeyi* [9]. The single cell oils produced by these oleaginous microorganisms vary in terms of fatty acid composition, which qualifies them for different applications. *L. starkeyi* for instance, produces large amounts of palmitic acid (33.3%), followed by *R. toluroides* (20.0%). *R. toluroides* also shows a high amount of the essential fatty acid linoleic acid (13.1%), which is more than double the share found in single cell oil of the other three yeasts, and has added nutritional value [9]. Among those however, *C. oleaginosus* is one of the least studied with regard to the availability of genetic tools, which currently complicates its genetic optimization [8, 9, 13]. At present, no plasmid-based system is known for *C. oleaginosus*, which makes genetic modification dependent on time-consuming genomic integration methods. All these methods depend on reliable selection markers, whereof only a limited number is available for this yeast. Until recently, *Agrobacterium tumefaciens* mediated transformation (ATMT) and electroporation-mediated random integration techniques were the only vector-based methods to introduce DNA into the genome of *C. oleaginosus* [13, 14]. Transformation with *A. tumefaciens* is a successful and reliable method used for the introduction of genetic material into yeasts and fungi for almost three decades [15–17]. While ATMT is a fast transformation method, it does not allow targeted genomic integration. Specifically, *A. tumefaciens* randomly introduces multiple gene copies at different genomic locations. As the integration site cannot be controlled, genetic insertions can have detrimental effects on the growth of the transformants and on the expression of the gene(s) of interest. While ATMT was successfully used to generate non-native fatty acids in *C. oleaginosus*, we recently reported a CRISPR-Cas based approach for targeted genomic integration and deletion to yield mutants with modified fatty acid profiles [13, 18].

However, targeted genetic and metabolic engineering of microbial cell factories not only builds on reliable genetic accession tools but is also highly dependent on the availability of different antibiotic resistance cassettes, as well as functional promotor sequences to facilitate tunable, homologous, or heterologous gene expression. For *Yarrowia lipolytica* as well as *Rhodosporidum toruloides* native and engineered endogenous promoters as well as synthetic combinations have been characterized, which can be used for targeted metabolic engineering approaches [19, 20]. For metabolic engineering in *C. oleaginosus*, only a total of three endogenous promoters have been used for gene expression in previous studies [13, 18]. Of these, the glyceraldehyde 3-phosphate dehydrogenase promoter (GAPDHp) was used for the heterologous expression of a dominant marker and other genes of interest. The other two promoters used for homologous expression originated from the aldo-keto reductase (AKR) and the transcription elongation factor (TEF), which were combined with different endogenous genes of *C. oleaginosus* in our previous work [18]. In the same study, also three native genes (URA5, D9FAD and D12FAD) were used for genetic engineering [18]. As *C. oleaginosus* is commonly used for lipid accumulation, promoters should be especially active under these conditions to be used for metabolic engineering. However, strongly reduced expression behavior was reported for the GAPDH promoter under nitrogen limitation, which is commonly used to induce accumulation of lipids [13]. The available promoters currently not allow diversified genetic engineering approaches to build a platform for oleochemical production beyond tailored triglycerides [12]. Consequently, to allow for more flexibility in genetic engineering approaches, the availability of a larger selection of promoters for *C. oleaginosus* to expand the molecular biology toolbox would be highly desirable. To that end, specifically constitutive promoters which act independently of the respective metabolic situation would be an important addition to the toolbox of metabolic engineering of the oleaginous yeast.

To date, the low availability of promoters is not the only limiting factor for genetic engineering of *C. oleaginosus*.

This issue extents to having only a few reliably working selection markers available including one auxotrophic marker (orotate phosphoribosyltransferase, URA5) for negative selection and three dominant resistance markers (HPH: hygromycin B phosphotransferase, PDR4: pleiotropic drug resistance 4, APH: aminoglycoside 3'-phosphotransferase) [13, 14, 18]. Auxotrophic markers allow for genetic engineering without antibiotics and mediate strong selection. However, a major drawback of using auxotrophic markers for selection is that an auxotrophic strain must be established before, which is often a rather work-intense effort. Also, once introduced, the markers should be expressed in the host at physiological levels, which can be difficult to balance [21]. To this end, dominant markers are a robust and faster alternative, because the wild type (wt) can be directly used for transformation. However, the introduction of large genes can result in a metabolic burden for the host cell, reduced growth, and productivity. Moreover, the antibiotics have to be well tolerated by the transformed cells [21].

In general, to introduce more than one genetic construct, it is useful to have several selection markers at hand. For other oleaginous yeasts like *Y. lipolytica* there are already several other auxotrophic markers such as *URA3*, *LEU2* and *LYS5* available, as well as dominant markers like the geneticin and nourseothricin resistance [22]. Both geneticin G418 and nourseothricin inhibit ribosomal translation [23, 24]. Geneticin G418 resistance can be mediated by the enzyme aminoglycoside 3 'phosphotransferase (APH). The transposon Tn903 from *Escherichia coli* carrying the APH sequence was established in *S. cerevisiae* as the resistance marker KanMX already in 1980 [23, 25]. In case of nourseothricin, the resistance gene for nourseothricin N-acetyl transferase (NAT) is found in the producer strain *Streptomyces noursei* and can be used as a dominant resistance marker [23, 26]. Both dominant markers have been successfully used and combined in genetic work using different conventional and oleaginous yeasts [22, 24].

The unconventional yeast *C. oleaginosus* is a promising candidate for the industrial production of single cell oils [9]. However, to allow efficient metabolic and genetic engineering strategies, it is required to extend the molecular biology toolbox for this microorganism. Until now, only a few promotors and selection markers have been used. The goal of this study was to extend the portfolio of the available genetic tools. Therefore, five endogenous promoters were tested for their activity for heterologous gene expression. Furthermore, the cytotoxic effect of the two antibiotics geneticin G418 and nourseothricin was investigated on *C. oleaginosus* wt cells. Finally, *A. tumefaciens*-mediated transformation was chosen as a convenient method to evaluate geneticin G418 and nourseothricin resistances as markers for positive selection in *C. oleaginosus* and to further assess their compatibility. The experiments aim at extending the current metabolic engineering tools available for *C. oleaginosus* to access the potential of this oleaginous yeast for the sustainable production of single cell oils and oleochemicals.

## Results and discussion

### In silico analysis of *Cutaneotrichosporon oleaginosus* promoter elements

To increase the number of available promoters for genetic engineering approaches, the corresponding regulatory elements had to be identified. However, gene regulation in eukaryotic organisms is still not fully understood, especially for non-model organisms like the oleaginous yeast *Cutaneotrichosporon oleaginosus*. Fortunately, modern sequencing technology simplifies access to genetic information. The genome of *C. oleaginosus* was sequenced and the corresponding transcriptome was annotated in 2015 by Kourist et al. [27]. These genomic and transcriptomic data were used for the *in-silico* analysis of promoter and regulatory elements of the non-conventional yeast. Known endogenous yeast promoters commonly consist of a core promoter, comprising the minimal sequences required for the transcription start, and further different regulatory elements, including the proximal promoter as well as regulatory upstream activation sequences (UAS) [19]. The core promoter in yeasts usually contains one or several transcription start sites (TSS) and a non-obligatory TATA-box upstream of the start codon [28–30].

#### TATA-box screening

For TATA-box motif screening, a dataset of up to 310 genes was selected from the highest expressed genes in *C. oleaginosus* cultivated with glucose as carbon source, as obtained from proteomics analysis of Fuchs et al. in 2021 [5]. Several sequence areas relative to the mRNA start (-800 to -1, -200 to -1, and −100 to -1) were selected with RSAT Fungi 'retrieve sequence' tool, mostly excluding other overlapping elements [31]. These sequence sets were analyzed with the MEME tool for motif discovery. Different settings for motif occurrence and motif lengths of 5 to 8 bp were tested [32]. Furthermore, other tools (FIMO and MAST) were employed to search for specific TATA-motifs known from *Saccharomyces cerevisiae* and other oleaginous yeasts [33]. However, no significant conserved TATA-box-like sequence could be identified. Therefore, the TATA-box annotation was neglected for the promoter description.

In this context, motif discovery with the MEME tool certainly has its limitations, specifically for short sequence motifs, such as the TATA-box, a strong conservation is required to find statistically significant results in

a dataset. Further, searching for known motifs originating from other yeast employing tools like MAST, can only identify patterns relevant for the corresponding yeast species. However, the transferability of these motif search algorithms from known species to genetically poorly understood organisms, such as *C. oleaginosus* might be very limited. Consequently, an enrichment of A and T bases at specific positions relative to the TSS, might not be identified with this approach but could nevertheless exist.

#### Search for transcription start site

The TSS can either be positioned before or around the start codon, and in the latter case, it is at the same position as the translation initiation site (TIS). However, the mRNA can also start with the first intron of a gene, the 5'-untranslated region (UTR) [28]. To this end, the importance of the intronic region for promoter activity has already been shown in the oleaginous yeast *Rhodotorula toruloides* [28]. The search for conserved TSS motifs in this study was performed with the data set of up to 310 highly expressed genes as mentioned above. The area from −50 to +50 relative to the annotated mRNA start was selected with RSAT [31]. However, the motif search with MEME did not reveal a statistically relevant sequence that exclusively occurs in the potential TSS region. Therefore, no TSS was annotated.

An obstacle that can influence the TSS motif search is the mRNA annotation. The mRNA is annotated from transcriptomics data and therefore has already been processed by the cell [34]. Hence, the exact position of the TSS for each gene is hard to identify, which makes the motif discovery relative to the mRNA start difficult. Surprisingly, during the search for the TATA-box and TSS motifs, both a general putative regulatory element and a motif for the TIS were found and further analyzed.

#### Discovery of CT-rich motif

Regulatory elements like the UAS can be versatile in position, length, orientation, and sequence [19]. Mostly, regulatory elements are recognition sites for transcription factors (TF), cofactors, RNA binding or act as (steric) their regulation sequences for [35–37]. The above-mentioned dataset of up to 310 genes was searched for these motifs. For this set the default RSAT settings were used to select the upstream sequence of the genes (-800 bp, excluding other annotated sequences, to -1). For 298 genes sequences longer than 8 bp were found and were included. Subsequently, a highly significant element could be identified, comprising a 41 bp long CT-rich motif, with an E-value of $2.3e^{-227}$. It was identified in 245 sites within 189 of the 298 sequences, with a position p-value less than 0.0001. The consensus sequence of the motif is YYYYYCYCYCYCCCYCCYCHYCHCYCYCHCYCYYYYYCYC, with Y coding for CTA and H for ACT, compare Fig. 1a. Notably, the CT-motif is most abundant in areas close to the gene start in 5' to 3' direction but was also found further upstream of the mRNA start as well as in the reverse direction, as shown in Figure S2.

However, the sequences are not necessarily restricted to the length of 41 bp, as very similar motifs are found differing in length, using different settings in the same or different sequence sets. The minimal and maximal length of the CT-rich motif is rather hard to specify. CT-rich stretches of over 100 bp, representing the potential maximal length, were identified manually within the data sets. The minimal length is challenging to identify as well, because some statistically relevant shorter motifs were found, but were always observed to be part of longer CT-rich regions. Repeating patterns were found comprising 4 to 12 bp. Therefore, the element can be summarized as a CT-rich repeat, accumulating in the areas before transcriptional initiation. The function of the repeats can be hypothesized to be of regulatory nature, like TF binding. Furthermore, for other basidiomycota related CT-motifs and repeats in promoter regions were described before, like for *Ceriporiopsis subvermispora* and *Pleurotus ostreatus* [38]. Nevertheless, the molecular function of these is not yet unraveled. Therefore, other approaches, aiming at the screening of TF binding site should be applied for a better understanding of the regulatory elements of *C. oleaginosus* promoters, such as DNA microarrays or Chip-seq [36, 39].

#### Translational initiation site identification

The translational initiation is coupled to the binding of ribosomes to the mRNA, therefore it does not only require a specific sequence but also a certain tertiary structure of the RNA [40]. In this study we only focused on the genetic sequence around the translational start site, specifically the ATG start codon. A sequence selection of -30 to +10 relative to the coding sequences (CDS) from the 310 gene-set described above was selected with RSAT and used for the sequence identification of the TIS. A conserved 21 bp motif was found at 54 sites within 301 provided sequences, with an E-value of $2.0e^{-40}$. The sequence spans from −17 to +4, relative to the start codon ATG. The motif consists of an A- and C-rich stretch from −17 to -7, a non-conserved position −5 and a highly conserved A at position −3. Position −2 and −1 again are AC-rich and the conserved ATG is followed by a G or T in most cases. The consensus sequence is MYMMMAHMMCAVYCAMMATGK (with M: CA, Y: CAT, H: ACT, V: GAC, K:GT), shown in Fig. 1b.

The start codon ATG is a conserved sequence for gene regulation across the kingdoms, for translational initiation the small ribosomal subunit (40 S) scans the mRNA from the m7G cap until the start codon is reached [41].

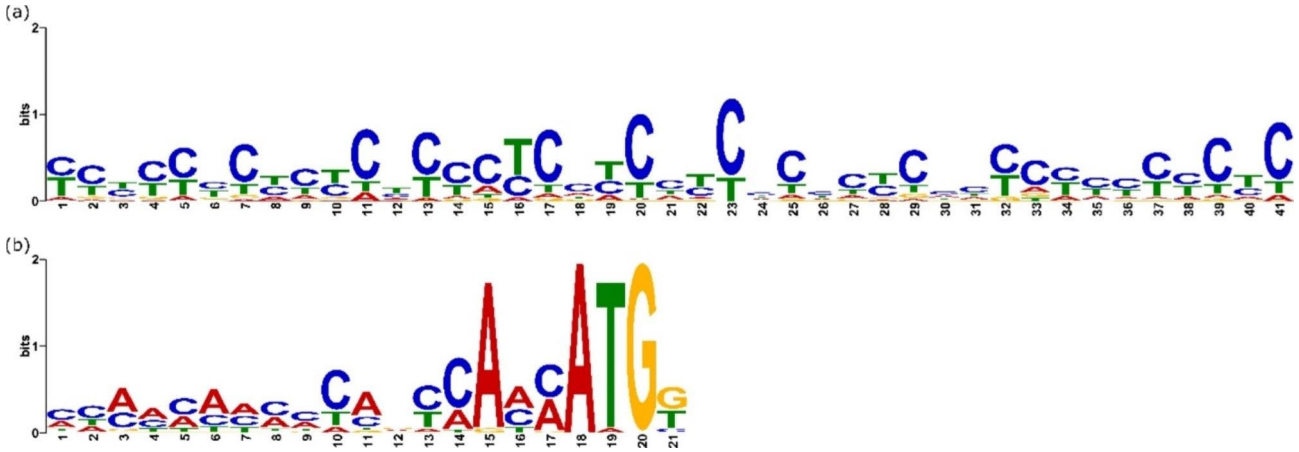


**Fig. 1** (**a**) 41 bp long CT-rich stretch, that was found in the promoter region in 245 sites within the 298 sequences of high expressed genes from *C. oleaginosus* with statistical significance with an E-value of $2.3e^{-227}$. (**b**) The translational initiation site of 21 bp Kozak-like sequence was found in 54 of 301 sequences and is located from −17 to +4, relative to the start codon ATG, with an E-value of $2.0e^{-40}$

This recognition is also influenced by the surrounding nucleotide sequence, the TIS [40]. The TIS motif found in *C. oleaginosus* is related to the general Kozak motif described for many eukaryotic organisms by Kozak (1989) [42]. In the Kozak motif also the nucleotide −3 and +4 are highly conserved with an optimal recognition of the start codon with the sequence GCCRCCaugG (R = A/G) [41]. The motif found in *C. oleaginosus* follows this structure with the exclusion of the −6 G in the Kozak sequence and a stronger emphasis on A in the position −3. The cropped sequence in a Kozak-like format is VYCAMMaugK (M: CA, Y: CAT, V: GAC, K:GT).

### Endogenous promoter for the heterologous gene expression in *Cutaneotrichosporon oleaginosus*

To identify putative endogenous promoters of *C. oleaginosus* for heterologous gene expression, suitable genes were manually selected according to the expression rates in the transcriptomics data published by Kourist et al. in 2015 [27]. As criteria transcription levels in both glucose media and in nitrogen-limited conditions were considered as well as the biological function of the genes. Based on these criteria, the five endogenous promoters GAPDHp, D9FADp, UBIp, PPIp, and 60Sp were selected for this study as listed in Table 1. The GAPDH promoter was the only one described in literature and used in a longer 800 bp version, as well as in a cropped 390 bp version [13]. For this study, the 800 bp version was employed.

The length of the novel putative promoters D9FAD, PPIp, and UBIp was selected to be the sequence upstream of the start codon at least including the annotated 5'UTR region. Further, the next CT-rich repeats region upstream of the 5'UTR was included in the promoter sequence. This resulted in respective promoter lengths of 191 bp for D9FADp, 154 bp for PPIp and 463 bp for UBIp. The 60 S promoter structure differed clearly from the others containing a less conserved region of CT-rich repeats, no 5'UTR and no ATG start codon at the beginning of the annotated CDS. It was, therefore, tentatively selected with 421 bp upstream of the annotated gene start. FIMO was employed for the annotation of the TIS, and CT-rich repeats described above [33]. The predicted TIS and the CT-motif identified before were used as indicators for the promoter annotation, as shown in Fig. 2a. In four of the five selected genes TIS motifs were identified according to the Kozak-like sequence. Only in the 60Sp gene no TIS motif was identified. The 41 bp long CT-motif was identified in all annotated sequences. In the promoter of GAPDH 96 hits for the CT-motif were found with a p-value $< 10^{-4}$, 76 hits in D9FADp, 70 hits in UBIp, 31 hits in PPIp and only 4 in 60Sp. The number and length of the CT-rich regions that span over all motif hits vary in each promoter sequence from 54 to 134, as listed in Table 1. The coverage of the regions with CT-motif hits is further different for each sequence, but quite high for GAPDHp, UBIp, D9FADp, and PPIp, but with only 4 hits on a 113 bp region very low for the 60Sp. For a clearer visualization only the CT-rich regions, including the identified CT-motifs, were annotated in Fig. 2b. As an example for the annotation of the CT-motif, Figure S1 shows the structure of the PPI promoter with all overlapping CT-motifs annotated by FIMO and the resulting CT-rich region stretches.

The annotations strengthen the hypothesis that the CT-motifs might be important for TF binding in the core promoter region in *C. oleaginosus*. In all promoters selected in this study, the motifs were cumulatively annotated in the region from 450 bp (mainly 200 bp) upstream, to the start of the CDS. In four of the five promoters a 5'UTR is annotated upstream of the start codon. In the case of UBIp there is a 5' intron annotated included within the putative promoter region. All 5'UTR

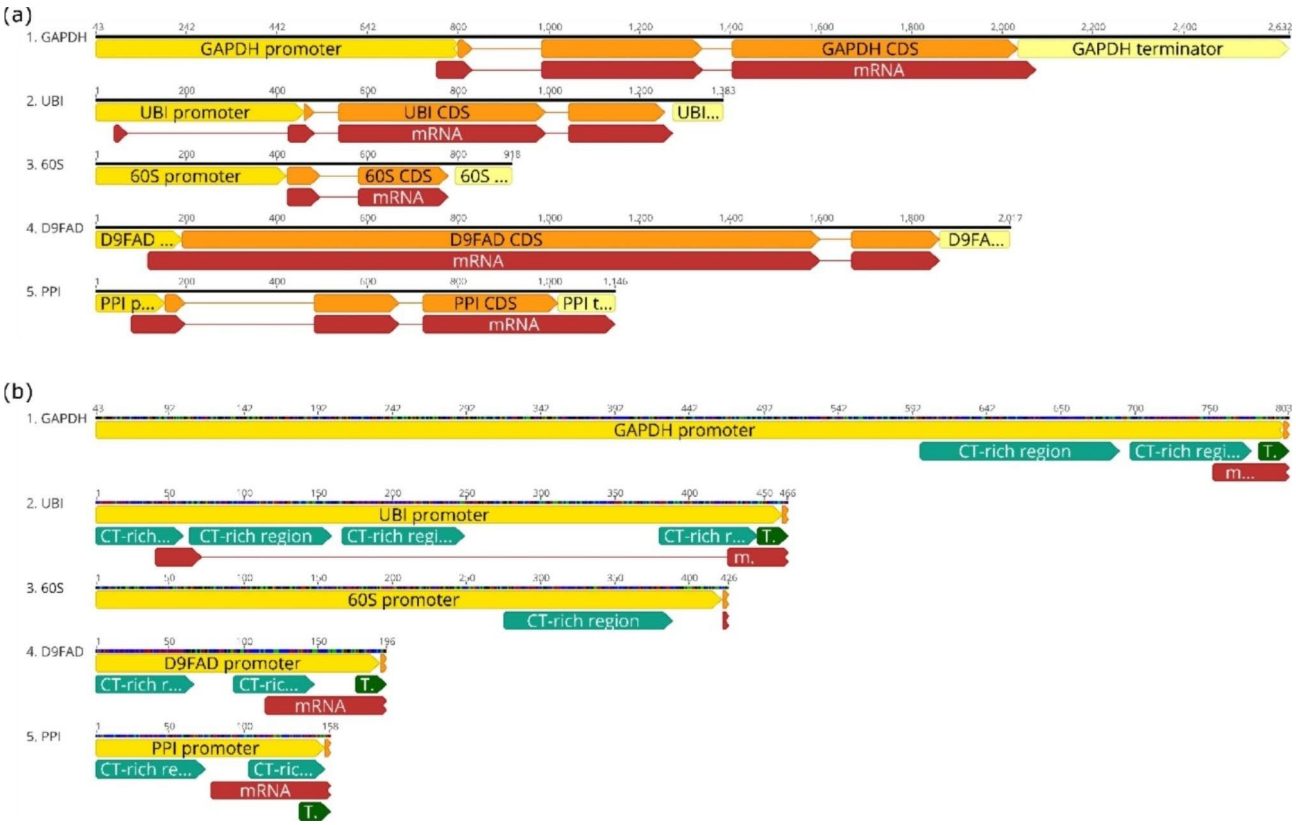


**Fig. 2** (**a**) Annotation of selected genes from *C. oleaginosus*, with promoters (yellow), terminators (light yellow), CDS (orange) and mRNA (red) annotated by Kourist et al. [3]. Putative promoters were annotated according to CT-motifs identified in this study and including the 5'UTR, shown in detail in (**b**). The CT-rich regions (green) within the putative promoter regions indicate where CT-motifs were identified. The identified TIS motifs (dark green) as well as the mRNA transcripts (red) and the first 4 bases of the CDS (orange) are also depicted

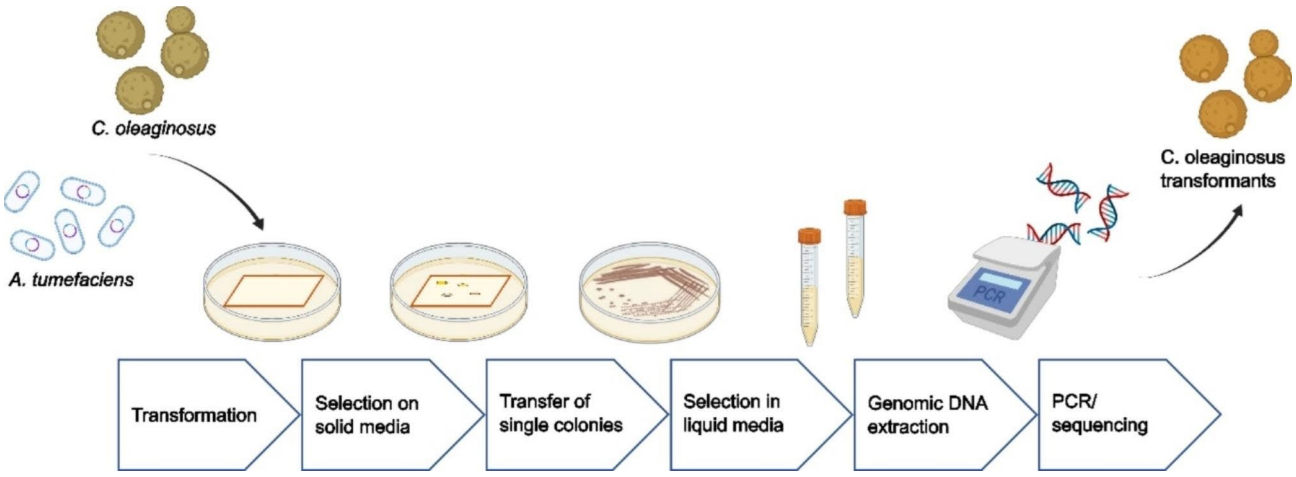


**Fig. 3** Workflow for the genetic modification of *C. oleaginosus* with an *Agrobacterium tumefaciens*-mediated transformation. *A. tumefaciens* cells with a plasmid containing a resistance were used to transfect *C. oleaginosus* followed by selection on solid media. After restreaking single colonies were used to inoculate liquid media. Finally, the genomic DNA was extracted for PCR amplification of the respective gene and sequencing for validation. Parts of the figure were created with BioRender

regions contain CT-motifs, this is in accordance with literature that showed that the 5'UTR and intronic regions are important for the promoter activity in other non-conventional yeast [28].

### Evaluation of different promoters for functional gene expression in *Cutaneotrichosporon oleaginosus*

Of the five promoters selected as described above, only GAPDHp was previously described as a promoter for

**Table 1** Selection of promoters from endogenous genes of *C. oleaginosus*. UBIp, 60Sp, D9FADp and PPIp were newly identified in this study

| # | Promoter | Gene of origin | Gene ID | Length selected | 5′UTR | Count of CT-motifs (41 bp) | Length of CT-rich regions (bp) |
|---|---|---|---|---|---|---|---|
| 1 | GAPDHp | Glyceraldehyde 3-phosphate dehydrogenase | 276,138 | 800 | yes | 96 | 134, 82 |
| 2 | UBIp | Ubiquitin and ubiquitin-like proteins | 289,369 | 463 | yes | 70 | 59, 96, 82, 66 |
| 3 | 60Sp | 60 S ribosomal protein L37 | 224,393 | 421 | no | 4 | 113 |
| 4 | D9FADp | delta-9 fatty acid desaturase | 308,253 | 191 | yes | 76 | 66, 54 |
| 5 | PPIp | Cyclophilin type peptidyl-prolyl cis-trans isomerase | 286,945 | 154 | yes | 31 | 74, 51 |

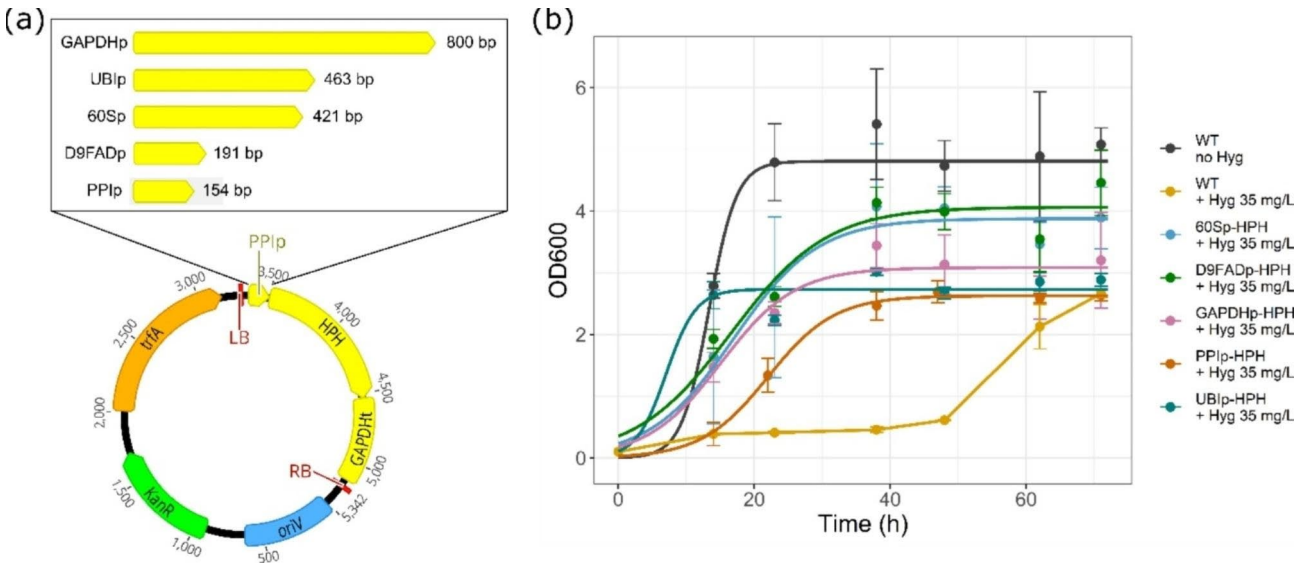


**Fig. 4** (**a**) pRF_Xp_HPH vector used for ATMT of *C. oleaginosus* with the five different promoters tested. Elements for plasmid replication and amplification in *E. coli* include KanR: kanamycin resistance; oriV: plasmid origin of replication; trfA: plasmid replication initiator protein. (**b**) Growth of *C. oleaginosus* mutants, with genomically integrated promoter-HPH constructs, and wt cells as controls with and without the addition of hygromycin B. The measurements were performed with four biological replicates. 60Sp, 60 S ribosomal protein L37 promoter; D9FADp, delta-9 fatty acid desaturase promoter; GAPDHp, glyceraldehyde 3-phosphate dehydrogenase promoter; HPH, hygromycin phosphotransferase; Hyg, hygromycin B; PPIp, cyclophilin type peptidyl-prolyl cis-trans isomerase promoter; UBIp, ubiquitin and ubiquitin-like protein promoter; wt, wild type. Plasmid maps were created with Geneious

heterologous gene expression in *C. oleaginosus*. The promoter was applied in a modified pRF-HU2 plasmid for *Agrobacteria*-mediated transformation to produce non-native fatty acids in *C. oleaginosus*. The method is summarized in Fig. 3 [13]. This construct contained the hygromycin B phosphotransferase (HPH) gene from the pRF-HU2 plasmid, originating from the bacterium *Streptomyces hygroscopicus*. The HPH gene mediates resistance towards hygromycin B, an aminoglycoside, which inhibits protein biosynthesis.

To further assess which of the four putative promoters identified in this study would initiate gene expression, GAPDHp was replaced with D9FADp, UBIp, PPIp, and 60Sp, which were amplified from genomic DNA of *C. oleaginosus.* The GAPDH terminator was kept as a regulatory element for all constructs, resulting in the plasmids pRF-D9FADp-HPH, pRF-UBIp-HPH, pRF-PPIp-HPH, and pRF-60Sp-HPH, described in Fig. 4a. The constructs were all subsequently tested by PCR for, potentially genomic, integration via ATMT of *C. oleaginosus*. The transformation of *C. oleaginosus* wt cells with all plasmids resulted in CFUs on the membrane in the first round of selection. These CFUs were then transferred and streaked out on YPD plates. Single colonies from the plates were subsequently used to inoculate hygromycin B-containing YPD broth. All the tested plasmids resulted in transformants capable of surviving in the presence of the antibiotic in liquid media, reaching similar ODs as the wt without exposure to hygromycin B. Figure 4b shows the growth behavior of the mean of four biological replicates for each construct in comparison to the wt with and without the addition of hygromycin B. The wt without addition of hygromycin B outperformed the mutants in all cases. The growth of the wt yeast was suppressed in the presence of hygromycin B at 35 µg/mL only up to 46 h after inoculation.

This allows for the conclusion that *C. oleaginosus* shows some inherent resistance against the antibiotic, making it prone to lead to false positive results. The high variability in growth between the five promoters and the wt may result from different activities of the promoters. However, a high variability between the mutants using the same construct was observed, resulting in a high standard deviation. In ATMT, genomic integration takes place in an untargeted way, leading to high biological variability and difficulties with the quantification of the promoter activity. This might result from differences in the transcription frequency within the different loci of gene integration. In addition, the number of integrations can vary between the transformants, resulting in different gene copy numbers. Growth on solid and in liquid media was also not stable for some of the mutants and some could not be re-cultivated after storage. Overall, the observations characterize the ATMT using hygromycin B as potentially error-prone and inconsistent. Under these circumstances, evaluation of the quantitative promoter strength is difficult, which was the reason that methods such as quantitative PCR or the expression of fluorescent proteins were not applied. The results further show, that there is a strong need for alternative dominant markers for *C. oleaginosus*, that show a lower background and produce more stable transformants. This led to the characterization of other dominant markers for *C. oleaginosus* in the following steps with a focus on selectivity and reproducibility for genetic modification.

Of the four promoter sequences newly identified, all initiated the expression of the HPH resistance marker. This confirms that the sequences were functional promoters, comprising at least the core regulatory elements. Hence, these promoters can be applied in future genetic engineering approaches in *C. oleaginosus*. Therefore, the applied methodology for promoter annotation qualifies for the identification of functional endogenous promoters, featuring elements like the described CT-rich repeats. Compared to other reported working promoters for gene expression in *C. oleaginosus*, UBIp, 60Sp, D9FADp, and PPIp are much shorter with PPIp being the shortest element with 154 bp. Of the four newly reported elements the longest was 463 bp (UBIp), which is still shorter compared to GAPDHp and AKRp with 800 bp, and TEFp with 913 bp previously described in literature for tailoring the fatty acid profile [13, 18]. Due to its small size, PPIp was used for further ATMT experiments in this study. This is an advantage as transformation efficiency might decrease with increasing size of the vector DNA, thus generally favoring shorter promoter sequences [43]. The four newly described promoter sequences for gene expression in *C. oleaginosus* are a valuable and convenient alternative to the long promoters described in previous studies. Having a larger set of different promoters is a requirement for more complex genetic engineering using several constructs because different promoters do not compete for the same TF.

### Dominant markers for the selection of genetically modified *Cutaneotrichosporon oleaginosus*

The promoters GAPDHp, D9FADp, UBIp, PPIp, and 60Sp tested in this study all effectively initiated expression of the HPH protein. All further plasmids used for ATMT in this study featured the PPI promoter in front of the resistance marker. Until now, there was only one dominant marker described in the literature, the HPH resistance gene. This marker proved to have its difficulties, as false positive clones were a substantial part of the screening process and recultivation of the selected clones was sometimes not possible anymore after storage. Therefore, two dominant markers, known from genetic studies with other yeasts, were tested, namely APH and NAT. The CDS of the two enzymes was used to replace the HPH sequence in the plasmid pRF_PPIp-HPH. The sequence for APH originates from the bacterial transposon Tn903 and acts as geneticin G418 resistance marker. The NAT sequence comes from *Streptomyces noursei* and is a nourseothricin resistance marker. The sequences were retrieved from a public database, codon-optimized for expression in *C. oleaginosus*, and inserted into pRF_PPIp-HPH, resulting in the plasmids pRF_PPIp-APH and pRF_PPIp-NAT, as shown in Figs. 5c and 6c. To assess the applicability of these dominant resistance markers in *C. oleaginosus*, the cytotoxicity of geneticin G418 and nourseothricin against the unconventional yeast was tested on solid media, shown in Figs. 5a and 6a. To this end, a serial dilution of *C. oleaginosus* culture was dropped onto plates containing increasing concentrations of the respective antibiotic. The growth at 28 °C was monitored for two days. Based on the growth inhibition, a suitable concentration of the respective antibiotic was selected. Geneticin G418 completely inhibited growth at 50 mg/L and above, and nourseothricin at 20 mg/L and above. Therefore, for solid media selection 50 mg/L geneticin G418 and 25 mg/L nourseothricin were chosen. The growth behavior of *C. oleaginosus* wt was further assessed in YPD liquid media containing different concentrations of one of the antibiotics. In the presence of geneticin G418, growth of *C. oleaginosus* in YPD broth was fully inhibited at 25 mg/L, see Fig. 5b. In the case of nourseothricin, the growth was fully inhibited already at 10 mg/L, as displayed in Fig. 6b. The determined concentrations were used in all further growth experiments for liquid media selection using geneticin G418 or nourseothricin, respectively.

In the next step, ATMT was performed using pRF_PPIp-APH and pRF_PPIp-NAT. The concentration of antibiotics in the solid media for membrane transfer was

doubled compared to the minimal inhibition concentration, following the common ATMT procedure described in Fig. 3. As substantial variation of the transformant numbers between the membranes of biological replicates is inherent to ATMT, the CFUs on the membranes were not analyzed quantitatively. From each of the three membranes 24 CFU were restreaked on solid media for single clone selection. *C. oleaginosus* wt transformed with the *A. tumefaciens* wt used as negative control did form up to 10 CFUs on the membranes in the presence of the respective antibiotic. The ATMT with pRF_PPIp-APH resulted in 65 out of 72 transformants growing on YPD plates with geneticin G418. In the case of pRF_PPIp-NAT, 70 out of 72 transformants survived on nourseothricin-containing plates. The streaked clones from the control ATMTs were not capable of surviving nourseothricin or geneticin selection on solid media (Figs. 5d and 6d). For the selection in liquid media, 32 transformants for each APH and NAT were used for inoculation of YPD with either nourseothricin or geneticin G418. For both dominant markers, all the selected CFU grew in liquid media in the presence of nourseothricin or geneticin G418, respectively (Figs. 5f and 6f). The integration was finally confirmed via PCR (Figs. 5e and 6e) and sequencing, leaving the uncertainty of the place of integration as, apart from a genomic site, an ectopic appearance of the DNA sequence might be possible. The results of the transformation experiments are summarized in Table 2.

The relatively high share of transformants (90% for APH and 97% for NAT) growing on plates with antibiotics allowed for an efficient transformation process with both dominant markers. The growth and validation of 100% of the *C. oleaginosus* mutants in liquid media showed that the approach leads to a reliable selection of transformants with confirmed, potentially genomic, integration of the marker. Furthermore, recovery from cryostocks worked consistently well. Thus, the experiments demonstrate that selection on solid media with the respective antibiotic is already a strong indicator for the integration of the genetic construct with APH or NAT. However, with 100% of the yeast clones surviving exposition to the antibiotic in liquid media, this allows for selection of transformants with a very low share of false positives, as confirmed by PCR. Overall, this study presents the use of the antibiotic resistance gene NAT for the genetic modification of *C. oleaginosus* for the first time. In comparison, both dominant markers qualify as reliable and efficient tools for selection using ATMT or any other transfection method for the genetic engineering of the unconventional yeast.

#### Combination of the two dominant markers

Until now, for the genetic modification of *C. oleaginosus*, only the HPH resistance gene has been established as a dominant maker. For the successive or simultaneous modification introducing more than one genetic construct, at least two compatible markers are required. APH and NAT are both aminoglycoside-modifying enzymes, but work with different molecule classes and have a different molecular reaction mechanism. APH is an aminoglycoside-3'-phosphotransferase phosphorylating an alcohol group of the target molecule geneticin G418. NAT is an N-acetyl transferase that acetylates the β-amino group of nourseothricin. Based on these differences, the two dominant markers could be compatible and might be used to independently integrate two separate constructs into the same target cell.

To assess this, APH and NAT were first tested for cross-reactivity. Transformants from ATMTs with pRF_PPIp-APH or pRF_PPIp-NAT were tested for cross-activity against nourseothricin or geneticin G418, respectively. No growth was observed on plates or in liquid media for transformants featuring either an integrated APH or NAT in presence of the respective other antibiotic. In a next step, the combination of the two marker genes was tested either with successive or simultaneous transformation. For successive transformation, a transformant with a confirmed genomically integrated APH or NAT was selected. The mutant was then used for an ATMT with the respective other dominant resistance marker. The efficiency of the cloning procedure is shown in Table 2. The transformation efficiency was high in the cases of successive transformation, CFUs on the membrane were more than 500 each for all three replicates. For the simultaneous transformation the efficiency was reduced significantly, with four to eight CFU on each transformation membrane. From the selected clones of the successive transformation of APH integration followed by NAT integration, all 32 grew (100%) on solid media containing both antibiotics. 18 further selected transformants were able to grow in liquid media. Further, all nine transformants used for genomic DNA extraction were positive for the gene sequence as shown by PCR and sequencing. The other successive combination, NAT followed by APH integration, was similarly successful. After restreaking, 30 out of 32 clones grew (94%) on solid media containing geneticin G418 and nourseothricin. All the 16 selected transformants survived in liquid broth with the antibiotics. The genomic DNA extracted from four of these clones featured both markers, as confirmed by PCR and sequencing. In case of the simultaneous integration of the APH and NAT marker, a total of 17 CFU on the three different transformation membranes were picked. Out of those 17 only 14 grew (82%) when restreaked on solid media, but from those all eleven, which were further selected, survived in liquid media. All four clones selected for sequencing tested positive for both markers. Liquid cultures for growth curves were measured

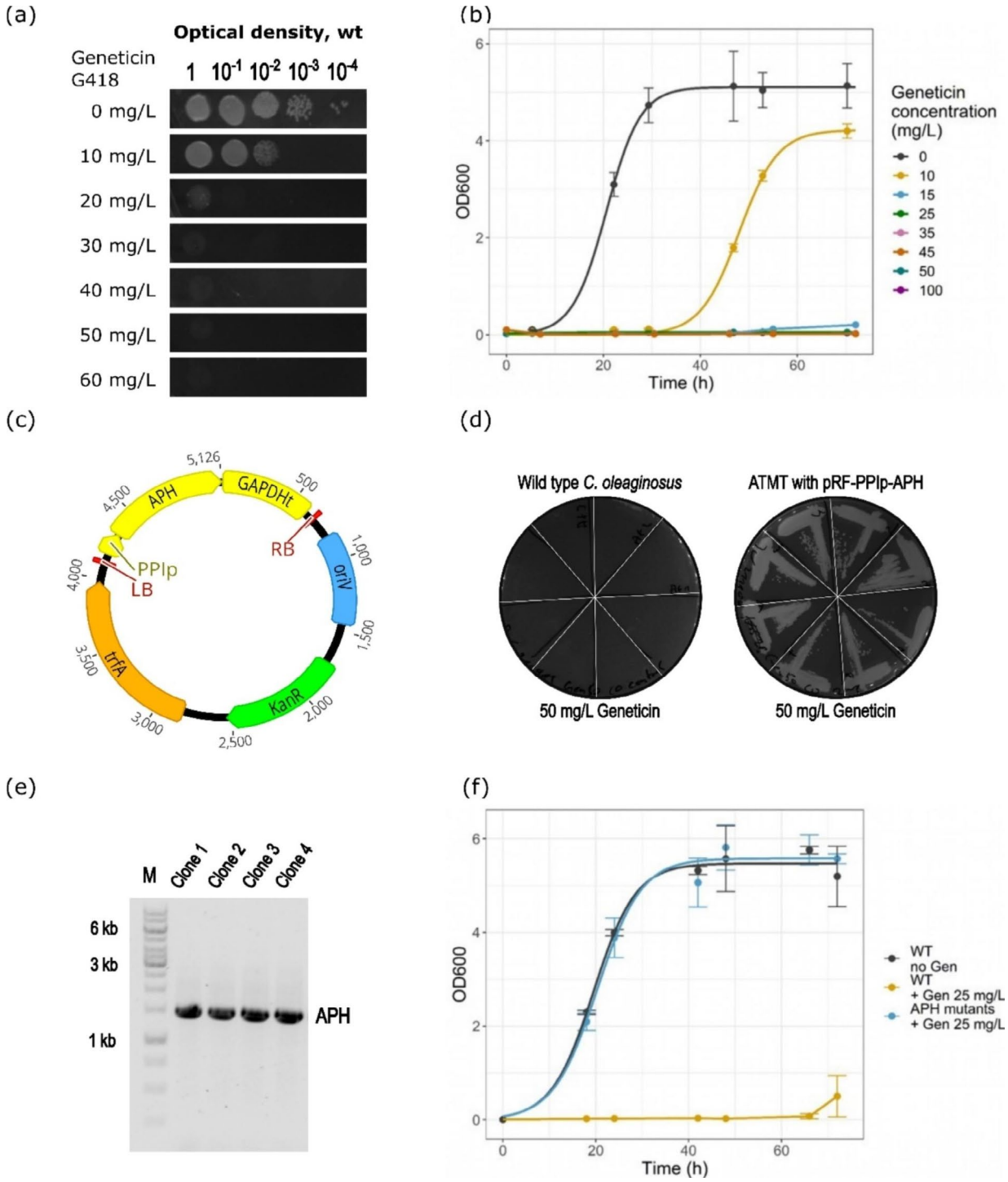


**Fig. 5** (**a**) Drop-test on solid media determining the minimal inhibitory concentration of geneticin G418 on *C. oleaginosus* wt. (**b**) Growth curves of *C. oleaginosus* wt with increasing concentrations of geneticin G418, determining the minimal inhibitory concentration in liquid media. (**c**) Map of the pRF_PPIp_APH plasmid, which was used for ATMT-derived integration of the APH resistance gene. Shown elements, besides the described gene cassette, include: KanR, bacterial kanamycin resistance; oriV, bacterial origin of replication; trfA, bacterial plasmid replication initiator protein. Plasmid maps were created with Geneious. (**d**) Restriped colonies after transformation of the wt control and the transformants on geneticin G418 plates. (**e**) Gel-electrophoresis of APH amplified by PCR (1599 bp) from genomic DNA of the transformants. The gel was cropped for clarity after lane 5, the complete gel picture is included in Figure S3. (**f**) Growth curves of the transformants and the wt, in triplicates, with and without the addition of geneticin. APH, aminoglycoside 3′-phosphotransferase; Gen, geneticin; wt, wild type

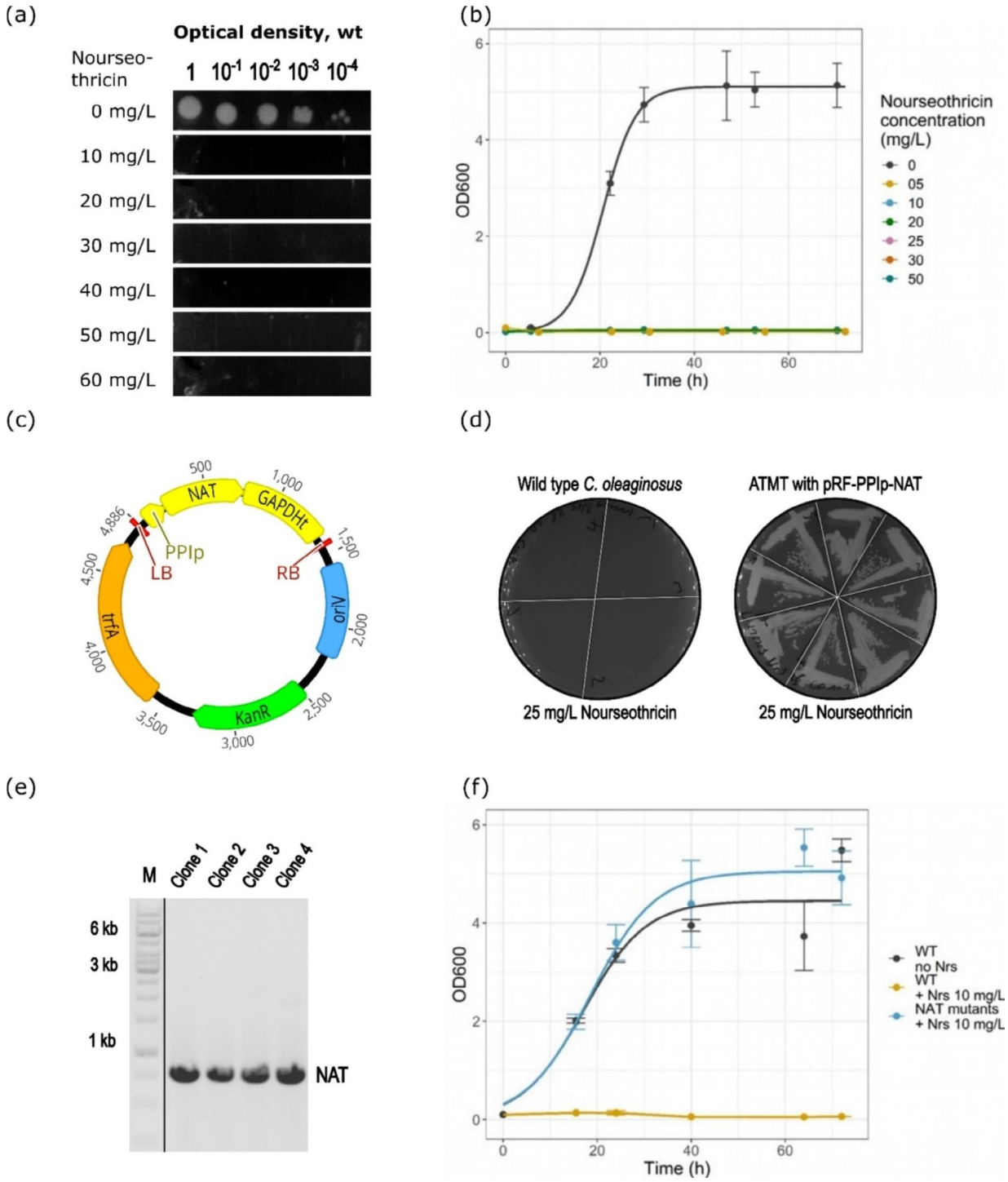


**Fig. 6** (**a**) Drop-test on solid media determining the minimal inhibitory concentration of nourseothricin on *C. oleaginosus* wt. (**b**) Growth curves of *C. oleaginosus* wt with increasing concentrations of nourseothricin, determining the minimal inhibitory concentration in liquid media. (**c**) Map of the pRF_PPIp_NAT plasmid, which was used for ATMT-derived integration of the NAT resistance gene. Shown elements, besides the described gene cassette, include: KanR, bacterial kanamycin resistance; oriV, bacterial origin of replication; trfA, bacterial plasmid replication initiator protein. Plasmid maps were created with Geneious. (d) Restriped colonies after transformation of the wt control and the transformants on nourseothricin plates. (**e**) Gel-electrophoresis of NAT amplified by PCR (783 bp) from genomic DNA of the transformants. The gel was cropped for clarity between the marker (**M**) and the lanes 2 to 5 and after lane 5, the complete gel picture is included in Figure S3. (**f**) Growth curves of the transformants and the wt, in triplicates, with and without the addition of nourseothricin. NAT, N-acetyl transferase; Nrs, nourseothricin; wt, wild type

**Table 2** Integration of the two dominant markers via ATMT into *C. oleaginosus*. Transformation efficiency, positive rate, and stability of the mutants are accessed by growth behavior and sequence confirmation. APH, aminoglycoside 3'-phosphotransferase; CFU, colony forming units; Gen, geneticin; NAT, N-acetyl transferase; Nrs, nourseothricin; suc, successive; sim, simultaneous

| Dominant marker integrated into *C. oleaginosus* | Antibiotics added | Picked CFUs from three membranes | Growth on solid media + antibiotics | Growth in liquid media + antibiotics | Sequence confirmed |
|---|---|---|---|---|---|
| APH | Gen | 72 | 65/72 (90%) | 32/32 (100%) | 3/3 (100%) |
| NAT | Nrs | 72 | 70/72 (97%) | 32/32 (100%) | 3/3 (100%) |
| APH/NAT suc | Gen + Nrs | 32 | 32/32 (100%) | 18/18 (100%) | 9/9 (100%) |
| NAT/APH suc | Gen + Nrs | 32 | 30/32 (94%) | 16/16 (100%) | 4/4 (100%) |
| APH/NAT sim | Gen + Nrs | 17 | 14/17 (82%) | 11/11 (100%) | 4/4 (100%) |

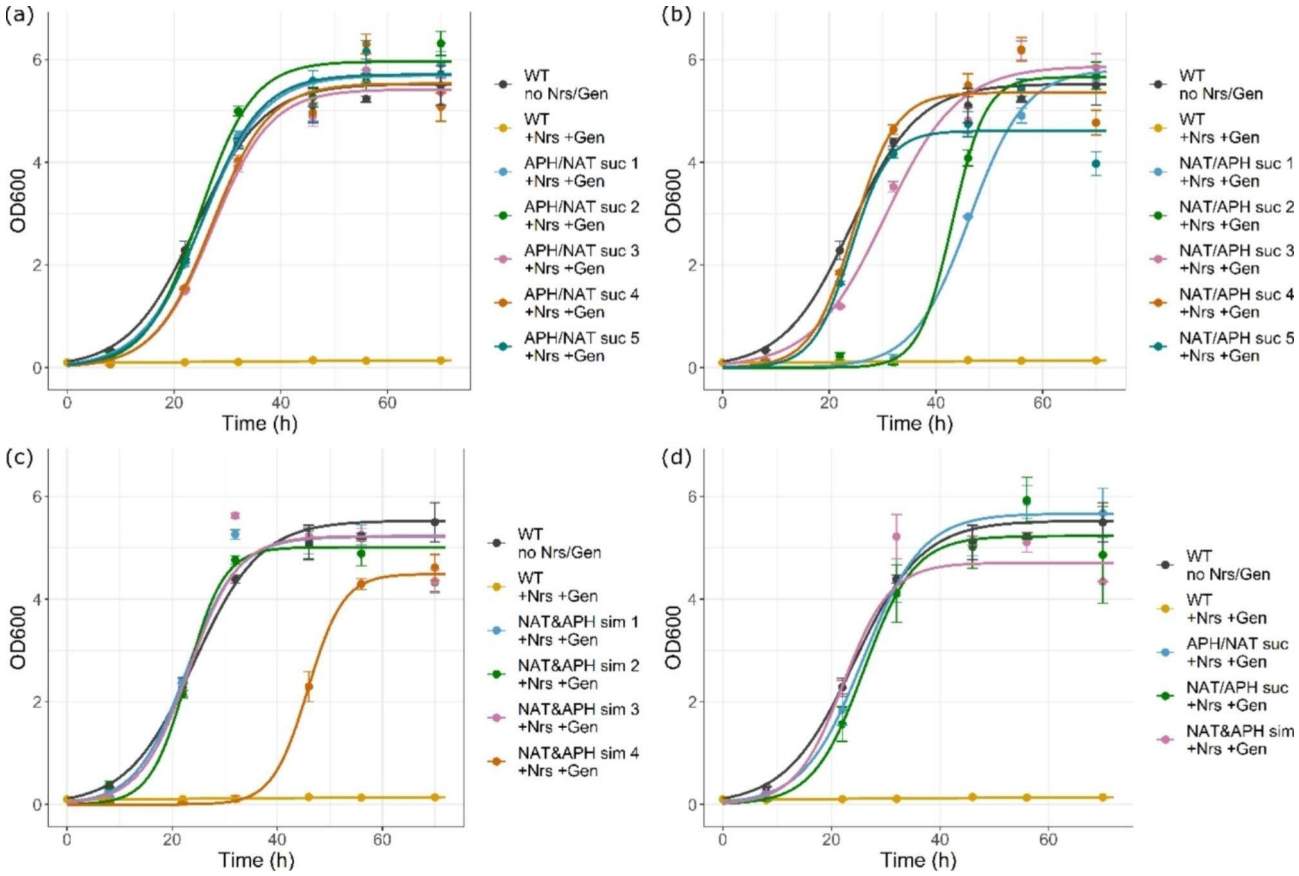


**Fig. 7** Growth curves of double mutants with the addition of both antibiotics (+ Nrs + Gen) in comparison to *C. oleaginosus* wt with and without the addition of both antibiotics. (**a**) Five double mutants from successive integration of APH/NAT in comparison to *C. oleaginosus* wt. (**b**) Five double mutants from successive integration of NAT/APH in comparison to *C. oleaginosus* wt. (**c**) Four double mutants from simultaneous integration of APH/NAT in comparison to *C. oleaginosus* wt. (**d**) Average from the biological replicates from (**a**, **b**, **c**), excluding the outliers with delayed growth behavior. APH, aminoglycoside 3'-phosphotransferase; Gen, geneticin; NAT, N-acetyl transferase; Nrs, nourseothricin; suc, successive; sim, simultaneous; wt, wild type

for four to five of the verified mutants. *C. oleaginosus* wt in YPD without the addition of antibiotics was used as a reference, and a negative control with the wt yeast and the addition of 25 mg/L geneticin and 10 mg/L nourseothricin was cultivated as well. The mutants for the successive APH/NAT integration showed very stable growth in between the different mutants and were comparable to the wt in YPD without the antibiotics, as shown in Fig. 7a. Using the other successive order NAT/APH for combined integration the growth curves were less uniform. Two mutants showed a much longer lag-phase in growth, compared to the positive control, see Fig. 7b. For the simultaneous integration of both APH and NAT, three of the four mutants showed a growth behavior very similar to the positive control. One clone had a much longer lag-phase, and the fifth clone did not grow in the pre-culture and was therefore excluded. Figure 7c shows the growth behavior of *C. oleaginosus* transformants from a simultaneous integration of APH and NAT. The variability in between the biological replicates was higher,

as one of the putative positive clones did not grow in recultivation conditions for the preculture, and therefore only four replicates were analyzed. All three transformation strategies were summarized for better comparison without the outliers in Fig. 7d.

The combinatory ATMT confirmed that APH and NAT show no cross-activity and thus can be considered compatible. The antibiotics could still be used to apply selection pressure on transformants which already had the respective other resistance gene integrated into their genome. This is in line with the findings in the literature for the yeast *Schizosaccharomyces pombe* [24]. Further, the successful integration of both markers in a successive as well as a simultaneous manner is possible and reliable. The method of selection and further cultivation of positive mutants is suitable for the generation of genetically modified *C. oleaginosus* using more than one construct, resulting in high rates of positives after primary selection of putative mutants from transformation. The order of the successive genetic modification is not crucial, but as the APH seems to show more variation, it is recommended to use the order APH/NAT. This way the variability between the generated mutants is lower than with the other order of markers. The transformational efficiency of the simultaneous integrated APH/NAT mutants was much lower, as the transfection and integration of two constructs at the same time is less likely than for one construct at a time. However, it can be a time-saving alternative to two separate ATMTs of *C. oleaginosus*.

## Conclusion

The non-conventional yeast *C. oleaginosus* has great potential as production organism for the biotechnological production of lipids and oleochemicals. Until recently, limited accounts on the genetic engineering of this yeast were published in the literature. However, metabolic engineering of *C. oleaginosus* might be of high value for the optimization of substrate adaptation, product specification, as well as growth optimization, and by-product variation. The genetic toolbox described in the literature was limited to three promoters with rather long sequences of up to 913 bp and one dominant resistance marker, which produced false positive transformants, and often could not be recultivated after storage. In this study, the sequences of putative endogenous promoters were analyzed based on more than 280 highly expressed genes of *C. oleaginosus*. The promoter regions of the genes featured a CT-rich motif which is suspected to have regulatory function in the oleaginous yeast. Based on this CT-rich motif and a TIS the four putative promoter sequences D9FADp, UBIp, PPIp, and 60Sp were selected and used for a qualitative expression tests in comparison to the known endogenous promoter GAPDHp. All putative promoters initiated the expression of the resistance gene HPH. PPIp (154 bp) as the shortest element was chosen for the construction of plasmids for ATMT with the two dominant markers APH and NAT. Both markers showed high positive rates (90% and 97% of the screened transformants, respectively) and resulted in stable mutants, which could be recultivated in the presence of geneticin G418 (in case of APH) or nourseothricin (in case of NAT). Selection by streaking and cultivation in liquid media resulted in transformants that were positive for the integration, which was finally confirmed via sequencing. This qualifies APH and NAT as functional dominant markers for the genetic modification of the non-conventional yeast. Furthermore, the compatibility of the two dominant markers was demonstrated. The two antibiotic-resistance genes were successfully integrated successively and simultaneously. In both combination orders, the successive integration had a high transformation efficiency, positive rate, and resulted in mutants with resistance to both markers. Transformation with both constructs at the same time in a simultaneous approach resulted in a reduced transformation efficiency, but both resistance genes were successfully integrated. Using ATMT as a screening method, the genetic toolbox of *C. oleaginosus* was considerably expanded with the novel endogenous promoters and dominant resistance markers. In combination with new targeted genomic integration methods as recently reported, the established tools from this study open up new opportunities for genetic and metabolic engineering of the industrially highly relevant yeast *C. oleaginosus*.

## Materials and methods

### Motif discovery

Genomic DNA sequences and transcriptional data of *C. oleaginosus* were used as published by Kourist et al. (2015) [3]. The selection of the 310 highest expressed genes was based on the proteomics data from Fuchs et al. (2021) with glucose as carbon source [5]. The extraction of specific sequence regions was performed with the RSAT retrieve sequence tool for fungi [31]. The regions were selected either relative to the start of the annotated coding sequence (CDS) or the mRNA start. TATA-box identification was mainly attempted with sequences from −200 bp to -1 bp relative to the mRNA start. For TSS identification the region from −30 bp to +10 bp relative to the mRNA start was selected. UAS identification was done with the RSAT default settings, selecting −800 bp to -1 bp (to mRNA) dismissing regions where other genetic elements are annotated. TIS annotation was performed with a dataset with 50 bp upstream and 50 bp downstream relative to CDS start. For motif discovery, the MEME suite was employed, with the MEME tool for novel motif discovery and FIMO for motif annotation

within specific sequences [32, 33]. For motif discovery with MEME, default settings were used, with edited minimal motif length for the TATA-box search. FIMO was employed with default settings.

### Strain and cultivation on plates

The oleaginous yeast *Cutaneotrichosporon oleaginosus* (ATCC 20509 / DSM-11815) was retrieved from the Deutsche Sammlung von Mikroorganismen und Zellkultur (DMSZ, Braunschweig, Germany). *C. oleaginosus* was cultivated on agar plates to obtain single colonies for cultivation, mutant screening, recovery from cryo-stocks, and the determination of the minimal inhibition concentration of antibiotics. Yeast extract peptone dextrose (YPD) with 1.2% agar was used as solid medium for the plates, optionally with the addition of different concentrations of antibiotics. The plates were incubated at 28 °C for at least one day or up to three days until visible colonies appeared. For cell separation, screening, and recovery, cells were streaked out to obtain single colonies.

**Table 3** Plasmids used in this study with two dominant resistance makers under the control of different endogenous *C. oleaginosus* promoters

| Plasmid no. | Plasmid name | Promoter regulating the resistance gene | Resistance gene | Origen |
|---|---|---|---|---|
| 1 | pRF_GAPDHp-HPH | Glyceraldehyde 3-phosphate dehydrogenase (GAPDH) | Hygromycin phosphotransferase (HPH) | Görner et al. [13] |
| 2 | pRF_D9FADp-HPH | Delta-9 Fatty acid desaturase (D9FAD) | Hygromycin phosphotransferase (HPH) | this study |
| 3 | pRF_UBIp-HPH | Ubiquitin and ubiquitin-like proteins (UBI) | Hygromycin phosphotransferase (HPH) | this study |
| 4 | pRF_PPIp-HPH | Cyclophilin type peptidyl-prolyl cis-trans isomerase (PPI) | Hygromycin phosphotransferase (HPH) | this study |
| 5 | pRF_60Sp-HPH | 60 S ribosomal protein L37 (60 S) | Hygromycin phosphotransferase (HPH) | this study |
| 6 | pRF_PPIp-APH | Cyclophilin type peptidyl-prolyl cis-trans isomerase (PPI) | Aminoglycoside 3'-phosphotransferase (APH) | this study |
| 7 | pRF_PPIp-NAT | Cyclophilin type peptidyl-prolyl cis-trans isomerase (PPI) | Nourseothricin N-acetyl transferase (NAT) | this study |

### Drop tests on plates

To assess the cytotoxicity and the minimal inhibitory concentration of different antibiotics towards *C. oleaginosus*, YPD plates were prepared with a dilution series of the respective antibiotics. YPD plates included 0–70 mg/L Geneticin sulfate G418 (Burlington, United States) or 0–60 mg/L nourseothricin (Carl Roth, Lausanne, Switzerland). An overnight *C. oleaginosus* culture in YPD was adjusted with fresh YPD to an $OD_{600}$ of 1. From that, a serial dilution was prepared in steps with a factor of 10 until the minimal count of colony-forming units (CFU) on a YPD plate was around between 0.1 and 1 CFU/µL. 2 µL of each dilution was dropped on the antibiotic-containing plate. The plates were incubated at 28 °C for two days and the growth was documented with the CHEMI Premium Imager (VWR International, Germany).

### Cultivation in liquid media

Cultivation was performed in YPD broth and incubated at 28 °C while shaking at 120 rpm. When using shaking flasks 20% of the total volume was used for cultivation. Pre-cultures were inoculated with single colonies from agar plates, main cultures were inoculated to an $OD_{600}$ of 0.1 from the pre-culture, measured with an Implen NanoPhotometer® (Implen, Munich, Germany). For growth curves, 24-well deep well plates were used with 2.5 mL culture in each well (total well volume of 10 mL) and incubated under humid conditions at 180 rpm shaking speed. $OD_{600}$ was measured in 100 µL volume with the EnSpire™ Multimode Plate Reader by PerkinElmer Inc. in 96-well clear microtiter plates, diluted to a measured $OD_{600}$ between 0.1 and 0.6.

### Promoters, resistance genes, and plasmids

To retrieve the promoter sequences for GAPDHp, 60Sp, PPIp, UBIp, and D9FADp primers flanking the identified promoter regions were used for amplification from genomic DNA, constructs are listed in Table 3. The primer sequences as well as the gene sequences are listed in the supplementary material Sequences.xslx. The plasmids featuring the HPH resistance gene (pRF_GAPDHp-HPH) were constructed based on a modified version of the plasmid pRF-HU2 previously described for *A. tumefaciens*-mediated transformation in *C. oleaginosus* [13]. The shuttle vector included the landing pads required for *A. tumefaciens*-mediated genomic integration as well as the bacterial kanamycin resistance cassette KanMX and the bacterial oriV system. GADPHp in the pRF_GAPDHp-HPH was replaced by any of the other promoters reported in this study, as indicated in the plasmid Table 3. The hygromycin B resistance gene in pRF_PPIp-HPH was replaced by the sequence of either APH or NAT, resulting in the two vectors pRF_PPIp-APH and pRF_PPIp-NAT.

The amino acid sequence for APH as the geneticine G418 resistance was obtained from the established dominant kanamycin resistance marker transposon Tn903 (Uniprot ID: P00551). In the case of NAT as the nourseothricin resistance marker, the protein sequence of the enzyme from *Streptomyces noursei* was used (Uniprot ID: Q08414). The enzyme amino acid sequences were reversely translated using the Kazusa webtool (www.kazusa.or.jp/codon, 2018, Kazusa DNA Research Institute, Japan) for codon-optimized expression in *C. oleaginosus* and synthesized by Eurofins Genomics Germany GmbH (Ebersberg, Germany). Cloning of the plasmids was done by restriction cloning and/or Gibson assembly. The *Escherichia coli* laboratory strain DH5 α strain was used for selection and amplification of all constructed plasmids. The sequences were verified by Sanger sequencing by Eurofins Genomics Germany GmbH (Ebersberg, Germany).

### *Agrobacterium tumefaciens*-mediated transformation

The integration of DNA sequences, potentially, into the genome of *C. oleaginosus* transformation was done with *Agrobacterium tumefaciens* according to Görner et al., 2016 [13]. In short, cells of *Agrobacterium tumefaciens* were transformed with the shuttle vector pRF containing the respective marker gene, using electroporation and selection on LB plates containing 30 µg/mL kanamycin. Overnight liquid cultures were then prepared from single colonies of the *A. tumefaciens* transformants in 5 mL LB medium with 30 µg/mL kanamycin at 28 °C. These cultures were used to inoculate 10 mL L-IMAS medium in shaking flasks, which were then incubated at 28 °C for 6 h. An overnight culture of *C. oleaginosus* was diluted to an $OD_{600}$ of 0.5. 50 µl of the *C. oleaginosus* dilution and 50 µL of the 6-hour *A. tumefaciens* culture were mixed. The mixture was then plated onto an Amersham Hybond-$N^+$ blotting membrane from GE Healthcare (Little Chalfont, United Kingdom) on top of an S-IMAS agar plate. The plates were incubated at 24 °C for 48 h and the membranes were subsequently transferred onto YPD agar plates containing an elevated concentration of the respective antibiotics: 150 µg/mL Hygromycin B (AppliChem GmbH, Darmstadt, Germany), 100 µg/mL geneticin G418 (Carl Roth GmbH, Karlsruhe, Germany) or 50 µg/mL nourseothricin (Carl Roth GmbH, Karlsruhe, Germany) or combinations thereof. To inhibit agrobacteria growth, also 300 µg/mL cefotaxime (Thermo Fisher Scientific Inc., Waltham, USA) was included in the plates. The method is visualized in Fig. 3.

### Screening of mutants

After transformation, single colonies were picked from the membrane and streaked out on YPD plates containing 300 µg/mL cefotaxime. To select for the respective antibiotic resistance 70 µg/mL hygromycin B, 50 µg/mL geneticin, or 25 µg/mL nourseothricin or combinations thereof were included in the solid media. Plates were incubated for two to three days until visible single colonies formed. Single colonies were then used for inoculation of 5 mL YPD medium supplemented with 35 µg/mL hygromycin B, 25 µg/mL geneticin G418, 10 µg/mL nourseothricin, or a combination thereof. Transformants that were able to grow in liquid cultures were pelleted and the genomic DNA was extracted using the Yeast DNA Extraction Kit from Thermo Fisher Scientific™ (Waltham, USA). PCR was then performed for the amplification of the DNA of the resistance markers and the results were versified via gel electrophoresis. Phusion™ High-Fidelity DNA Polymerase was employed and all reactions were performed with GC buffer and at annealing temperatures according to primer melting temperature. Elongation time was calculated with 20 s/kb for each individual fragment. Final verification of genomic gene integration was done by sanger sequencing at Eurofins Genomics GmbH (Ebersberg, Germany) after DNA purification with NEB Monarch® DNA Gel Extraction Kit (Ipswich, USA).

#### Abbreviations

| | |
|---|---|
| 60Sp | 60 S ribosomal protein L37 promoter |
| AKR | aldo-keto reductase AKR |
| APH | aminoglycoside 3′-phosphotransferase |
| ATMT | *Agrobacterium tumefaciens*-mediated transformation |
| CFU | colony forming units |
| D9FADp | delta-9 fatty acid desaturase promoter |
| GAPDHp | glycerinaldehyde 3-phosphate dehydrogenase promoter |
| Gen | geneticin G418 |
| HPH | hygromycin B phosphotransferase |
| KanR | kanamycin resistance cassette |
| NAT | N-acetyl transferase |
| Nrs | nourseothricin |
| PPIp | cyclophilin type peptidyl-prolyl cis-trans isomerase promoter |
| sim | simultaneous |
| suc | successive |
| TEF | transcription elongation factor |
| TF | transcription factor |
| TIS | translation initiation site |
| TSS | transcription start site |
| UAS | upstream activation sequences |
| UBIp | ubiquitin, and ubiquitin-like proteins promoter |
| UTR | untranslated region |
| wt | wild type |

## Supplementary Information

The online version contains supplementary material available at https://doi.org/10.1186/s12896-023-00812-7.

Supplementary Material 1

Supplementary Material 2

#### Acknowledgements

We would like to thank Petra Graban for her valuable assistance with the mutant screening. We thank Anna Drabarek for her diligent help with the cloning of the promoter constructs. Further, we thank Elisa Werner for her committed help with the cross-reactivity tests of the dominant markers. Finally, we thank Jeremias Widmann for his reliable support with cultivation and mutant handling.

**Author contributions**
Conceptualization, T.B., N.M., N.S. and Z.R.; methodology, N.S. and Z.R.; software, N.S. and Z.R.; validation, T.B., N.M., and M.R.; investigation, N.S. and Z.R.; resources, T.B.; data curation, M.R., N.S., and Z.R.; writing-original draft preparation, N.S. and Z.R.; writing-review and editing, M.R., and T.B.; visualization, N.S. and Z.R.; supervision, N.M., M.M., and M.R. All authors reviewed the manuscript.

**Funding**
Open Access funding enabled and organized by Projekt DEAL. This work was financially supported by The German Federal Ministry of Education and Research (Bundesministerium für Bildung und Forschung), grant number: FKZ 031B0662B. The funding body played no role in the design of the study and collection, analysis, interpretation of data, and in writing the manuscript.

**Data Availability**
The cloning vectors constructed during the current study are available in the GenBank repository, BankIt2716325, with the accession numbers: OR166493 (1_pRF_GAPDHp_HPH), OR166494 (2_pRF_D9FADp_HPH), OR166495 (3_pRF_UBIp_HPH), OR166496 (4_pRF_PPIp_HPH), OR166497 (5_pRF_60Sp_HPH), OR166498 (6_pRF_PPIp_APH), OR166499 (7_pRF_PPIp_NAT).

## Declarations

**Competing interests**
Thomas B. Brueck and Mahmoud Masri are board members at Global Sustainable Transformation GmbH. Nikolaus I. Stellner, Zora S. Rerop, Norbert Mehlmer, and Marion Ringel declare that they have no competing interests.

**Ethical approval and consent**
Not applicable.

**Consent to publish**
Not applicable.

Received: 9 June 2023 / Accepted: 8 September 2023
Published online: 18 September 2023

**References**

1. Spagnuolo M, Yaguchi A, Blenner M. Oleaginous yeast for biofuel and oleochemical production. Curr Opin Biotechnol. 2019;57:73–81.
2. Rerop ZS, Stellner NI, Graban P, Haack M, Mehlmer N, Brück TB et al. Bioconversion of a Lignocellulosic Hydrolysate to Single Cell Oil for Biofuel Production in a Cost-Efficient Fermentation Process. fermentation. 2023;9.
3. Kourist R, Bracharz F, Lorenzen J, Kracht ON, Chovatia M, Daum C, et al. Genomics and Transcriptomics Analyses of the Oil-Accumulating Basidiomycete Yeast. 2015;6:1–13.
4. Shaigani P, Awad D, Redai V, Fuchs M, Haack M, Mehlmer N, et al. Oleaginous yeasts- substrate preference and lipid productivity: a view on the performance of microbial lipid producers. Microb Cell Fact. 2021;20:1–18.
5. Fuchs T, Melcher F, Rerop ZS, Lorenzen J, Shaigani P, Awad D, et al. Identifying carbohydrate-active enzymes of Cutaneotrichosporon oleaginosus using systems biology. Microb Cell Fact. 2021;20:1–18.
6. Yaguchi A, Franaszek N, O'Neill K, Lee S, Sitepu I, Boundy-Mills K et al. Identification of oleaginous yeasts that metabolize aromatic compounds. J Ind Microbiol Biotechnol. 2020;47.
7. Masri M, Garbe D, Mehlmer N, Brück T. A sustainable, high-performance process for the economic production of waste-free microbial oils that can replace plant-based equivalents. Energy Environ Sci. 2019;12:2717–32.
8. Pham N, Reijnders M, Suarez-Diez M, Nijsse B, Springer J, Eggink G, et al. Genome-scale metabolic modeling underscores the potential of Cutaneotrichosporon oleaginosus ATCC 20509 as a cell factory for biofuel production. Biotechnol Biofuels. 2021;14:1–17.
9. Abeln F, Chuck CJ. The history, state of the art and future prospects for oleaginous yeast research. Microb Cell Fact. 2021;20:1–31.
10. Bracharz F, Beukhout T, Mehlmer N, Brück T. Opportunities and challenges in the development of Cutaneotrichosporon oleaginosus ATCC 20509 as a new cell factory for custom tailored microbial oils. Microb Cell Fact. 2017;16:1–15.
11. Di Fidio N, Minonne F, Antonetti C, Galletti AMR. Cutaneotrichosporon oleaginosus: a versatile whole-cell biocatalyst for the production of single-cell oil from agro-industrial wastes. Catalysts. 2021;11.
12. Stellner NI, Rerop ZS, Kyselka J, Alishevich K, Beneš R, Filip V, et al. Value-added squalene in single cell oil produced with Cutaneotrichosporon oleaginosus for food applications. J Agric Food Chem. 2023.
13. Görner C, Redai V, Bracharz F, Schrepfer P, Garbe D, Brück T. Genetic engineering and production of modified fatty acids by the non-conventional oleaginous yeast Trichosporon oleaginosus ATCC 20509. Green Chem. 2016;18:2037–46.
14. Koivuranta K, Castillo S, Jouhten P, Ruohonen L, Penttilä M, Wiebe MG. Enhanced triacylglycerol production with genetically modified Trichosporon oleaginosus. Front Microbiol. 2018;9 JUN:1–15.
15. Hooykaas PJJ, van Heusden GPH, Niu X, Roushan MR, Soltani J, Zhang X, et al. Agrobacterium-mediated Transformation of yeast and Fungi. Curr Top Microbiol Immunol. 2018;418:435.
16. Bundock P, Den Dulk-Ras A, Beijersbergen A, Hooykaas PJJ. Trans-kingdom T-DNA transfer from Agrobacterium tumefaciens to Saccharomyces cerevisiae. EMBO J. 1995;14:3206–14.
17. De Groot MJA, Bundock P, Hooykaas PJJ, Beijersbergen'. AGM. Agrobacterium tumef aciens-n1ediate d transforn1ation of filan1entous fungi. Nat Biotechnol. 1998;16:839–42.
18. Shaigani P, Fuchs T, Graban P, Prem S, Haack M, Masri M, et al. Mastering targeted genome engineering of GC – rich oleaginous yeast for tailored plant oil alternatives for the food and chemical sector. Microb Cell Fact. 2023;22:1–14.
19. Shabbir Hussain M, Gambill L, Smith S, Blenner MA. Engineering promoter Architecture in oleaginous yeast Yarrowia lipolytica. ACS Synth Biol. 2016;5:213–23.
20. Park YK, Nicaud JM, Ledesma-Amaro R. The Engineering potential of Rhodosporidium toruloides as a workhorse for Biotechnological Applications. Trends Biotechnol. 2018;36:304–17.
21. Solis-Escalante D, Kuijpers NGA, Bongaerts N, Bolat I, Bosman L, Pronk JT, et al. amdSYM, a new dominant recyclable marker cassette for Saccharomyces cerevisiae. FEMS Yeast Res. 2013;13:126–39.
22. Kretzschmar A, Otto C, Holz M, Werner S, Hübner L, Barth G. Increased homologous integration frequency in Yarrowia lipolytica strains defective in non-homologous end-joining. Curr Genet. 2013;59:63–72.
23. Wach A, Brachat A, Pöhlmann R, Philippsen P. New heterologous modules for classical or PCR-based gene disruptions in Saccharomyces cerevisiae. Yeast. 1994;10:1793–808.
24. Hentges P, Van Driessche B, Tafforeau L, Vandenhaute J, Carr AM. Three novel antibiotic marker cassettes for gene disruption and marker switching in Schizosaccharomyces pombe. Yeast. 2005;22:1013–9.
25. Young R, Grillo DS, Isberg R, Way J, Syvanen M. Transposition of the kanamycin-resistance transposon Tn903. MGG Mol Gen Genet. 1980;178:681–9.
26. Van Driessche B, Tafforeau L, Hentges P, Carr AM, Vandenhaute J. Additional vectors for PCR-based gene tagging in Saccharomyces cerevisiae and Schizosaccharomyces pombe using nourseothricin resistance. Yeast. 2005;22:1061–8.
27. Kourist R, Bracharz F, Lorenzen J, Kracht ON, Chovatia M, Daum C, et al. Genomics and Transcriptomics analyses of the oil-accumulating basidiomycete yeast. MBio. 2015;6:1–13.
28. Liu Y, Yap SA, Koh CMJ, Ji L. Developing a set of strong intronic promoters for robust metabolic engineering in oleaginous Rhodotorula (Rhodosporidium) yeast species. Microb Cell Fact. 2016;15:1–9.
29. Basehoar AD, Zanton SJ, Pugh BF, Erratum. Identification and distinct regulation of yeast TATA box-containing genes (cell (March 2004). Cell. 2004;116:699–709.
30. Rhee HS, Pugh BF. Genome-wide structure and organization of eukaryotic pre-initiation complexes. Nature. 2012;483:295–301.
31. Nguyen NTT, Contreras-Moreira B, Castro-Mondragon JA, Santana-Garcia W, Ossio R, Robles-Espinoza CD, et al. RSAT 2018: Regulatory sequence analysis tools 20th anniversary. Nucleic Acids Res. 2018;46:W209–14.
32. Bailey TL. Discovering Novel sequence motifs with MEME. Current protocols in Bioinformatics. John Wiley & Sons, Inc.; 2003. p. 2.4.1–35.
33. Grant CE, Bailey TL, Noble WS. FIMO: scanning for occurrences of a given motif. Bioinformatics. 2011;27:1017–8.
34. Kourist R, Bracharz F, Lorenzen J, Kracht ON, Chovatia M, Daum C, et al. Genomics and transcriptomics analyses of the oil-accumulating basidiomycete yeast Trichosporon oleaginosus: insights into substrate utilization

and alternative evolutionary trajectories of fungal mating systems. MBio. 2015;6:1–13.
35. Randise-Hinchliff C, Brickner JH. Transcription factors dynamically control the spatial organization of the yeast genome. Nucleus. 2016;7:369–74.
36. Levo M, Segal E. In pursuit of design principles of regulatory sequences. Nat Rev Genet. 2014;15:453–68.
37. Kirkpatrick DT, Fan Q, Petes TD. Maximal stimulation of meiotic recombination by a yeast transcription factor requires the transcription activation domain and a DNA-binding domain. Genetics. 1999;152:101–15.
38. Nguyen DX, Sakaguchi T, Nakazawa T, Sakamoto M, Honda Y. A 14-bp stretch plays a critical role in regulating gene expression from β1 -tubulin promoters of basidiomycetes. Curr Genet. 2019;66:217–28.
39. Chua G. Identification of transcription factor targets by phenotypic activation and microarray expression profiling in yeast. In: Stagljar I, editor. Yeast Functional Genomics and Proteomics. Humana Press; 2009. pp. 19–36.
40. Robbins-Pianka A, Rice MD, Weir MP. The mRNA landscape at yeast translation initiation sites. Bioinformatics. 2010;26:2651–5.
41. Kozak M. Pushing the limits of the scanning mechanism for initiation of translation. Gene. 2002;299:1–34.
42. Kozak M. The scanning model for translation: an update. J Cell Biol. 1989;108:229–41.
43. Schiestl RH, Gietz RD. High efficiency transformation of intact yeast cells using single stranded nucleic acids as a carrier. Curr Genet. 1989;16:339–46.

## Publisher's Note

# Part IV.

# Discussion

# 5 Discussion

## 5.1 Single-cell oil as value creation from waste streams

### Traditional oil production and its limitations

The extensive land use associated with traditional agriculture is a drawback that will become increasingly problematic as the global population continues to grow [125]. Palm oil production, for instance, has a particularly detrimental impact on the rainforests and the environment on a global scale, with an annual production volume of 75.8 million metric tons [5]. The valuable carbon sink of the rainforest is currently being destroyed, the use of pesticides has increased, resulting in a drastically reduced biodiversity and barren soils [5]. In addition, palm oil production contributes to the emission of nitrous oxide and methane, two potent greenhouse gases [126]. Unfortunately, the yield per hectare of palm, at 5,950 L/ha, still surpasses that of other vegetable oil crops such as rapeseed (1,190 L/ha) and soybean (446 L/ha) [5]. Therefore, vegetable oil production cannot be the only solution to the growing demand for oil in the future. Innovative approaches are required to develop sustainable and environmentally friendly methods of oil production, such as the bioconversion of lignocellulosic waste into yeast oil. These alternative routes can help to reduce pressure on land resources while providing renewable and more sustainable options to meet the future oil demand.

### Single-cell oil as an alternative

Single-cell oil has the potential to be a solution for a circular and environmentally friendly industrial oil production. Notably, SCO production requires only a tiny fraction of the land used in traditional agriculture [4, 127]. Studies demonstrated that SCO can be effectively produced through a three-day fermentation process. Although additional time is required for subsequent processing, the overall timeframe remains considerably shorter compared to growing oil crops. In addition, climate change, in such forms as heat waves or rising temperatures, has less impact on bioreactor-based production than on regional crops. In addition, SCO production is flexible and can be adapted to climate-related changes in agriculture that will provide new raw materials in the future.

The composition of SCO can differ significantly from vegetable oil or animal fats, as shown in table 5.1. Protists such as *Thrautromyces* species often have odd-chain fatty acids in their spectrum and high levels of long poly-unsaturated fatty acids [128]. The long poly-unsaturated fatty acids are also very abundant in microalgae such as *Dunaliella* [129]. These profiles do not match the vegetable oils and animal fats, which usually do not have uneven or no long poly-unsaturated fatty acids [5]. Tropical vegetable oils, as well as animal fats, are rich in palmitic acid and monounsaturated fatty acids (C16:1, C18:1), while vegetable oil plants from temperate climates like soybean have a much higher content of longer and saturated fatty acids such as C16:1, C18:1, C16:2, C18:2, and

**Table 5.1.:** Comparison of the fatty acid profiles of different oil sources with a general range and a specific example. sum - summary.

| Category | Organism of origin | Fatty acid profile (%) | | | | | | | Ref. |
|---|---|---|---|---|---|---|---|---|---|
| | | Medium chain (8:0-14:0) | Odd (15:0, 17:0) | Palmitic (16:0) | Steric (18:0) | Mono-unsat. (16:1, 18:1) | poly-unsat. (16:2, 18:2, 18:3) | long poly-unsat. (20:4-20:5, 22:4-22:6) | |
| Vegetable, tropical | Tropical crops | 0-66 | | 6-45 | 2-41 | 6-49 | 1-11 | | [5] |
| | Palm | 0 | | 45 | 5 | 38 | 11 | | [5] |
| Vegetable, temperate | Temperate crops | 0 | | 5-13 | 1-5 | 22-61 | 32-69 | | [5] |
| | Soybean | 0 | | 11 | 4 | 22 | 62 | | [5] |
| Animal | Livestock | 2-3 | | 27 | 7-11 | 48-59 | 2-11 | | [5] |
| | Tallow | 3 | | 27 | 7 | 59 | 2 | | [5] |
| Microbial, protists | Thraustro-myces | 0-1.8 | 4-50 | 4-35 | 0-8 | 0-16 | 0-1 | 42-70 | [128] |
| | *Aurantiochy-trium* sp. JS702 | 0.6 | 25 | 11 | 0.2 | 0.1 | 0 | 62 | [128] |
| Microbial, algae | sum. Mi-croalgae | 0-43 | | 10-46 | 0-18 | 11-74 | 0-51 | 0-46 | [129] |
| | *Dunaliella primolecta* | 0.4 | | 22 | 0.8 | 11 | 48 | 4 | [129] |
| Microbial, fungi | sum. Oleagi-nous yeast | | | 15-32 | 0-25 | 44-67 | 6-23 | | [60] |
| | *Cutaneotrichc oleaginosus* | 0.4 | | 24.5 | 16 | 54.8 | 5.4 | | this work [63] |

C18:3 [5]. These differences in fatty acid composition pose challenges in replacing tropical palm oil with other vegetable oils, often difficult because the oils have different properties, such as the cloud and the melting points [5]. With a higher proportion of saturated fatty acids, tropical oils usually have a higher melting point, which is about 30-38°C for palm oil [130]. These oils are, therefore, semi-liquid and solid at room temperatures of about 25°C, while temperate vegetable oils are usually completely liquid above 0°C [130].

Fortunately, oils derived from oleaginous yeasts can in some cases approach the fatty acid profile of tropical oils, making them suitable substitutes. By selecting strains with desired fatty acid profiles or optimizing process parameters, it is possible to modify the fatty acid composition [131, 132, 133]. Strain development strategies involving random and targeted genetic modification can also be employed to specifically tailor the fatty acid profile of oleaginous yeasts [18, 134].

In addition to fatty acids, other components of oils and fats are important, particularly pigments, flavors, oxidative stability, and bioactive compounds such as sterols. The presence of these compounds, such as tocopherols, sterols and squalene, is highly dependent on the production organism. Some of these compounds are tocopherols, sterols, and squalene. While animal fat contains

cholesterol, plants produce $\beta$-sitosterol, campesterol, and stigmasterol, which are known to reduce cholesterol levels and have anti-inflammatory properties [135]. Fungi, including yeast, produce ergosterol, a natural precursor of vitamin D, as well as various hormones and secondary metabolites [136]. Some vegetable oils, such as olive oil, can contain significant amounts of pigments and off-flavors when extracted from the fruit [137, 138]. Single-cell oils may also contain pigments, but not all do, and often only in smaller quantities, such as the oil of *C. oleaginosus*. The flavor profile of single-cell oils has not been extensively studied, but an internal evaluation revealed a flavor profile close to that of refined palm oil for *C. oleaginosus* [oral communication Dr. Mahmoud Masri].

**Benefits and future potential of waste stream utilization**

Waste streams are ideal substrates for biotechnological processes due to their potential to provide low-cost and widely available carbon sources for bioconversion [139]. To make industrial biotechnological processes economically viable, it is desirable to avoid costly purified monomeric sugars as feedstocks. Therefore, a key priority for upscaling biotechnological processes is to identify and utilize low-cost feedstocks that are abundant by-products or waste streams from extensive industrial processes. Ideally, the feedstocks will be low-cost but high in biodegradable carbon. Lignocellulosic materials are particularly interesting in this regard, as they are readily available in large quantities as waste from agricultural and forestry processes [11]. The choice of the raw material also depends on the future application and the desired purity, especially for hydrophobic compounds. Substrates containing potential fat-soluble toxins may not be suitable for food or cosmetic applications but could still be utilized for oleochemicals or biofuels. On the other hand, substrates that are free of hydrophobic toxins or that can be degraded by microorganisms have potential applications in pharmaceuticals, cosmetics, animal feed, or food.

In many agricultural products and processes, digestible carbohydrates and proteins are primarily found in seeds or fruits. These components include carbohydrates such as starch, oligo- and disaccharides such as sucrose and lactose, and monomeric sugars such as glucose and fructose [140]. On the other hand, nondigestible plant parts often contain significant amounts of cellulose, lignin, and hemicellulose. These feedstocks can be derived from crops such as grains, rice, corn, or others, as well as associated by-products such as bran, husks, hulls, stover, or straw [13, 25]. In addition, fast-growing crops such as poplar, miscanthus, or microalgae offer interesting feedstock options [4, 25]. Forestry waste streams such as wood chips, sawdust, bark, or spent liquor from pulp production in which cellulose has been separated can be used as well [22]. Of particular interest are materials that have already undergone other processes and have been pretreated or separated into their constituent parts. Examples include manure, sugarcane bagasse, brewer's spent grains, or spent pulp liquor [11, 25]. Although these waste streams may still contain pentose sugars, lignins, and organic acids, they are not suitable to be included in the main processes and products but are highly attractive for SCO production with *C. oleaginosus*.

Pretreatment of lignocellulosic waste is a critical step in bioconversion, as it reduces the structural complexity of the biomass and improves biological accessibility. Enzymatic hydrolysis can be a subsequent step, releasing fermentable sugars, mainly glucose, and xylose. Potential inhibitors or high levels of inorganic material need to be removed before the hydrolysate can be transferred to a fermentation medium. The pretreatment process must be cost-effective while retaining the

carbon sources needed for bioconversion. In addition, the process must be designed to avoid storing the material in non-sterile and potentially good microbial growth conditions, as the microbial load should not increase drastically. This study demonstrated the successful pretreatment of an abundant waste stream from the pulp industry. By optimizing the pretreatment, a highly potent fermentation medium was formulated that was suitable for the cultivation of *C. oleaginosus* to produce high amounts of single-cell oil. Lignin compounds and small amounts of furans are not a problem for *C. oleaginosus*, but may potentially be for other yeasts. Pretreatment and media formulation must be specific to each substrate, as different biomasses may present additional challenges, such as salinity, pH, inhibitors, or hydrolysis. Based on the pretreatment strategy developed in this work, related waste streams can be accessed easier in the future.

Industrial waste streams feature various constituents, each with its own structural complexity and chemical composition. Effective pretreatment strategies are essential to overcome these challenges and improve nutrient accessibility for microorganisms. Different methods thereof, such as physical, chemical, and biological treatments, need to be optimized to maximize substrate conversion and SCO production. Bioconversion of lignocellulosic wastes to yeast oil offers significant environmental benefits. The use of waste biomass as a feedstock can help reduce greenhouse gas emissions and decrease dependence on fossil fuels and extensive monocultures. In addition, it helps address the waste management challenges associated with lignocellulosic residues [141]. From an economic perspective, the production of high-quality SCO offers opportunities for revenue generation and a modern marketing strategy that considers environmental aspects.

## 5.2 *C. oleaginosus*, a complex and versatile organism

**Substrate spectrum and metabolism**

The unconventional yeast *C. oleaginosus* has a broad spectrum of carbon sources that can be metabolized and used for cell growth and energy storage in the form of lipid bodies. Interestingly, it can utilize xylose, a pentose sugar that is not bio-accessible by all organisms [72]. *C. oleaginosus* does not show diauxic growth behavior and can metabolize xylose to glucose simultaneously [4]. Furthermore, it has the ability to utilize certain aromatic compounds and organic acids as carbon sources [118]. This substrate flexibility makes *C. oleaginosus* an ideal candidate for the production of SCO from lignocellulosic hydrolysates. Especially with acetic acid as feed during fermentation, high lipid yields can be achieved, as shown in this work. Although it is not known how the uptake of acetic acid and conversion to acetate takes place inside the cell, the metabolic pathway from acetate to fatty acid synthesis has been analyzed by Pham et al. as shown in Figure 2.3 [72, 121]. Furthermore, unlike other oleaginous yeasts, the growth of *C. oleaginosus* is not inhibited by aromatics and organic acids [142]. These characteristics expand the range of potential low-cost by-products and waste streams from modern industries that could be utilized as feedstock for SCO production using this yeast. However, pretreatment of the feedstock may be required to hydrolyze carbohydrates, neutralize pH, or remove high levels of salts. Formulating a suitable fermentation medium for *C. oleaginosus* is also crucial, and the optimization of its composition, including carbon source, nitrogen source, salts, vitamins, and trace elements, is essential to achieve high yields and productivity. It is important that the added medium components are as cost-effective as possible

while maintaining excellent growth and lipid accumulation behavior. For this medium optimization, a high to moderate throughput approach could be helpful to customize the medium depending on the feedstock used.

**Productivity and process optimization**

Lipid conversion, yields, and titers are already high for the wild type yeast *C. oleaginosus*, making it a very interesting host for GMO-free SCO production, see table 2.1. With up to 80%, the lipid content of the cell dry weight is relatively high compared to other yeasts, which typically range from 20 to 70% [4, 61, 63]. More industrially relevant is the lipid titer and, especially, the productivity, which determines the cost of oil production. Using industrial waste as a substrate, a lipid productivity of 0.58 g/L/h was achieved in this study. This is significantly higher than the yield reported in other studies using natural substrates, such as the maximum of 0.4 g/L/h for the conversion of lignocellulosic hydrolysate from corn stover with *R. toruloides* [66]. Increasing the yield and productivity of SCO production is a critical aspect of industrial-scale bioconversion. Process optimization strategies, such as fed-batch or continuous cultivation systems, can be implemented to improve productivity and efficiency. In addition, genetic engineering and strain development techniques can be employed to enhance lipid synthesis pathways, improve substrate utilization, and increase lipid content, see section 5.2.

Both growth medium composition and process parameters significantly impact SCO productivity. Factors such as pH, temperature, agitation, aeration, and feed must also be carefully adjusted to provide an optimal environment for growth and lipid accumulation. Optimization of these factors must be carried out in laboratory scale bioreactors and scaled up to an industrial scale using the knowledge gained from the smaller scale. In addition to lipid production, the downstream processing needs to be further optimized. Efficient cell lysis and separation techniques are essential for recovering SCO from microbial biomass. Various methods, including mechanical disruption, enzymatic hydrolysis, and solvent extraction, can be used for cell lysis, followed by separation techniques such as centrifugation, filtration, or membrane-based processes [143, 144]. Downstream processing depends on the final application of the product and also affects the yield and quality of the oil, as oxidation can occur during the process [144]. Therefore, downstream processing strategies must be optimized for efficient SCO production to ensure high recovery yields, maintain oil quality, and minimize the energy and resources required in the process.

**Strain development of *C. oleaginosus***

Traditional strain development methods have been successful in improving certain properties of production hosts, such as yeasts used for baking and brewing. However, breeding is often time-consuming, error-prone, and limited in achieving some desired phenotypes. Genetic engineering, on the other hand, offers a more efficient and precise approach by allowing the introduction of genes from other organisms and targeted manipulation of specific genes.

Genetic engineering tools already exist for some oleaginous microorganisms, allowing the targeted introduction of genes into the organisms, through plasmids or by genomic integration. *C. oleaginosus* has been genetically engineered, although mainly with physical or chemical random mutagenesis approaches and with untargeted integration methods [86, 98]. Plasmids or extrachromosomal

DNA constructs have not yet been demonstrated for this yeast. Breeding approaches with chemical and physical mutagenesis were used in the 1980s and 1990s to adapt the fatty acid profile [98]. These methods are still relevant in modern biotechnology, as the resulting strains are not regulated as GMOs. Lengthy approval procedures can thus be avoided. However, the drawbacks of these methods are many off-target mutations and a long and labor-intensive screening process. The resulting strain may have the desired phenotype but may be impaired in other aspects, depending on the screening method used.

Since 2016, ATMT methods have been applied for the untargeted integration of homologous and heterologous genes into the genome of *C. oleaginosus* [86]. However, with this method, the integration loci and the copy number of gene integration are unknown. Nevertheless, it is a suitable approach for strain development because it requires relatively little time and cost. On the other hand, screening is critical to identify clones with the desired mutation and gene expression leading to the desired phenotype. Similar to random mutagenesis, off-target integration with these methods can manipulate clones and unintentionally alter cellular functions. Another obstacle may be the local chromatin structure at the loci of gene insertion, which can prevent expression. In 2023, a study demonstrated the modern method CRISPR-Cas9-mediated genetic engineering for *C. oleaginosus* [18]. This method allows targeted genomic integration. This opens up the possibility of gene deletion or regulation, which is of great interest for metabolic engineering approaches. However, both untargeted and targeted genetic engineering methods require tools such as promoters and markers. The experimental results presented in the second publication could expand the tools for the genetic manipulation of *C. oleaginosus*. The two novel dominant markers, APH and NAT, are more potent than the previously described HPH and work in combination with each other. This allows them to be combined into independent gene constructs. Alternatively, a clone already modified with one of the markers can still be manipulated. With the five promoters described for heterogeneous gene expression in yeast, it is much easier to integrate multiple genes without fear of transcription factor competition when using the same promoter multiple times. The combination of the markers and promoters established in this work with the targeted CRISPR-Cas approach opens up a new field of genetic engineering possibilities for further strain development.

Targets for metabolic engineering strategies can be substrate metabolism, increasing the range of convertible carbohydrates, e.g. by integrating media-secreted hydrolases [116]. Fatty acid metabolism or TAG production can also be manipulated to increase lipid production. The lipid body-associated proteins may also be an interesting target as they regulate lipid droplet formation and TAG metabolism [90, 122]. Another approach would be to target the fatty acid profile, including fatty acid chain length and desaturation, which are mainly regulated within the ER, may be more relevant [72]. Further manipulation of the TAG metabolism can be achieved by introducing specific enzymes such as lipoxygenases or TAG hydrolyzing enzymes like diacylglycerol-O-acyltransferase, lipases, phospholipases, or thioesterases. These enzymes can modulate the synthesis, degradation, and modification of TAGs, potentially resulting in altered lipid properties. In addition to optimized lipid production, there is potential for the production of value-added products in addition to the SCO. For instance, targets such as sterols, tocopherols, and squalene may be considered, as their production in parallel with SCO may increase the commercial value of the products [127]. Other approaches can also be used to facilitate downstream processing, such as with the heterologous

expression of CFL1, a flocculation protein, that assists in the separation of biomass from lipids, as shown by Donzella et al. [124]. This can simplify the recovery and purification of SCO, thereby increasing the efficiency of the overall process.

**Economic challenges**

The bioconversion of industrial waste streams into SCO has emerged as a promising approach for sustainable resource utilization and the production of valuable compounds. However, several process parameters need to be optimized to enable large-scale industrial production.

The techno-economic analysis (TEA) of the process reported in the first publication of this work revealed a putative production cost of 2,938 USD/t for SCO derived from LCH pulping. The price of palm oil that could be substituted with SCO varies, especially since the Covid-19 crisis [145]. In 2022, the price of palm oil was at 2,000 USD/t, and that of certified organic palm oil was between 2,000 and 3,000 USD/t [63, 145]. This renders SCO an economically attractive alternative. However, in 2023, the price of palm oil dropped to 700 - 1,000 USD/t [145]. To obtain more realistic input data for the TEA and to evaluate the technical and practical challenges, further scale-up of the process is required. An industrially relevant pilot scale with a fermentation volume of 100 $m^3$ should be carried out to provide a more comprehensive evaluation of the process. Such a test run could also provide more accurate data for more detailed TEA and LCA studies. This approach would enable a closer assessment of economic feasibility and environmental sustainability, which are essential for scaling up lignocellulosic waste bioconversion.

A successful industrial-scale implementation of SCO bioconversion requires upscaling of the process. Challenges related to large-scale cultivation, process control, and engineering aspects need to be addressed. Bioreactor design, fermentation strategies, and robust process monitoring systems are essential for efficient and reliable SCO production at a commercial scale. Reducing production costs is vital for the economic viability of SCO bioconversion processes. This can be achieved by using inexpensive and abundant biogenic waste streams as feedstocks, minimizing the need for expensive nutrient additives, optimizing process parameters to reduce energy consumption, and implementing simple, cost-effective downstream processing techniques.

## 5.3 Applications, products, and co-products of single-cell oil

SCOs have a wide range of applications in industries such as biofuels, lubricants, biopolymers, cosmetics, nutraceuticals, animal feed, and the food industry. These versatile oils offer a more sustainable and environmentally friendly alternative to conventional oils, meeting the growing demand for renewable resources and reducing environmental impact [121, 143, 146]. Ongoing research and development in this field will likely lead to further advancements and broader adoption of SCOs in various industries, contributing to a more sustainable and circular bioeconomy.

SCO is a promising alternative to fossil or vegetable oils as a source of oleochemicals. The high lipid content and composition of SCOs make them a promising feedstock for biodiesel production. The lipids can be converted into biodiesel through a transesterification process. SCO-based biodiesel offers a renewable and sustainable alternative to fossil fuels, reducing greenhouse gas emissions and dependence on finite resources. To this end, SCO-derived oleochemicals, such as fatty acids, esters, and alcohols, can find applications in various industries. These include the production of lubri-

cants, surfactants, emulsifiers, detergents, personal care products, and industrial chemicals. The versatility of SCO-based oleochemicals helps reduce dependence on petroleum-based compounds and supports the transition to more sustainable and environmentally friendly alternatives.

The unique composition of specific SCO can be a valuable resource for pharmaceuticals and cosmetics, especially if it can be tailored to meet specific requirements. Lipid compounds derived from SCO can also be a source of bioactive compounds, including antimicrobial agents, antioxidants, and anti-inflammatory substances. The development of SCO-based pharmaceutical products holds potential for the treatment and prevention of various diseases and disorders. By using SCO, cosmetics can be produced with improved specifications and in a more sustainable manner without relying on palm oil. SCO can also be used in the food and feed industries. Certain oleaginous microorganisms produce lipids that are rich in essential fatty acids, such as omega-3 and omega-6 fatty acids. These lipids can be extracted and incorporated into functional foods, dietary supplements, and animal feed additives to enhance nutritional value. SCO-derived lipids can contribute to a balanced lipid intake in humans, promote cardiovascular health, and support brain function. Most importantly, SCO from *C. oleaginosus* can be used as a substitute for palm oil due to its unique fatty acid profile, as discussed in section 5.1.

In addition to primary SCO, the cultivation of oleaginous microorganisms often yields valuable co-products. These co-products can improve the overall economics and sustainability of SCO production processes. Notable co-products include protein-rich biomass, nutrients, antioxidants, biofertilizers, and soil amendments. The protein and nutrient-rich biomass can be used as a feed ingredient, providing a valuable nutrient source for the livestock and aquaculture industries. The spent biomass generated during SCO production can be used as biofertilizers or soil amendments improving soil fertility, increasing crop productivity, and reducing dependence on synthetic fertilizers. Nutrients and bioactive compounds can be extracted from the oil or biomass for use as food supplements or in other areas such as cosmetics or pharmaceuticals. These compounds can include sterols, squalene, and tocopherols, among others [127]. The co-products generated during SCO production further contribute to the economic and environmental sustainability of the overall process. Continued research and development efforts are essential to optimize SCO production and utilization.

# Appendix

# A Appendix

## A.1 List of Abbreviations

| | |
|---|---|
| 60S | 60S ribosomal protein L37 |
| AKR | Aldo-keto reductase |
| APH | Aminoglycoside 3'-phosphotransferase |
| ATMT | *Agrobacterium tumefaciens* mediated transformation |
| cb-feed | Consumption-based acetic acid feed |
| CDS | Coding sequence |
| CFU | Colony forming units |
| co-feed | Combined feed of constant LCH feed and cb-feed |
| D9FAD | Delta 9 fatty acid desaturase |
| DCW | Dry cell weight |
| FAS | Fatty acid synthase |
| GAPDH | Glycerinaldehyde 3-phosphate dehydrogenase |
| Gen | Geneticin |
| HPH | Hygromycin B phosphotransferase |
| HygB | Hygromycine B |
| Kana | Kanamycine |
| LCH | Lignocellulosic hydrolysate |
| n.a. | Not available |
| n.d. | Not detected |
| NAT | N-acetyl transferase |
| Nrs | Nourseothricin |
| TEA | Techno-economic analysis |
| TEF | Transcription elongation factor |
| TF | Transcription factor |
| TIS | Translation initiation site |
| TSS | Transcription start site |
| PPI | Cyclophilin type peptidyl-prolyl cis-trans isomerase |
| SCO | Single-cell oil |
| sim | Simultaneous |
| suc | Successive |
| UAS | Upstream activation sequences |
| UBI | Ubiquitin, and ubiquitin-like proteins |
| UTR | Untranslated region |
| wt | Wild type |
| XGA | Xylose, glucose, and acetic acid mix |

## A.2 List of Publications

| | | |
|---|---|---|
| 1. | Research article | Z.S. Rerop, N.I. Stellner, P. Graban, M. Haack, N. Mehlmer, M. Masri, T.B. Brück; Bioconversion of a Lignocellulosic Hydrolysate to Single Cell Oil for Biofuel Production in a Cost-Efficient Fermentation Process. Fermentation 2023, 9, 189. https://doi.org/10.3390/fermentation9020189 |
| 2. | Research article | N.I. Stellner, Z.S. Rerop, J. Kyselka, K. Alishevich, Radek Beneš, Vladimír Filip, Gülnaz Celik, Martina Haack, Marion Ringel, Mahmoud Masri, and Thomas Brück; Value-Added Squalene in Single-Cell Oil Produced with Cutaneotrichosporon oleaginosus for Food Applications. J. Agric. Food Chem. 2023, 71, 22, 8540–8550; https://doi.org/10.1021/acs.jafc.3c01703 |
| 3. | Research article | N.I. Stellner, Z.S. Rerop, N. Mehlmer, M. Masri, M. Ringel and T.B. Brück; Expanding the genetic toolbox for *Cutaneotrichosporon oleaginosus* employing newly identified promoters and a novel antibiotic resistance marker. BMC Biotechnology 2023, 23, 40, https://doi.org/10.1186/s12896-023-00812-7 |
| 4. | Patent | European Patent filed, no. 22 215 578.0; Titel: Pretreatment of salt-containing hydrolysate, particularly for use in fermentation processes; Owner: Technische Universität München, Date:21.12.2022 |

## A.3 List of Figures

## A.4 List of Tables

## A.5 Reprint Permissions

### Bioconversion of a Lignocellulosic Hydrolysate to Single Cell Oil for Biofuel Production in a Cost-Efficient Fermentation Process

#### MDPI - Copyright and Licensing

For all articles published in MDPI journals, copyright is retained by the authors. Articles are licensed under an open access Creative Commons CC BY 4.0 license, meaning that anyone may download and read the paper for free. In addition, the article may be reused and quoted provided that the original published version is cited. These conditions allow for maximum use and exposure of the work, while ensuring that the authors receive proper credit.

#### MDPI - Permissions

No special permission is required to reuse all or part of article published by MDPI, including figures and tables. For articles published under an open access Creative Common CC BY license, any part of the article may be reused without permission provided that the original article is clearly cited. Reuse of an article does not imply endorsement by the authors or MDPI.

### Expanding the genetic toolbox for *Cutaneotrichosporon oleaginosus* employing newly identified promoters and a novel antibiotic resistance marker

#### Permissions BMC Biotechnology

The article is published and available under the Creative Commons CC BY license.

SPRINGER NATURE

**Expanding the genetic toolbox for Cutaneotrichosporon oleaginosus employing newly identified promoters and a novel antibiotic resistance marker**

**Author:** Nikolaus I. Stellner et al
**Publication:** BMC Biotechnology
**Publisher:** Springer Nature
**Date:** Sep 18, 2023



**Creative Commons**

# References


[1] European Commission. The European Green Deal. *European Commission*, 53(9):2019, 2019.

[2] European Commission. REPowerEU Plan. Technical report, European Commission, Brussels, 2022.

[3] Lisa Klug and Günther Daum. Yeast lipid metabolism at a glance. *FEMS Yeast Research*, 14:369–388, 2014.

[4] Mahmoud Masri, Daniel Garbe, Norbert Mehlmer, and Thomas Brück. A sustainable, high-performance process for the economic production of waste-free microbial oils that can replace plant-based equivalents. *Energy and Environmental Science*, 12(9):2717–2732, 2019.

[5] Sophie Parsons, Sofia Raikova, and Christopher J. Chuck. The viability and desirability of replacing palm oil. *Nature Sustainability*, 3:412–418, 2020.

[6] Sujeong Je and Yasuyo Yamaoka. Biotechnological Approaches for Biomass and Lipid Production Using Microalgae Chlorella and Its Future Perspectives. *Journal of Microbiology and Biotechnology*, 32(11):1357–1372, 2022.

[7] Sheetal Bandhu, Anita Srivastava, Debashish Ghosh, and Tapan Kumar Chaudhuri. Yeast Single Cell Oils from Bioresources : Current Developments in Production and Applications. *Current Sustainable/Renewable Energy Reports, BIOCONVERSION*, 7:109–120, 2020.

[8] Aristotle T. Ubando, Charles B. Felix, and Wei Hsin Chen. Biorefineries in circular bioeconomy: A comprehensive review. *Bioresource Technology*, 299:122585, 2020.

[9] Torsten Meyer and Elizabeth A. Edwards. Anaerobic digestion of pulp and paper mill wastewater and sludge. *Water Research*, 65:321–349, 2014.

[10] A. N. Hassan and B. K. Nelson. Invited review: Anaerobic fermentation of dairy food wastewater. *Journal of Dairy Science*, 95(11):6188–6203, 2012.

[11] Leif J. Jönsson and Carlos Martín. Pretreatment of lignocellulose: Formation of inhibitory by-products and strategies for minimizing their effects. *Bioresource Technology*, 199:103–112, 2016.

[12] Charles E. Wyman, Bruce E. Dale, Richard T. Elander, Mark Holtzapple, Michael R. Ladisch, and Y. Y. Lee. Coordinated development of leading biomass pretreatment technologies. *Bioresource Technology*, 96(18 SPEC. ISS.):1959–1966, 2005.

[13] Eva Schmitz, Savvina Leontakianakou, Siri Norlander, Eva Nordberg Karlsson, and Patrick Adlercreutz. Lignocellulose degradation for the bioeconomy: The potential of enzyme synergies between xylanases, ferulic acid esterase and laccase for the production of arabinoxylo-oligosaccharides. *Bioresource Technology*, 343(August 2021):126114, 2022.

[14] Pooja Sharma, Surendra Pratap Singh, Hafiz M.N. Iqbal, Roberto Parra-Saldivar, Sunita Varjani, and Yen Wah Tong. Genetic modifications associated with sustainability aspects for

sustainable developments. *Bioengineered*, 13(4):9509–9521, 2022.

[15] Marion Ringel, Nicole Dimos, Stephanie Himpich, Martina Haack, Claudia Huber, Wolfgang Eisenreich, Gerhard Schenk, Bernhard Loll, and Thomas Brück. Biotechnological potential and initial characterization of two novel sesquiterpene synthases from Basidiomycota Coniophora puteana for heterologous production of $\delta$-cadinol. *Microbial Cell Factories*, 21(1):1–15, 2022.

[16] Alok Patel, Maurizio Bettiga, Ulrika Rova, Paul Christakopoulos, and Leonidas Matsakas. Microbial genetic engineering approach to replace shark livering for squalene. *Trends in Biotechnology*, 40(10):1261–1273, 2022.

[17] Harmeet Kaur, Swati Chahal, Priyanka Jha, Manoj M. Lekhak, Mahipal S. Shekhawat, Devashan Naidoo, Ariel D. Arencibia, Sergio J. Ochatt, and Vijay Kumar. Harnessing plant biotechnology-based strategies for in vitro galanthamine (GAL) biosynthesis: a potent drug against Alzheimer's disease. *Plant Cell, Tissue and Organ Culture*, 149(1-2):81–103, 2022.

[18] Pariya Shaigani, Tobias Fuchs, Petra Graban, Sophia Prem, Martina Haack, Mahmoud Masri, Norbert Mehlmer, and Thomas Brueck. Mastering targeted genome engineering of GC - rich oleaginous yeast for tailored plant oil alternatives for the food and chemical sector. *Microbial Cell Factories*, 22(25):1–14, 2023.

[19] Jacopo Paini, Vittoria Benedetti, Snehesh Shivananda Ail, Marco J. Castaldi, Marco Baratieri, and Francesco Patuzzi. Valorization of Wastes from the Food Production Industry: A Review Towards an Integrated Agri-Food Processing Biorefinery. *Waste and Biomass Valorization*, 13(1):31–50, 2022.

[20] Apostolis A. Koutinas, Anestis Vlysidis, Daniel Pleissner, Nikolaos Kopsahelis, Isabel Lopez Garcia, Ioannis K. Kookos, Seraphim Papanikolaou, Tsz Him Kwan, and Carol Sze Ki Lin. Valorization of industrial waste and by-product streams via fermentation for the production of chemicals and biopolymers. *Chemical Society Reviews*, 43(8):2587–2627, 2014.

[21] Pratik R. Pawar, Poornima Rao, Gunjan Prakash, and Arvind M. Lali. Organic waste streams as feedstock for the production of high volume-low value products. *Environmental Science and Pollution Research*, 28(10):11904–11914, 2021.

[22] Juan-rodrigo Bastidas-Oyanedel and Jens Ejbye Schmidt. *Biorefinery - Integrated Sustainable Processes for Biomass Conversion to Biomaterials, Biofuels, and Fertilizers*. Springer Nature Switzerland AG, 2019.

[23] Chun Hui Zhou, Xi Xia, Chun Xiang Lin, Dong Shen Tong, and Jorge Beltramini. Catalytic conversion of lignocellulosic biomass to fine chemicals and fuels. *Chemical Society Reviews*, 40(11):5588–5617, 2011.

[24] Martin B. Hocking. Production of Pulp and Paper. *Handbook of Chemical Technology and Pollution Control*, pages 453–504, 2005.

[25] A. Duwe, N. Tippkötter, and R. Ulber. Lignocellulose-biorefinery: Ethanol-focused. *Advances in Biochemical Engineering/Biotechnology*, 166, 2017.

[26] Jan Christoph Peinemann and Daniel Pleissner. Continuous pretreatment, hydrolysis, and fermentation of organic residues for the production of biochemicals. *Bioresource Technology*, 295:122256, 2020.

[27] Lalitha Devi Gottumukkala, Kate Haigh, François Xavier Collard, Eugéne van Rensburg, and Johann Görgens. Opportunities and prospects of biorefinery-based valorisation of pulp and paper sludge. *Bioresource Technology*, 215:37–49, 2016.

[28] Fredrik Nielsen, Mats Galbe, Guido Zacchi, and Ola Wallberg. The effect of mixed agricultural feedstocks on steam pretreatment, enzymatic hydrolysis, and cofermentation in the lignocellulose-to-ethanol process. *Biomass Conversion and Biorefinery*, 10(2):253–266, 2020.

[29] European Commission. New market niches for the Pulp and Paper Industry waste based on circular economy approaches. *H2020-Eu*, pages 1–4, 2017.

[30] Gaurav Saxena and Ram Naresh Bharagava. *Bioremediation of Industrial Waste for Environmental Safety*, volume I. 2020.

[31] Pratima Bajpai. *Green Chemistry and Sustainability in Pulp and Paper Industry*. Springer International Publishing Switzerland, 2015.

[32] Shuzhen Zhou, Miaomiao Zhang, Linying Zhu, Xiaoling Zhao, Junying Chen, Wei Chen, and Chun Chang. Hydrolysis of lignocellulose to succinic acid: a review of treatment methods and succinic acid applications. *Biotechnology for Biofuels and Bioproducts*, 16(1):1–17, 2023.

[33] Adane Haile, Gemeda Gebino Gelebo, Tamrat Tesfaye, Wassie Mengie, Million Ayele Mebrate, Amare Abuhay, and Derseh Yilie Limeneh. Pulp and paper mill wastes: utilizations and prospects for high value-added biomaterials. *Bioresources and Bioprocessing*, 8(1), 2021.

[34] Herbert Sixta and Lenzinger AG. Zellstoffherstellung und Recycling von Roh- und Hilfsstoffen nach dem Lenzinger Mg- Bisulfitverfahren. *Lenzinger Berichte*, 61:5–11, 1986.

[35] Anil Kumar Singh, Muhammad Bilal, Hafiz M.N. Iqbal, Anne S. Meyer, and Abhay Raj. Bioremediation of lignin derivatives and phenolics in wastewater with lignin modifying enzymes: Status, opportunities and challenges. *Science of the Total Environment*, 777, 2021.

[36] Bhupendra Koul, Mohammad Yakoob, and Maulin P. Shah. Agricultural waste management strategies for environmental sustainability. *Environmental Research*, page 112285, oct 2021.

[37] Christos K. Nitsos, Konstantinos A. Matis, and Kostas S. Triantafyllidis. Optimization of hydrothermal pretreatment of lignocellulosic biomass in the bioethanol production process. *ChemSusChem*, 6(1):110–122, 2013.

[38] V. Ananthi, G. Siva Prakash, Soon Woong Chang, Balasubramani Ravindran, Dinh Duc Nguyen, Dai Viet N. Vo, Duong Duc La, Quang Vu Bach, J. W.C. Wong, Sanjay Kumar Gupta, Arokiyaraj Selvaraj, and A. Arun. Enhanced microbial biodiesel production from lignocellulosic hydrolysates using yeast isolates. *Fuel*, 256(July):115932, 2019.

[39] Nikki Sjulander and Timo Kikas. Origin, impact and control of lignocellulosic inhibitors in bioethanol production—A review. *Energies*, 13(4751), 2020.

[40] David Cannella, Per Viktor Sveding, and Henning Jørgensen. PEI detoxification of pretreated spruce for high solids ethanol fermentation. *Applied Energy*, 132:394–403, 2014.

[41] Nancy N. Nichols, Bruce S. Dien, Gema M. Guisado, and Maria J. López. Bioabatement to remove inhibitors from biomass-derived sugar hydrolysates. *Applied Biochemistry and Biotechnology - Part A Enzyme Engineering and Biotechnology*, 121-124(1-3):379–390, 2005.

[42] Guangli Cao, Eduardo Ximenes, Nancy N. Nichols, Sarah E. Frazer, Daehwan Kim, Michael A. Cotta, and Michael Ladisch. Bioabatement with hemicellulase supplementation

to reduce enzymatic hydrolysis inhibitors. *Bioresource Technology*, 190:412–415, 2015.

[43] Jeremy M. Berg, John L. Tymoczko, and Lubert Stryer. *Biochemistry.* 5th editio edition, 2002.

[44] Eoin Fahy, Dawn Cotter, Manish Sud, and Shankar Subramaniam. Lipid classification, structures and tools. *Biochim Biophys Acta.*, 1811(11):637–647, 2011.

[45] Colin Ratledge. Single cell oils - have they a biotechnological future? *Trends in Biotechnology*, 11(July):278–284, 1993.

[46] Patrick J. McGinn, Kathryn E. Dickinson, Shabana Bhatti, Jean-Claude Frigon, Serge R. Guiot, and Stephen J. B. O'Leary. Integration of microalgae cultivation with industrial waste remediation for biofuel and bioenergy production : opportunities and limitations. *Photosynth Res*, 109:231–247, 2011.

[47] Liang Wan, Yixiao Wu, Xuemei Zhang, and Weihao Zhang. Nutrient removal from pickle industry wastewater by cultivation of Chlorella pyrenoidosa for lipid production. *Water Science & Technology*, 79(11):2166–2174, 2019.

[48] Alifha Severes, Shashank Hegde, L D'Souza, and Smitha Hegde. Use of light emitting diodes (leds) for enhanced lipid production in micro-algae based biofuels. *Journal of photochemistry and photobiology. B, Biology*, 170:235–240, 2017.

[49] Ben Leyland, Stefan Leu, and Sammy Boussiba. Are thraustochytrids algae? *Fungal Biology*, 121(10):835–840, 2017.

[50] Kenshi Watanabe, Miho Nishijima, Shinzo Mayuzumi, and Tsunehiro Aki. Utilization of Sugarcane Bagasse as a Substrate for Lipid Production by Aurantiochytrium sp. *Journal of Oleo Science*, 71(10):1493–1500, 2022.

[51] Yousuke Taoka, Naoki Nagano, Yuji Okita, Hitoshi Izumida, Shinichi Sugimoto, and Masahiro Hayashi. Influences of culture temperature on the growth, lipid content and fatty acid composition of aurantiochytrium sp. strain mh0186. *Marine Biotechnology*, 11(3):368–374, 2009.

[52] Sara A. Shields-Menard, Marta Amirsadeghi, Badamkhand Sukhbaatar, Emmanuel Revellame, Rafael Hernandez, Janet R. Donaldson, and W. Todd French. Lipid accumulation by Rhodococcus rhodochrous grown on glucose. *Journal of Industrial Microbiology and Biotechnology*, 42(5):693–699, 2015.

[53] Antonio Caporusso, Angela Capece, and Isabella De Bari. Oleaginous yeasts as cell factories for the sustainable production of microbial lipids by the valorization of agri-food wastes. *Fermentation*, 7(2):1–33, 2021.

[54] Sirawich Sapsirisuk, Pirapan Polburee, Wanlapa Lorliam, and Savitree Limtong. Discovery of Oleaginous Yeast from Mountain Forest Soil in Thailand. *Journal of Fungi*, 8(10), 2022.

[55] Felix Abeln and Christopher J. Chuck. The history, state of the art and future prospects for oleaginous yeast research. *Microbial Cell Factories*, 20(221):1–31, 2021.

[56] Colin Ratledge. Microorganisms for lipids. *Acta Biotechnologica*, 11(5):429–438, 1991.

[57] Luis A. Garay, Irnayuli R. Sitepu, Tomas Cajka, Idelia Chandra, Sandy Shi, Ting Lin, J. Bruce German, Oliver Fiehn, and Kyria L. Boundy-Mills. Eighteen new oleaginous yeast species. *Journal of Industrial Microbiology and Biotechnology*, 43(7):887–900, 2016.

[58] Macarena Larroude, Ewelina Celinska, Alexandre Back, Stephan Thomas, Jean Marc Nicaud,

and Rodrigo Ledesma-Amaro. A synthetic biology approach to transform Yarrowia lipolytica into a competitive biotechnological producer of $\beta$-carotene. *Biotechnology and Bioengineering*, 115(2):464–472, 2018.

[59] Rodrigo Ledesma-Amaro and Jean Marc Nicaud. Yarrowia lipolytica as a biotechnological chassis to produce usual and unusual fatty acids. *Progress in Lipid Research*, 61:40–50, 2016.

[60] Pariya Shaigani, Dania Awad, Veronika Redai, Monika Fuchs, Martina Haack, Norbert Mehlmer, and Thomas Brueck. Oleaginous yeasts- substrate preference and lipid productivity: a view on the performance of microbial lipid producers. *Microbial Cell Factories*, 20(1):1–18, 2021.

[61] Rujiralai Poontawee, Wanlapa Lorliam, Pirapan Polburee, and Savitree Limtong. Oleaginous yeasts: Biodiversity and cultivation. *Fungal Biology Reviews*, 44:100295, 2023.

[62] Xochitl Niehus, Anne Marie Crutz-Le Coq, Georgina Sandoval, Jean Marc Nicaud, and Rodrigo Ledesma-Amaro. Engineering Yarrowia lipolytica to enhance lipid production from lignocellulosic materials. *Biotechnology for Biofuels*, 11(1):1–10, 2018.

[63] Zora S. Rerop, Nikolaus I. Stellner, Petra Graban, Martina Haack, Norbert Mehlmer, Thomas B. Brück, and Mahmoud Masri. Bioconversion of a Lignocellulosic Hydrolysate to Single Cell Oil for Biofuel Production in a Cost-Efficient Fermentation Process. *fermentation*, 9(189), 2023.

[64] Nicola Di Fidio, Federico Liuzzi, Silvio Mastrolitti, Roberto Albergo, and Isabella de Bari. Single cell oil production from undetoxified Arundo donax L. Hydrolysate by cutaneotrichosporon curvatus. *Journal of Microbiology and Biotechnology*, 29(2):256–267, 2019.

[65] Seraphim Papanikolaou, Isabelle Chevalot, Michael Komaitis, George Aggelis, and Ivan Marc. Kinetic profile of the cellular lipid composition in an oleaginous Yarrowia lipolytica capable of producing a cocoa-butter substitute from industrial fats. *Antonie van Leeuwenhoek, International Journal of General and Molecular Microbiology*, 80(3-4):215–224, 2001.

[66] Qiang Fei, Marykate O'Brien, Robert Nelson, Xiaowen Chen, Andrew Lowell, and Nancy Dowe. Enhanced lipid production by Rhodosporidium toruloides using different fed-batch feeding strategies with lignocellulosic hydrolysate as the sole carbon source. *Biotechnology for Biofuels*, 9(1):1–12, 2016.

[67] M. C.A. Xavier, A. L.V. Coradini, A. C. Deckmann, and T. T. Franco. Lipid production from hemicellulose hydrolysate and acetic acid by Lipomyces starkeyi and the ability of yeast to metabolize inhibitors. *Biochemical Engineering Journal*, 118:11–19, 2017.

[68] Marika Ngamsirisomsakul, Mallika Boonmee Kongkeitkajorn, Sittipong Amnuaypanich, and Alissara Reungsang. An Approach for Incorporating Glycerol as a Co-Substrate into Unconcentrated Sugarcane Bagasse Hydrolysate for Improved Lipid Production in Rhodotorula glutinis. *Fermentation*, 8(10), 2022.

[69] Ezhaveni Sathiyamoorthi, Prasun Kumar, and Beom Soo Kim. Lipid production by Cryptococcus albidus using biowastes hydrolysed by indigenous microbes. *Bioprocess and Biosystems Engineering*, 42(5):687–696, 2019.

[70] Zhiwei Gong, Wenting Zhou, Hongwei Shen, Zhonghua Yang, Guanghui Wang, Zhenyu Zuo, Yali Hou, and Zongbao K. Zhao. Co-fermentation of acetate and sugars facilitating microbial

lipid production on acetate-rich biomass hydrolysates. *Bioresource Technology*, 207:102–108, 2016.

[71] Athanasios Beopoulos, Jean Marc Nicaud, and Claude Gaillardin. An overview of lipid metabolism in yeasts and its impact on biotechnological processes. *Applied Microbiology and Biotechnology*, 90(4):1193–1206, 2011.

[72] Nhung Pham, Maarten Reijnders, Maria Suarez-Diez, Bart Nijsse, Jan Springer, Gerrit Eggink, and Peter J. Schaap. Genome-scale metabolic modeling underscores the potential of Cutaneotrichosporon oleaginosus ATCC 20509 as a cell factory for biofuel production. *Biotechnology for Biofuels*, 14(2):1–17, 2021.

[73] Zbigniew Lazar, Nian Liu, and Gregory Stephanopoulos. Holistic Approaches in Lipid Production by Yarrowia lipolytica. *Trends in Biotechnology*, 36(11):1157–1170, 2018.

[74] Michael Spagnuolo, Allison Yaguchi, and Mark Blenner. Oleaginous yeast for biofuel and oleochemical production. *Current Opinion in Biotechnology*, 57:73–81, 2019.

[75] Ke Jin, Hongzhi Xia, Yanfeng Liu, Jianghua Li, Guocheng Du, Xueqin Lv, and Long Liu. Compartmentalization and transporter engineering strategies for terpenoid synthesis. *Microbial Cell Factories*, 21(1):1–12, 2022.

[76] Zhiwei Zhu, Yunfeng Ding, Zhiwei Gong, Li Yang, Sufang Zhang, Congyan Zhang, Xinping Lin, Hongwei Shen, Hanfa Zou, Zhensheng Xie, Fuquan Yang, Xudong Zhao, Pingsheng Liu, and Zongbao K. Zhaoa. Dynamics of the lipid droplet proteome of the oleaginous yeast Rhodosporidium toruloides. *Eukaryotic Cell*, 14(3):252–264, 2015.

[77] Aglaia Burlacu, Florentina Israel-roming, and Călina Petruța Cornea. Fungal Strains Improvement for Xylanase Over Production Through Physical. *Agrolife Scientific Journal*, 6(1):40–47, 2017.

[78] Adrie Ykema, Elizabeth C. Verbree, H. John J. Nijkamp, and Henk Smit. Isolation and characterization of fatty acid auxotrophs from the oleaginous yeast Apiotrichum curvatum. *Applied Microbiology and Biotechnology*, 32(1):76–84, 1989.

[79] Gary A. Sega. A review of the genetic effects of ethyl methanesulfonate. *Mutation Research/Reviews in Genetic Toxicology*, 134(2-3):113–142, 1984.

[80] Takashi Sugimura, Minako Nagao, and Yoshikiyo Okada. Carcinogenic action of N-methyl-N-nitro-N-nitrosoguanidine. *Nature*, 210(5039):962–963, 1966.

[81] Chaolei Zhang, Hongwei Shen, Xibin Zhang, Xue Yu, Han Wang, Shan Xiao, Jihui Wang, and Zongbao K. Zhao. Combined mutagenesis of Rhodosporidium toruloides for improved production of carotenoids and lipids. *Biotechnology Letters*, 38(10):1733–1738, 2016.

[82] Ryosuke Yamada, Tomomi Kashihara, and Hiroyasu Ogino. Improvement of lipid production by the oleaginous yeast Rhodosporidium toruloides through UV mutagenesis. *World Journal of Microbiology and Biotechnology*, 33(99):1–9, 2017.

[83] Roland S. Kun, Ana Carolina S. Gomes, Kristiina S. Hildén, Sonia Salazar Cerezo, Miia R. Mäkelä, and Ronald P. de Vries. Developments and opportunities in fungal strain engineering for the production of novel enzymes and enzyme cocktails for plant biomass degradation. *Biotechnology Advances*, 37(6):107361, 2019.

[84] Yanbin Liu, Sihui Amy Yap, Chong Mei John Koh, and Lianghui Ji. Developing a set of

strong intronic promoters for robust metabolic engineering in oleaginous Rhodotorula (Rhodosporidium) yeast species. *Microbial Cell Factories*, 15(1):1–9, 2016.

[85] Young Kyoung Park, Jean Marc Nicaud, and Rodrigo Ledesma-Amaro. The Engineering Potential of Rhodosporidium toruloides as a Workhorse for Biotechnological Applications. *Trends in Biotechnology*, 36(3):304–317, 2018.

[86] Christian Görner, Veronika Redai, Felix Bracharz, Patrick Schrepfer, Daniel Garbe, and Thomas Brück. Genetic engineering and production of modified fatty acids by the non-conventional oleaginous yeast Trichosporon oleaginosus ATCC 20509. *Green Chemistry*, 18(7):2037–2046, 2016.

[87] David M. Ogrydziak and Stephen J. Scharf. A1 kalin e Ex t rac ellula r Pro t ease Produced by Saccharomycopsis lipolytica CX 161- IB. *Journal of General Microbiology*, 128:1225–1234, 1982.

[88] Sven Müller, Thomas Sandal, Peter Kamp-Hansen, and Henrik Dalbøge. Comparison of expression systems in the yeasts Saccharomyces cerevisiae, Hansenula polymorpha, Klyveromyces lactis, Schizosaccharomyces pombe and Yarrowia lipolytica. Cloning of two novel promoters from Yarrowia lipolytica. *Yeast*, 14(14):1267–1283, 1998.

[89] Farshad Darvishi, Mehdi Ariana, Eko Roy Marella, and Irina Borodina. Advances in synthetic biology of oleaginous yeast Yarrowia lipolytica for producing non-native chemicals. *Applied Microbiology and Biotechnology*, 102(14):5925–5938, 2018.

[90] Athanasios Beopoulos, Julien Cescut, Ramdane Haddouche, Jean Louis Uribelarrea, Carole Molina-Jouve, and Jean Marc Nicaud. Yarrowia lipolytica as a model for bio-oil production. *Progress in Lipid Research*, 48(6):375–387, 2009.

[91] Cory M. Schwartz, Murtaza Shabbir Hussain, Mark Blenner, and Ian Wheeldon. Synthetic RNA Polymerase III Promoters Facilitate High-Efficiency CRISPR-Cas9-Mediated Genome Editing in Yarrowia lipolytica. *ACS Synthetic Biology*, 5(4):356–359, 2016.

[92] Akram Muhammad, Xudong Feng, Aamir Rasool, Wentao Sun, and Chun Li. Production of plant natural products through engineered Yarrowia lipolytica. *Biotechnology Advances*, 43(April):107555, 2020.

[93] Christophe Leplat, Jean Marc Nicaud, and Tristan Rossignol. Overexpression screen reveals transcription factors involved in lipid accumulation in Yarrowia lipolytica. *FEMS Yeast Research*, 18(5):1–9, 2018.

[94] Nancy J. Moon, E. G. Hammond, and Bonita A. Glatz. Conversion of Cheese Whey and Whey Permeate to Oil and Single-Cell Protein. *Journal of Dairy Science*, 61(11):1537–1547, 1978.

[95] American Type Culture Collection (ATCC). Cutaneotrichosporon oleaginosum (Zhou et al.) Liu et al. (ATCC® 20509™). Technical report, 2016.

[96] A. Ykema, E. C. Verbree, H. W. van Verseveld, and H. Smit. Mathematical modelling of lipid production by oleaginous yeasts in continuous cultures. *Antonie van Leeuwenhoek*, 52(6):491–506, 1986.

[97] D. J. Bell and R. J. Davies. Cell harvesting of oleaginous yeast by cross-flow filtration. *Biotechnology and Bioengineering*, 29(9):1176–1178, 1987.

[98] Adrie Ykema, Elizabeth C. Verbree, Ira I.G.S. Verwoert, Karin H. van der Linden, H. John J. Nijkamp, and Henk Smit. Lipid production of revertants of Ufa mutants from the oleaginous yeast Apiotrichum curvatum. *Applied Microbiology and Biotechnology*, 33(2):176–182, 1990.

[99] James A. Barnett, Roger W. Payne, and David Yarrow. *Yeasts: Characteristics and Identification*. Cambridge University Press, 1990.

[100] Jonathan Depree, George W. Emerson, and Patrick A. Sullivan. The cell wall of the oleaginous yeast Trichosporon cutaneum. *Journal of General Microbiology*, 139(9):2123–2133, 1993.

[101] P. A.E.P. Meesters, G. N.M. Huijberts, and G. Eggink. High-cell-density cultivation of the lipid accumulating yeast Cryptococcus curvatus using glycerol as a carbon source. *Applied Microbiology and Biotechnology*, 45(5):575–579, 1996.

[102] Mainul Hassan, Philippe J. Blanc, Alain Pareilleux, and Gérard Goma. Selection of fatty acid auxotrophs from the oleaginous yeast Cryptococcus curvatus and production of cocoa butter equivalents in batch culture. *Biotechnology Letters*, 16(8):819–824, 1994.

[103] Pushpa Gujjari, Sung-Oui Suh, Kendra Coumes, and Jianlong J. Zhou. Characterization of oleaginous yeasts revealed two novel species: Trichosporon cacaoliposimilis sp. nov. and Trichosporon oleaginosus sp. nov. *Mycologia*, 103, 2011.

[104] Robert Kourist, Felix Bracharz, Jan Lorenzen, Octavia N. Kracht, Mansi Chovatia, Chris Daum, Shweta Deshpande, Anna Lipzen, Matt Nolan, Robin A. Ohm, Igor V. Grigoriev, Sheng Sun, Joseph Heitman, Thomas Brück, and Minou Nowrousian. Genomics and transcriptomics analyses of the oil-accumulating basidiomycete yeast Trichosporon oleaginosus: Insights into substrate utilization and alternative evolutionary trajectories of fungal mating systems. *mBio*, 6(4), 2015.

[105] Jia Liu, Ming Yuan, Jia Nan Liu, and Xiang Feng Huang. Bioconversion of mixed volatile fatty acids into microbial lipids by Cryptococcus curvatus ATCC 20509. *Bioresource Technology*, 241:645–651, 2017.

[106] X. Z. Liu, Q. M. Wang, M. Göker, M. Groenewald, A. V. Kachalkin, H. T. Lumbsch, A. M. Millanes, M. Wedin, A. M. Yurkov, T. Boekhout, and F. Y. Bai. Towards an integrated phylogenetic classification of the Tremellomycetes. *Studies in Mycology*, 81:85–147, 2015.

[107] Yalda Rahbar Saadat, Ahmad Yari Khosroushahi, and Bahram Pourghassem Gargari. Yeast exopolysaccharides and their physiological functions. *Folia Microbiologica*, 66(2):171–182, 2021.

[108] Adrie Ykema, Elizabeth C. Verbree, Martin M. Kater, and Henk Smit. Optimization of lipid production in the oleaginous yeast Apiotrichum curvatum in wheypermeate. *Applied Microbiology and Biotechnology*, 29(2-3):211–218, 1988.

[109] Yubin Zheng, Zhanyou Chi, Birgitte Kiær Ahring, and Shulin Chen. Oleaginous yeast Cryptococcus curvatus for biofuel production: Ammonia's effect. *Biomass and Bioenergy*, 37:114–121, 2012.

[110] Felix Bracharz, Teun Beukhout, Norbert Mehlmer, and Thomas Brück. Opportunities and challenges in the development of Cutaneotrichosporon oleaginosus ATCC 20509 as a new cell factory for custom tailored microbial oils. *Microbial Cell Factories*, 16(1):1–15, 2017.

[111] Cuimin Hu, Siguo Wu, Qian Wang, Guojie Jin, Hongwei Shen, and Zongbao K. Zhao. Si-

multaneous utilization of glucose and xylose for lipid production by Trichosporon cutaneum. *Biotechnology for Biofuels*, 4(1):25, 2011.

[112] Christopher T. Evans and Colin Ratledge. A comparison of the oleaginous yeast, Candida curvata, grown on different carbon sources in continuous and batch culture. *Lipids*, 18(9):623–629, 1983.

[113] Christopher Thomas Evans and Colin Ratledge. Induction of xylulose-5-phosphate phosphoketolase in a variety of yeasts grown on i)-xylose: the key to efficient xylose metabolism. *Archives of Microbiology*, 139:48–52, 1984.

[114] Allison Yaguchi, Nicole Franaszek, Kaelyn O'Neill, Stephen Lee, Irnayuli Sitepu, Kyria Boundy-Mills, and Mark Blenner. Identification of oleaginous yeasts that metabolize aromatic compounds. *Journal of Industrial Microbiology & Biotechnology*, 47, 2020.

[115] Dania Awad, Frank Bohnen, Norbert Mehlmer, and Thomas Brueck. Multi-factorial-guided media optimization for enhanced biomass and lipid formation by the oleaginous yeast Cutaneotrichosporon oleaginosus. *Frontiers in Bioengineering and Biotechnology*, 7(MAR), 2019.

[116] Tobias Fuchs, Felix Melcher, Zora Selina Rerop, Jan Lorenzen, Pariya Shaigani, Dania Awad, Martina Haack, Sophia Alice Prem, Mahmoud Masri, Norbert Mehlmer, and Thomas B. Brueck. Identifying carbohydrate-active enzymes of Cutaneotrichosporon oleaginosus using systems biology. *Microbial Cell Factories*, 20(1):1–18, 2021.

[117] Guochang Zhang, William Todd French, Rafiel Hernandez, Jaclyn Hall, Darrell Sparks, and William E. Holmes. Microbial lipid production as biodiesel feedstock from N-acetylglucosamine by oleaginous microorganisms. *Journal of Chemical Technology and Biotechnology*, 86(5):642–650, 2011.

[118] Allison Yaguchi, Alana Robinson, Erin Mihealsick, and Mark Blenner. Metabolism of aromatics by Trichosporon oleaginosus while remaining oleaginous. *Microbial Cell Factories*, 16(1):1–12, 2017.

[119] Juan Wang, Qiuqiang Gao, Huizhan Zhang, and Jie Bao. Inhibitor degradation and lipid accumulation potentials of oleaginous yeast Trichosporon cutaneum using lignocellulose feedstock. *Bioresource Technology*, 218:892–901, 2016.

[120] Andrea Meo, Xenia Laura Priebe, and Dirk Weuster-Botz. Lipid production with Trichosporon oleaginosus in a membrane bioreactor using microalgae hydrolysate. *Journal of Biotechnology*, 241:1–10, 2017.

[121] Nicola Di Fidio, Filippo Minonne, Claudia Antonetti, and Anna Maria Raspolli Galletti. Cutaneotrichosporon oleaginosus: A versatile whole-cell biocatalyst for the production of single-cell oil from agro-industrial wastes. *Catalysts*, 11(11), 2021.

[122] Amir Sapir. Not so slim anymore—evidence for the role of sumo in the regulation of lipid metabolism. *Biomolecules*, 10(8):1–19, 2020.

[123] Kari Koivuranta, Sandra Castillo, Paula Jouhten, Laura Ruohonen, Merja Penttilä, and Marilyn G. Wiebe. Enhanced triacylglycerol production with genetically modified Trichosporon oleaginosus. *Frontiers in Microbiology*, 9(JUN):1–15, 2018.

[124] Silvia Donzella and Concetta Compagno. Heterologous Expression of CFL1 Confers Flocculating Ability to Cutaneotrichosporon oleaginosus Lipid-Rich Cells. *Journal of Fungi*, 8(12):1–

12, 2022.

[125] European Commission. A Farm to Fork Strategy for a fair, healthy and environmentally-friendly food system, 2020.

[126] Kanokwan Saswattecha, Melissa Cuevas Romero, Lars Hein, Warit Jawjit, and Carolien Kroeze. Non-CO2 greenhouse gas emissions from palm oil production in Thailand. *Journal of Integrative Environmental Sciences*, 12:67–85, 2015.

[127] N I Stellner, Z S Rerop, Jan Kyselka, Katsiaryna Alishevich, Radek Benes, Gülnaz Celik, Martina Haack, Marion Ringel, Mahmoud Masri, and Thomas Brück. Value-Added Squalene in Single-Cell Oil Produced with Cutaneotrichosporon oleaginosus for Food Applications. *Journal of Agricultural and Food Chemistry*, 2023.

[128] Panida Unagul, Satinee Suetrong, Sita Preedanon, Anupong Klaysuban, Wunna Gundool, Chanwit Suriyachadkun, and Jariya Sakayaroj. Isolation, fatty acid profiles and cryopreservation of marine thraustochytrids from mangrove habitats in Thailand. *Botanica Marina*, 60(4):363–379, 2017.

[129] Imke Lang, Ladislav Hodac, Thomas Friedl, and Ivo Feussner. Fatty acid profiles and their distribution patterns in microalgae: a comprehensive analysis of more than 2000 strains from the SAG culture collection. *BMC Plant Biology*, 11(124):1–16, 2011.

[130] Fritz Ullmann. *Ullmann's Encyclopedia of Industrial Chemistry*. Weinheim, 6th editio edition, 1995.

[131] R. Julian Davies, Jane E. Holdsworth, and Sarah L. Reader. The effect of low oxygen uptake rate on the fatty acid profile of the oleaginous yeast Apiotrichum curvatum. *Applied Microbiology and Biotechnology*, 33(5):569–573, 1990.

[132] Irnayuli R. Sitepu, Ryan Sestric, Laura Ignatia, David Levin, J. Bruce German, Laura A. Gillies, Luis A.G. Almada, and Kyria L. Boundy-Mills. Manipulation of culture conditions alters lipid content and fatty acid profiles of a wide variety of known and new oleaginous yeast species. *Bioresource Technology*, 144:360–369, 2013.

[133] Dennis Lamers, Nick van Biezen, Dirk Martens, Linda Peters, Eric van de Zilver, Nicole Jacobs-van Dreumel, René H. Wijffels, and Christien Lokman. Selection of oleaginous yeasts for fatty acid production. *BMC Biotechnology*, 16(1):1–10, 2016.

[134] Yeshitila Asteraye Tsigie, Chun Yuan Wang, Chi Thanh Truong, and Yi Hsu Ju. Lipid production from Yarrowia lipolytica Po1g grown in sugarcane bagasse hydrolysate. *Bioresource Technology*, 102(19):9216–9222, 2011.

[135] Ashok K. Batta, Guorong Xu, Akira Honda, Teruo Miyazaki, and Gerald Salen. Stigmasterol reduces plasma cholesterol levels and inhibits hepatic synthesis and intestinal absorption in the rat. *Metabolism: Clinical and Experimental*, 55(3):292–299, 2006.

[136] Valeria Polzonetti, Stefania Pucciarelli, Silvia Vincenzetti, and Paolo Polidori. Dietary intake of vitamin d from dairy products reduces the risk of osteoporosis. *Nutrients*, 12(6):1–15, 2020.

[137] Michael Murkovic, Sonja Lechner, Ariane Pietzka, Michael Bratacos, and Evangellos Katzogiannos. Analysis of minor components in olive oil. *Journal of biochemical and biophysical methods*, 61:155–160, 2004.

[138] Ioannis Martakos, Marios Kostakis, Marilena Dasenaki, and Michalis Pentogennis. Toco-

pherols , and Squalene in Greek Olive Oils :. *Foods*, 9:31, 2019.

[139] Saithip Sae-Ngae, Benjamas Cheirsilp, Yasmi Louhasakul, Thunwadee Tachapattaworakul Suksaroj, and Punyanich Intharapat. Techno-economic analysis and environmental impact of biovalorization of agro-industrial wastes for biodiesel feedstocks by oleaginous yeasts. *Sustainable Environment Research*, 30(1), 2020.

[140] K. N. Englyst, S. Liu, and H. N. Englyst. Nutritional characterization and measurement of dietary carbohydrates. *European Journal of Clinical Nutrition*, 61:S19–S39, 2007.

[141] Ewelina Gołębiewska and Monika Kalinowska. Agricultural Residues as a Source of Bioactive Substances—Waste Management with the Idea of Circular Economy. *environmental sciences proceedings*, 9(2), 2021.

[142] Irnayuli R. Sitepu, Luis A. Garay, Ryan Sestric, David Levin, David E. Block, J. Bruce German, and Kyria L. Boundy-Mills. Oleaginous yeasts for biodiesel: Current and future trends in biology and production. *Biotechnology Advances*, 32(7):1336–1360, 2014.

[143] Katrin Ochsenreither, Claudia Glück, Timo Stressler, Lutz Fischer, and Christoph Syldatk. Production strategies and applications of microbial single cell oils. *Frontiers in Microbiology*, 7(OCT), 2016.

[144] Colin Ratledge, Hugo Streekstra, Zvi Cohen, and Jaouad Fichtali. *Downstream Processing, Extraction, and Purification of Single Cell Oils*. ©2010 by AOCS Press. All rights reserved., second edition edition, 2010.

[145] Markets Insider. Palm oil Commodity, 2023.

[146] Brett D. Glencross, David Huyben, and Johan W. Schrama. The application of single-cell ingredients in aquaculture feeds—a review. *Fishes*, 5(3):1–39, 2020.